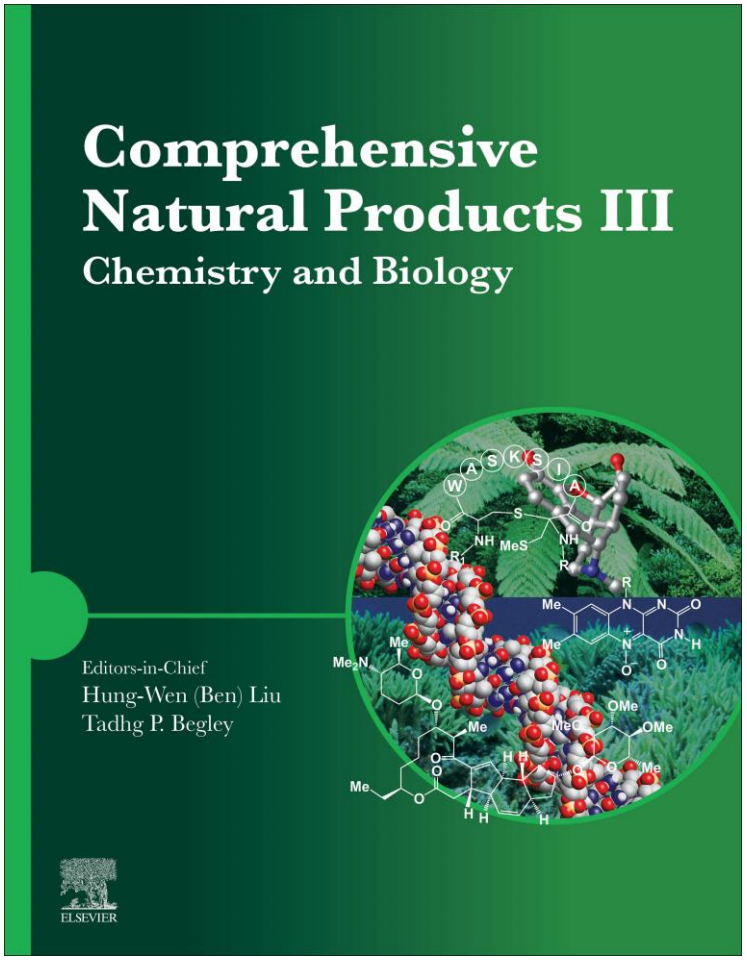

Chung Khoa, and O'Connor Sarah E. (2020) Biosynthesis of Vinblastine. In: Hung-Wen (Ben) Liu, Tadhg P. Begley (eds.) *Comprehensive Natural Products III: Chemistry and Biology*. vol. 2, pp. 642-685. Elsevier.

dx.doi.org/10.1016/B978-0-12-409547-2.14618-9

2.24 Biosynthesis of Vinblastine

Khoa Chung, University of Oxford, Oxford, United Kingdom
Sarah E O'Connor, John Innes Centre, Norwich, United Kingdom

2.24.1 Introduction

In 1958, Noble et al. published a seminal paper on the "chance" discovery of vinblastine as a potential chemotherapeutic agent.[1] According to Noble and coworkers, what started out as a search for an insulin alternative turned into exhaustive efforts to extract, purify, and characterize a compound that caused rats to exhibit a marked decrease in their white blood cell count and depression of bone marrow function.[1] Thus, the potential for vinblastine to cure leukemia and Hodgkin's lymphoma, cancers associated with a heightened level of white blood cells, was realized.[1]

In the same year, a meeting between Noble and the director of research at Eli Lilly, Dr. Johnson, revealed that the pharmaceutical conglomerate had been simultaneously searching for anticancer agents, including those from plant extracts.[2] While it remains controversial which group first noted the antitumor activity of vinblastine, a collaboration between Johnson and Noble soon ensued, and in 1961, Eli Lilly introduced vinblastine (Velban®) as their first oncology drug.[2] Not long after, vincristine (Oncovin®), a close analog of vinblastine, was also released to market.[2] The story of the discovery of vinblastine from the perspectives of both the well-known players and "unsung heroes" has been reported.[2]

Vinblastine and vincristine hold important places in the annals of chemotherapy drugs. Unfortunately, the low levels of these compounds in plant extracts mean that commercial access is limited, with current production relying on low-yield plant extraction and semisynthesis from rare precursors.[3] Elucidation of the biosynthesis of these compounds in planta will allow development of modern metabolic engineering and synthetic biology approaches for heterologous expression of the genes encoding these pathway enzymes to enable wider access to these life-saving drugs. In this article, we recount the biosynthesis of vinblastine. We emphasize the later stages of the pathway, since these steps involve chemistry that is unprecedented, and has proven to be the most challenging to solve. We summarize the model chemistry that has been developed for this pathway over the past five decades, and we highlight how these chemical studies guided the discoveries of the genes that encode the biosynthetic enzymes in planta. Only through using a combination of organic chemistry, biochemistry and plant molecular biology could this long-standing biosynthetic question be solved.

2.24.2 Discussion

2.24.2.1 Biosynthesis of the MIA Precursor Strictosidine

The chemical steps leading to the central intermediate strictosidine (**1**) were initially determined by numerous feeding studies in several iridoid and alkaloid-producing plants.[4] Strictosidine biosynthetic genes were the first genes in the monoterpene indole alkaloid (MIA) pathway to be identified. Strictosidine synthase (*STR*, Scheme 1) was identified from a cDNA library from *Rauvolfia serpentina* cell culture in 1988,[6] using a synthetic oligodeoxynucleotide hybridization probe. The *STR* homolog from *Catharanthus roseus* was identified shortly after in 1990.[7] Tryptophan decarboxylase (*TDC*), cloned in 1989,[8] was identified by antibody screening of a *C. roseus* cDNA expression library. Secologanin synthase (*SLS*) was discovered in 2000 by heterologous expression of cytochrome P450 genes that showed upregulation in response to induction conditions known to stimulate MIA biosynthesis.[9,10] Geraniol 8-hydroxylase (*G8H*, and named *G10H* at that time) was cloned in 2001 using degenerate PCR primers based on limited amino acid sequence information.[11] Expressed sequence tags (EST) libraries became more widely used after this period, and loganic acid methyltransferase (*LAMT*) was identified in 2008 using an EST library derived from *C. roseus* epidermal cells. With the advent of next generation sequencing, transcriptomic datasets became available for the first time for medicinal plants. Iridoid synthase (*IS*)

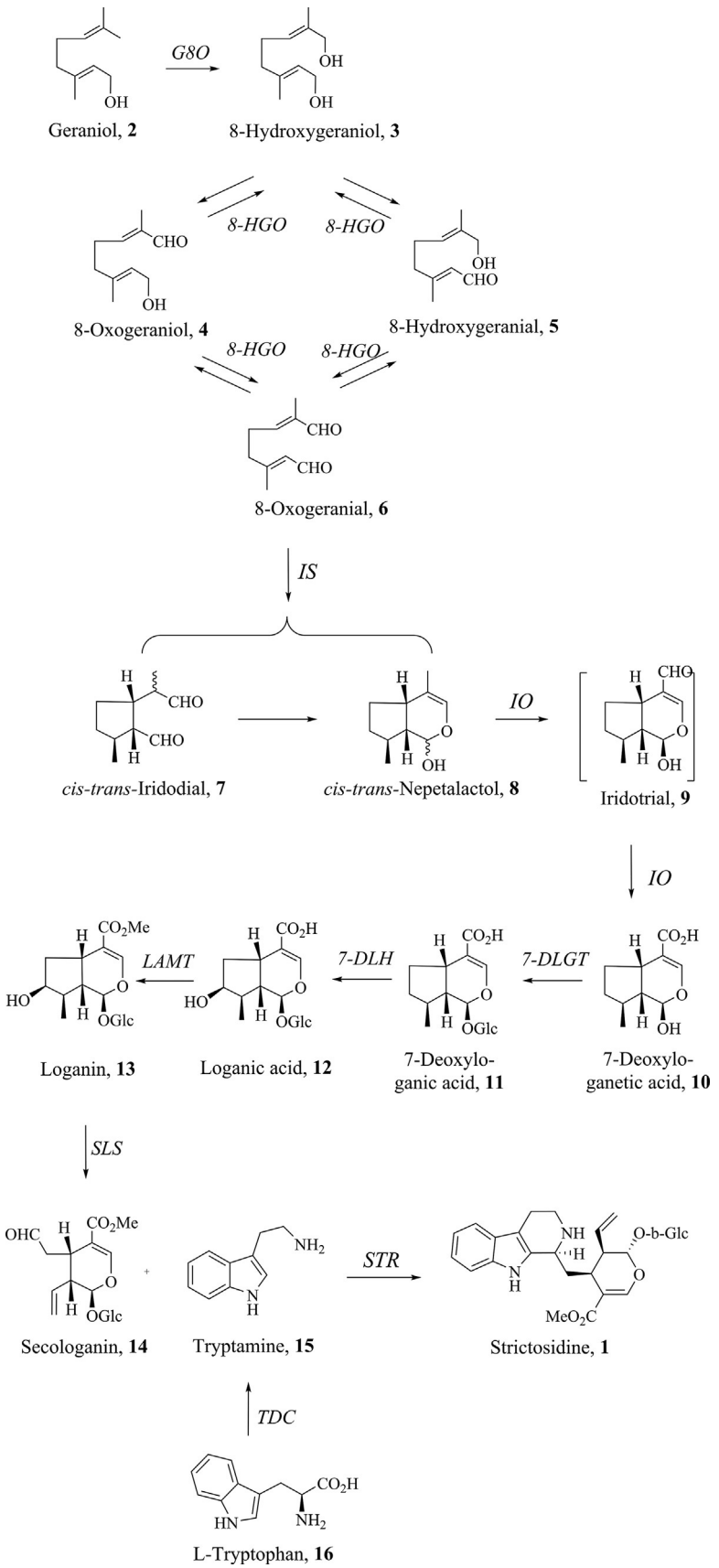

Scheme 1 The strictosidine pathway. Iridotrial (**9**) has been proposed to be an intermediate in the conversion from iridodial (**7**) to 7-deoxyloganetic acid (**10**) but has never been detected in planta or in enzymatic reactions.[5] *G8O*, geraniol 8-hydroxylase; *8-HGO*, 8-hydroxygeraniol oxidoreductase; *IS*, iridoid synthase; *IO*, iridoid oxidase; *7-DLGT*, 7-deoxyloganetic acid glucosyl transferase; *7-DLH*, 7-deoxyloganic acid hydroxylase; *LAMT*, loganic acid *O*-methyltransferase; *SLS*, secologanin synthase; *STR*, strictosidine synthase; *TDC*, tryptophan decarboxylase.

was cloned in 2012 using coexpression analysis with a transcriptomic dataset from *C. roseus*.[12] Coexpression analysis was also used to identify the last remaining genes in strictosidine biosynthesis, *GOR*, *IO*, *7DLGT*, and *7DLH*. These were reported in 2014 along with the reconstitution of strictosidine in *Nicotiana benthamiana*.[5] The genes *IO*,[13] *7DLGT*,[14] and *7DLH*[15] were also reported simultaneously in separate studies.

2.24.2.2 Chemical Studies—From Strictosidine to Catharanthine and Tabersonine

The chemistry involved in the transformation of strictosidine (**1**) to the central intermediates leading to vinblastine (**17**) and vincristine (**18**) is challenging, and was largely elucidated from chemical studies during the 1960s and 1970s.[4] The intermediary steps, from **1** to the monomeric building blocks, tabersonine (**19**, Aspidosperma type, a vindoline precursor) and catharanthine (**20**, Iboga type), via the putative intermediate stemmadenine (**21**), were hypothesized from these studies (Scheme 2). The model chemical experiments, isolation of reaction intermediates, and extensive feeding studies from this period were an essential part of recent efforts to complete the vinblastine pathway (Fig. 1).

In 1962, Wenkert developed the first hypothesis for the generation of the Aspidosperma and Iboga alkaloid backbones.[17] By observing that the structure of many nonalkaloidal glycosides, now formally known as iridoids, exemplified by indole alkaloids such as corynantheine (**24**) and strychnine (**25**), could be traced back to that of the *seco*-prephenate-formaldehyde (SPF, **26**) unit, Wenkert postulated that **26** could act as the basis from which seemingly disparate plant natural products are derived.[17] Thus, α-oxidation of anthranilic acid derivative (**27**) followed by Mannich condensation with **26** (at C*) would yield complex **29**, whose in vivo metabolism was expected to give indole **31** (Scheme 3). Replacement of the β-glycosyl side chain by an ethylamino group could then form structure **33**, which, following an initial (C-15)–(C-16) bond cleavage to give **34**, is primed to undergo

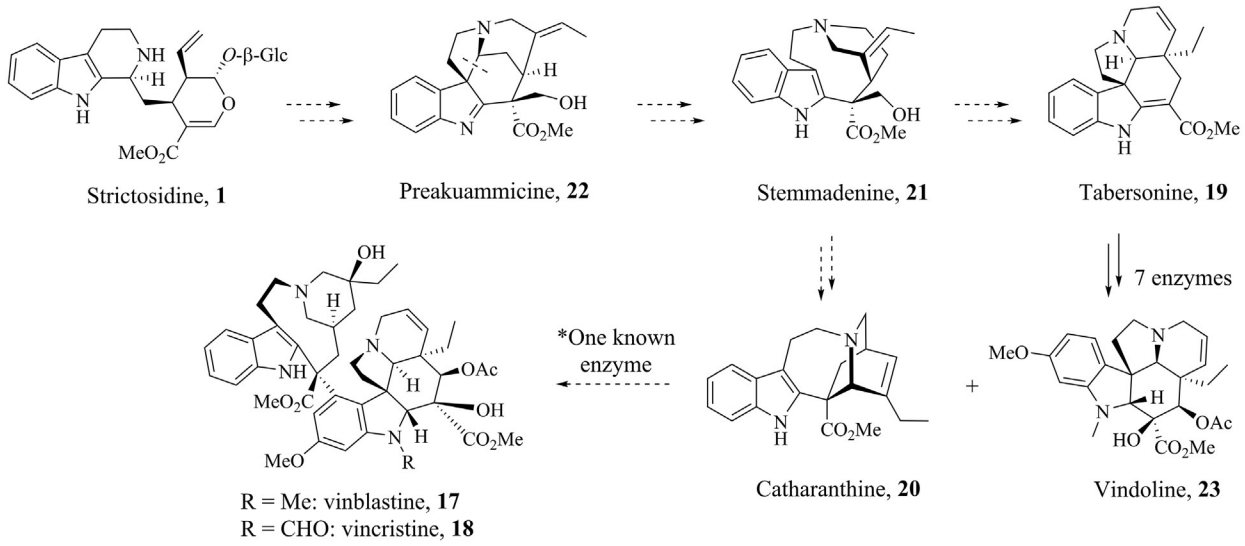

Scheme 2 Biosynthetic steps in the middle—late stage of the vinblastine pathway; dotted arrows denote transformations catalyzed by enzymes determined since 2017.

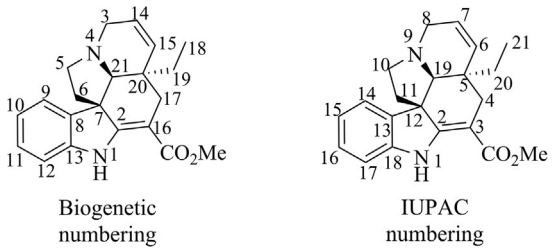

Fig. 1 Different numbering methods for **19**. Although the biogenetic numbering is employed throughout this article, the IUPAC system will be used for "Tabersonine-Vindoline Biosynthesis" section specifically, as the designations for the enzymes within the tabersonine-vindoline pathway are consistent with the latter system. Additionally, some of the nomenclature has changed over the years.[16] Specifically "pseudocatharanthine" in referring to an isomer of **19** and **20** whereas herein, "pseudotabersonine" is used.

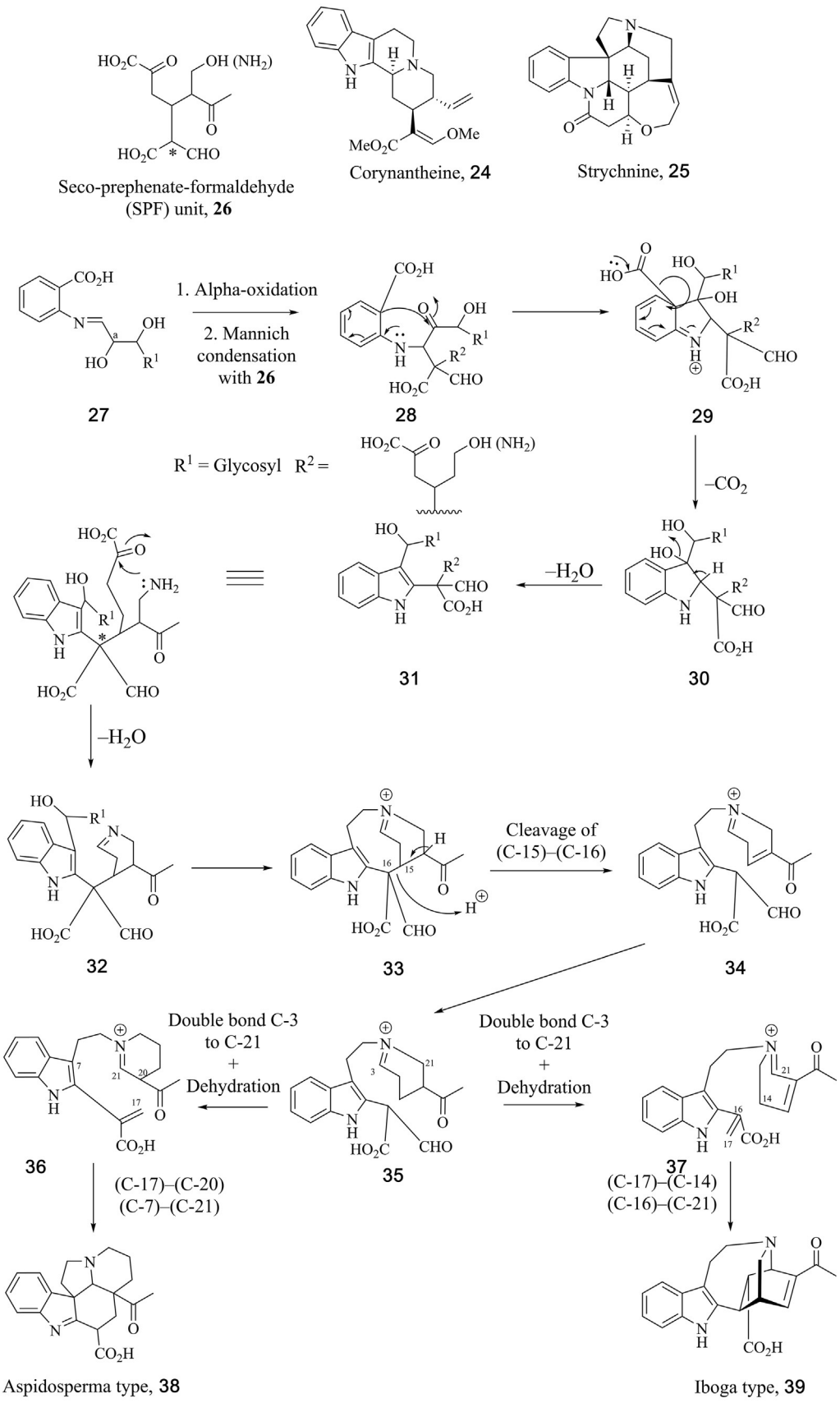

Scheme 3 Wenkert's original transannular cyclization hypothesis for the formation of the Aspidosperma and Iboga backbones from **26.**[17]

intramolecular Michael/Mannich reactions to give either Aspidosperma-**38** or Iboga-type **39**.[17] Despite the highly speculative and facile nature of this reaction sequence, Wenkert's hypothesis was widely accepted.[18–21]

Scott and coworkers were the first to propose the crucial involvement of the highly reactive dehydrosecodine **B** (**40**) in 1968, generated via a formal dehydration of isomerized stemmadenine (**41**, Scheme 4).[22] Kutney and colleagues also arrived at the same conclusion through a retrosynthetic analysis of the prototype of **19**.[19] The first notable feature in Scott's hypothesis is the importance of unsaturation at the (C-20)–(C-21) bond, which he proposed could arise through isomerization of the exocyclic double bond in **21** to furnish **41**. From here, ring-opening by cleavage of the (C-15)–(C-16) bond, mediated by the tertiary nitrogen, with concomitant dehydration, followed by tautomerization of the dihydropyridine ring could give **40**.

It is speculated that the conjugated system present in **40** could undergo different [4 + 2] Diels-Alder reactions (DAR), and, depending on which component is acting as the diene/dienophile, could form either **19** or **20**. Provided that **40** is the true intermediate in this pathway, an alternative stepwise ionic mechanism could lead to the same products, and it remains to be seen which of these mechanisms is operative in these systems. For the purposes of this article, the Diels-Alder mechanism will be assumed. Notably, Diels–Alderases are uncommon in biological systems.[23–26] Indeed, the first characterization of such enzymes only appeared in 1995;[27,28] and only a handful of reported cases of the involvement of Diels-Alderases in nature have since come about,[24–26,29–32] making the enzymology behind formation of **19** and **20** particularly exciting.

The experiments by Scott and coworkers dispelled Wenkert's transannular cyclization proposal (Scheme 3) in favor of a mechanism where **40** plays a pivotal role in forming **19** and **20**, and Scott's hypothesis has since been widely accepted by researchers of this field (Scheme 4). Nonetheless, Scott's biosynthetic proposal was clearly inspired by Wenkert's initial hypothesis.

Scott's biosynthetic proposal was supported by model chemistry as well as feeding studies. When Scott and coworkers refluxed (+)-**21** in acetic acid, a separable mixture of (±)-**19**, (±)-**20**, and (±)-pseudotabersonine (**43**) was observed (Scheme 5).[22] In another instance, Scott et al. observed the formation of (±)-**20** and **43** when they refluxed (−)-**19** in acetic acid.[22] Thus, although this reaction's product distribution is extremely sensitive to minor variations in experimental conditions, the fact that racemic mixtures of the dehydration products were observed from optically pure starting materials—an obvious consequence for any mechanism involving **40**—provided the first piece of experimental evidence to support Scott's hypothesis. This result led Scott's group to speculate the biosynthetic sequence: **21** → **19** → **20**.[22,33] Further evidence in support of this sequence was provided when administration of isotopically labeled **21** to germinating seeds yielded **19**, **20**, and the tabersonine derivative vindoline (**23**) with the appropriately labeled components.[34] The significant incorporation of labeled **19** into **20**, and not vice versa, was also detected,

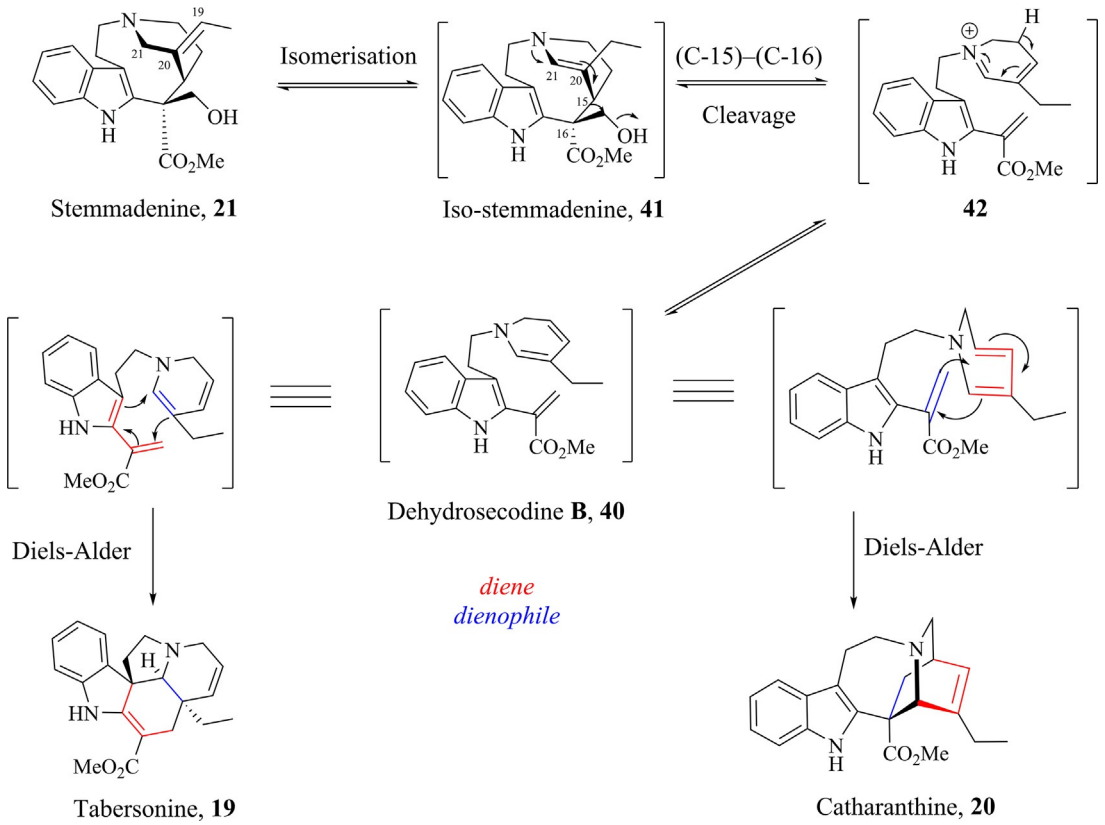

Scheme 4 Scott's dehydrosecodine hypothesis leading to tabersonine (**19**) and catharanthine (**20**) from stemmadenine (**21**). *Red* bonds denote the dieno, whereas those in blue denote the dienophile components.

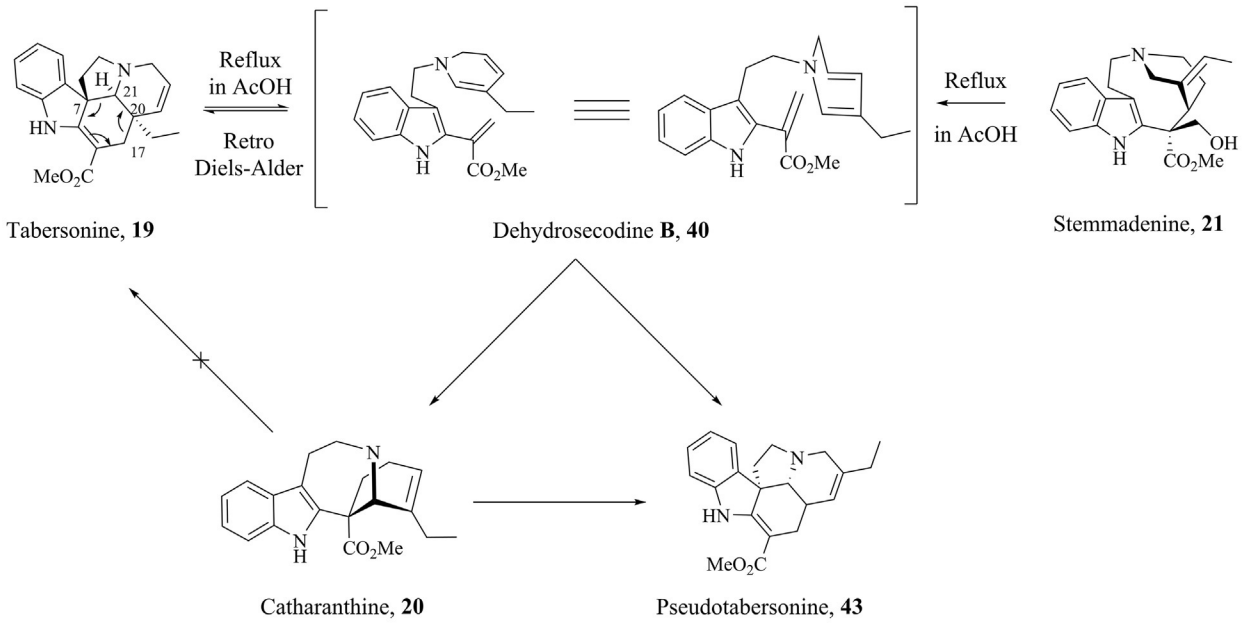

Scheme 5 Scott's initial hypothesis to explain the reactions of **21**, and **19** in refluxing acetic acid.[22]

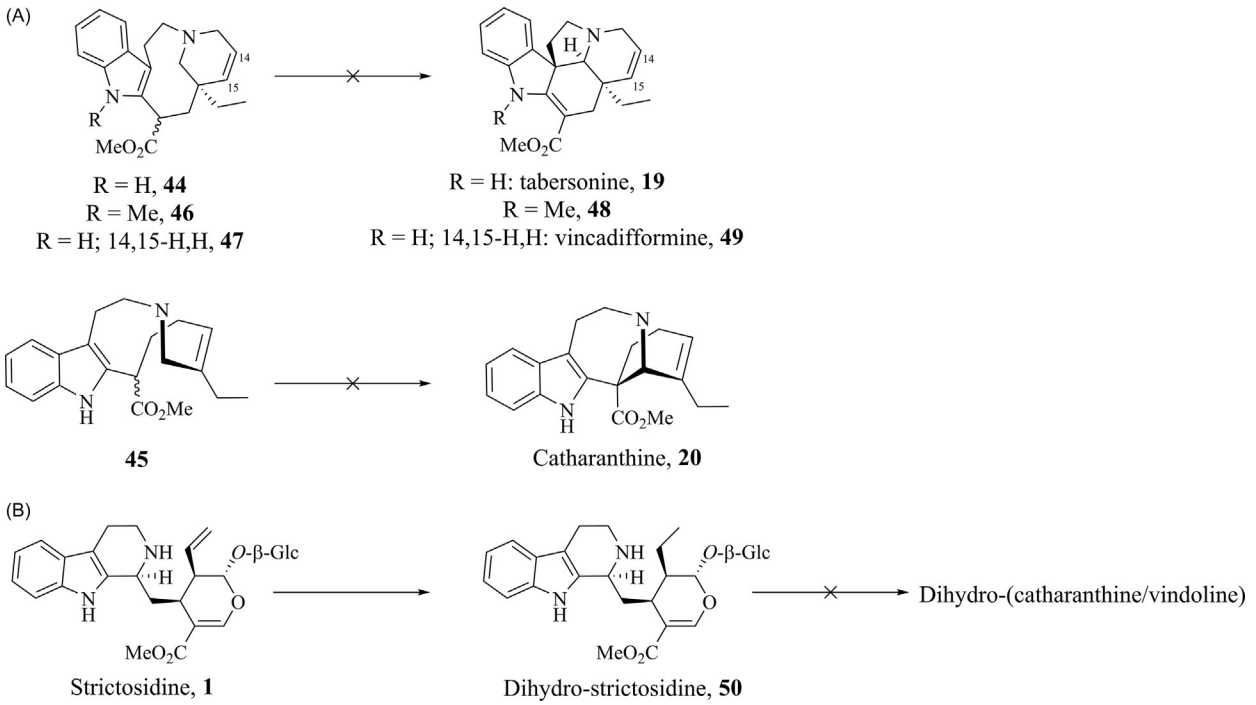

Scheme 6 Experiments to (**A**) disfavor Wenkert's transannular cyclization hypothesis and (B) support the importance of unsaturation of the ethylidene side chain.[19,35–39]

suggesting the conversion from **19** to **20** is irreversible.[34] Kutney et al. independently arrived at the interrelationship between **19** and **20** by analogous feeding studies.[19,35] Evidence disfavoring an operative transannular cyclization was also provided by Kutney and coworkers, as feeding of **44** and **45**, immediate precursors of **19** and **20** according to Wenkert's hypothesis, showed negligible incorporation (cf. Schemes 3 and 6).[19,35]

Furthermore, a detailed feeding study of DL-tryptophan-3-^{14}C (**A**), a known precursor of these MIAs, and isolation of the nine-membered ring structures **46** and **47** and their respective pentacyclic structures **48** and **49** confirmed the insignificance of the transannular process in forming the Aspidosperma backbone (Table 1).[19,36] Table 1 reveals two obvious trends. First, the

Table 1 Incorporation of **A** into **46–49** at different time intervals disfavoring Wenkert's transannular cyclization hypothesis[19,36]

	Combined % incorporation of A into		
Time	*46 + 47 (B)*	*48 + 49 (C)*	*C/B*
4 h	0.003	0.057	19
1 day	0.015	0.24	16
2 days	0.010	0.21	21
7 days	0.009	0.13	14
14 days	0.003	0.06	20

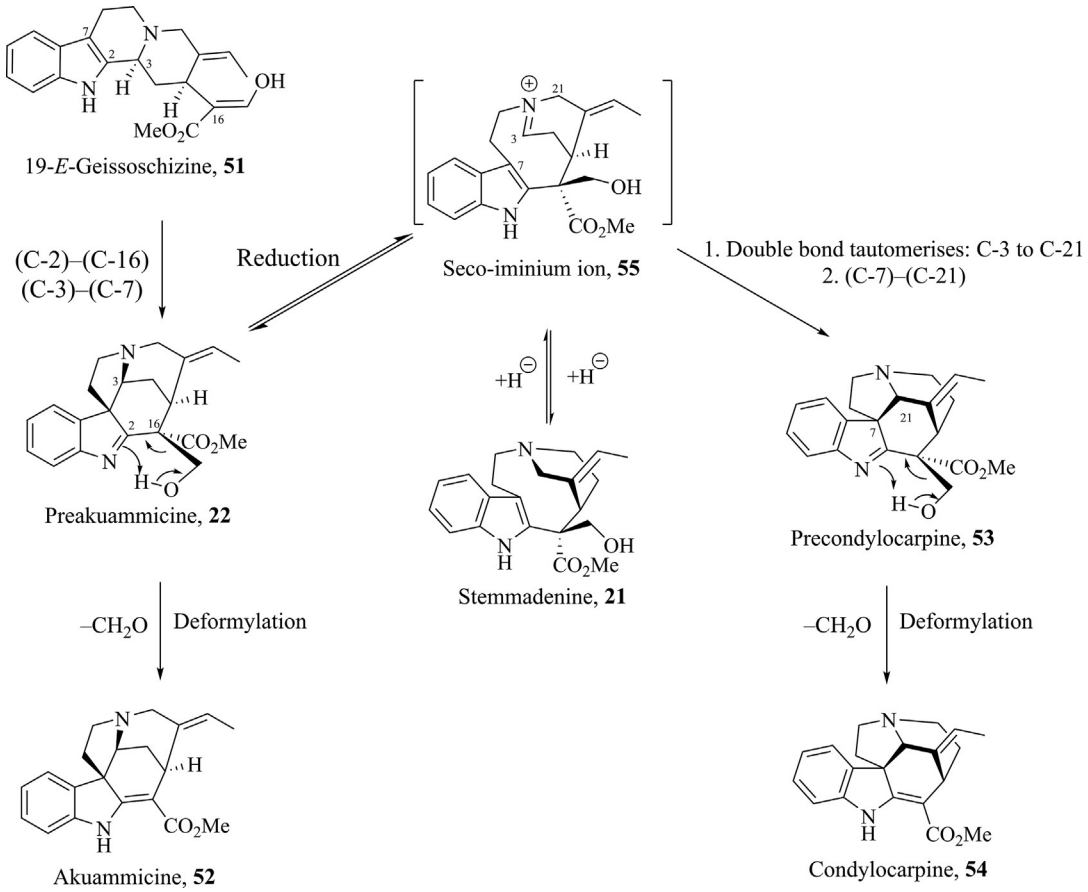

Scheme 7 Scott's proposed pathway for the intimate relationships between **22**, **21**, and **53** via iminium ion **55**.[46,47]

incorporation of **A** into the pentacycles **48** and **49** (**C**) was consistently higher than that of the nine-membered rings **46** and **47** (**B**). Second, the **C**/**B** ratio remains relatively constant with time, which once again does not support the codependence between the opened and cyclized systems.

Further evidence favoring Scott's hypothesis was provided by the Battersby group. As stated above, the centerpiece in Scott's hypothesis is the double bond at (C-20)–(C-21), formation of which would be mediated by the exocyclic side chain (Scheme 4). Hence, when labeled **1**, known precursor of **19**, **20**, and **22**, was reduced to form dihydro-strictosidine (**50**), and fed to *C. roseus* shoots, minimal incorporation into the corresponding downstream products was observed (Scheme 6).[37,38,40]

A year later, novel intermediates central to the vinblastine pathway were independently reported by the Scott and Battersby groups. The first, 19-*E*-geissoschizine (**51**), was shown to be the precursor of **20**, **22**, and akuammicine (**52**) through labeling experiments.[39,41–43] Scott also described identification of a new compound extracted from *C. roseus* seedlings, preakuammicine (**22**), which coeluted with **51**.[44,45] It had been suggested that structures such as **22** could act as the missing link between **51** and **21** (Scheme 7).[46,48,49] Thus, **22**'s coelution with **51** as well as its structural similarity to **21** made its fortuitous discovery all the more

gratifying. Despite lacking concrete evidence proving the biosynthetic order between **22** and **21**, the order of **21**'s appearance in young seedlings and mechanistic considerations suggest that **21** follows, or is in equilibrium with **22**, and this order has been assumed in the literature since.[39,50,51]

Partial spectral data of preakuammicine (**22**) appeared similar to that of structural isomer precondylocarpine (**53**).[46] Mass spectra of **22** and **53** contain base peaks corresponding to the retroaldol loss of C-17 as formaldehyde, forming akuammicine (**52**) and condylocarpine (**54**), respectively (Scheme 7).[46] This evidence could now be used to rationalize the high incorporation of labeled **51** into **52**, as previously observed by Battersby et al.[42] More concrete evidence came when Scott and Qureshi reduced **22** with sodium borohydride to give a mixture of **52** and **21**, which was proposed to have proceeded via the seco-iminium ion (**55**).[46,47] The latter compound, when subjected to catalytic oxidation with platinum, gave **22** and **53**, and their respective deformylated products. Thus, the coisolation of **21** with **22** and **52** strongly suggested **52**'s intermediacy in the vinblastine pathway, and illustrates the intimate relationship between the open structure **21** and cyclized forms **22** and **53**—interconversion of which could be achieved by sequential redox processes.[47] Notably, enzymes catalyzing the biosynthetic sequence **51** → **22** → **21** have been recently reported by the O'Connor and De Luca groups, a welcome tribute to the painstaking efforts of the researchers of this field in the 1960s and 1970s (see "Strictosidine-preakuammicine biosynthesis", "Preakuammicine-stemmadenine acetate biosynthesis," and "Stemmadenine acetate-tabersonine and catharanthine biosynthesis" sections).[50,52]

Research groups working in this area then focused on establishing the validity of the process delineated in Scheme 5, specifically in showing that (+)-**21** could be converted to the cyclized products (±)-**19** and (±)-**20**. To this end, the Kunesch group attempted to repeat Scott's experiments with **21** in refluxing acetic acid.[53] However, Kunesch et al. were unable to form **19**, **20**, and **43** as previously reported by Scott; only stemmadenine acetate (**56**), together with a small amount of unreacted **21**, was recovered.[53] Likewise, their results with **19** were incongruous with those obtained by Scott, with unreacted **19** being the main component recovered, along with its 15,20-dihydro-derivative, vincadifformine (**49**), and a mixture of (+)-allocatharanthine (**57**) and its reduced and acetoxylated analogs (**58** and **59**, respectively).[53] The absence of racemic **57** led Kunesch to propose a sequence as shown in Scheme 8 to rationalize the transformation from **19** to the allocatharanthine series. Notably, Kunesch proposed that the exclusive stereo-preference for (+)-**57** must preclude cleavage of the (C-17)–(C-20) bond, a conclusion which impinges on Scott's dehydrosecodine hypothesis.

Their inability to replicate earlier results by Scott was subsequently reported in a number of reviews.[39,54,55] Thus, Scott's dehydrosecodine theory, which had by then unified the results of a multitude of feeding studies and provided a rationale for how the Aspidosperma and Iboga alkaloid structures were biosynthetically linked, was now in question. Aside from a review and an article,[47] the Scott group reported little on the biosynthesis of MIA in the following years, and it seemed that the MIA community was consigned to come up with a new theory to rationalize these conflicting outcomes.

However, in 1972, Scott published a series of papers to address Kunesch's previous contradictory results.[30,45,56–58] The first of these was a rather strongly worded commentary directed at the Kunesch group.[56] Therein, Scott accounted for his 3-year absence in the field, the purpose of which was to identify a reliable source of the stemmadenine (**21**) substrate. Furthermore, Scott also noted that the reference compound which was used by Kunesch to ascertain their reaction progress was, in fact, "mixtures of uncertain optical purity" which Scott concluded would have invalidated the conclusions drawn from their work.[56] Nonetheless, Scott admitted that due to the scarcity of **21** and **19**, and the inherent difficulties associated with microgram-scale biomimetic

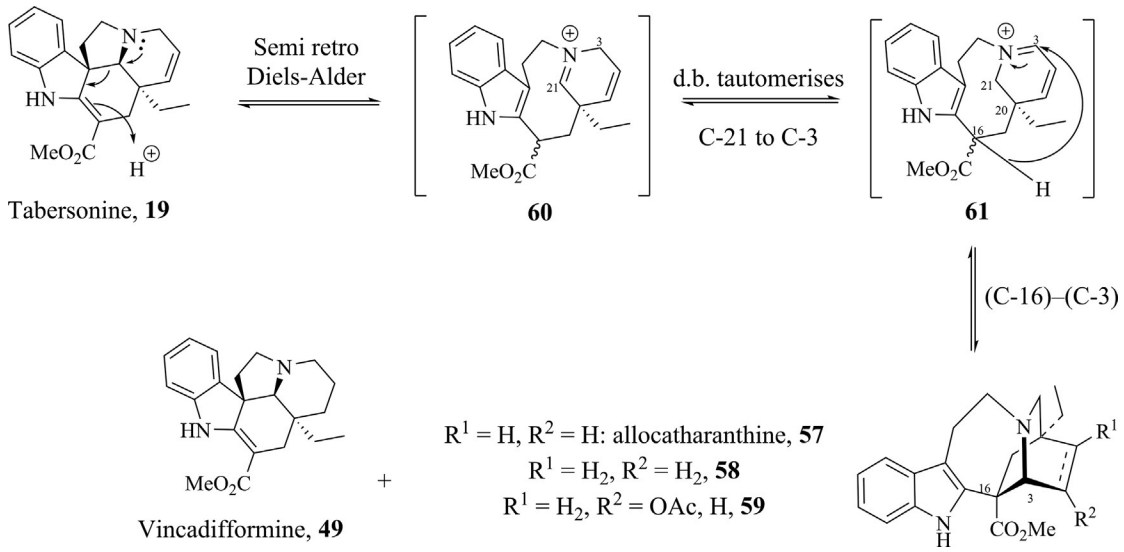

Scheme 8 Kunesch's proposed pathway for the transformation of **19** into **49**, **57** and its derivatives in refluxing acetic acid.[53]

experiments, his group was not able to report explicit details relating to their protocols.[56] Moreover, reexamination of the essential factors leading to their earlier observations revealed the high sensitivity of this particular reaction to external conditions.[44,47,56,57] Notwithstanding the newly gained knowledge, Scott admitted that such biogenetic-type interconversion had severe shortcomings in terms of reproducibility.[44] The next phase of Scott's experimental work thus relied on more chemically guided approaches, specifically redox reactions carried out on **21**.

The first hurdle was to discover a more predictable method for the isomerization of the exocyclic double bond to the (C-20)–(C-21) position in **21**. Their endeavor in this domain led to the discovery that, whereas platinum-catalyzed reduction of **21** led to the formation of the 19,20-dihydro derivative (**62**), when the same reduction was applied to stemmadenine acetate (**56**), tetrahydrosecodine (**70**) was formed in 75% yield (Scheme 9, path *a*).[44,45] The difference in behavior toward hydrogenation between the alcohol and acetate suggested that the acetyl group at C-17 facilitated the irreversible loss of the acetoxy moiety from the *endo* isomer, which is in equilibrium with its 19,20-*exo* counterpart.[44] The distinct reactivity imparted by the acetyl versus hydroxyl group in **21** in relation to cleavage of the (C-15)–(C-16) bond directed the group's attention to more rigorous studies on the acetylated derivative **56**.

Initial thermolysis of **56** formed (±)-**49** exclusively, while its unsaturated analog (±)-**19** was not observed. Formation of the former, Scott reasoned, was via initial Michael attack of a hydride onto the ring-opened intermediate (**42**), forming a tetrahydropyridine derivative (**71**), which could then undergo cyclization (Scheme 9, path *b*).[44,45] Explanation as to why

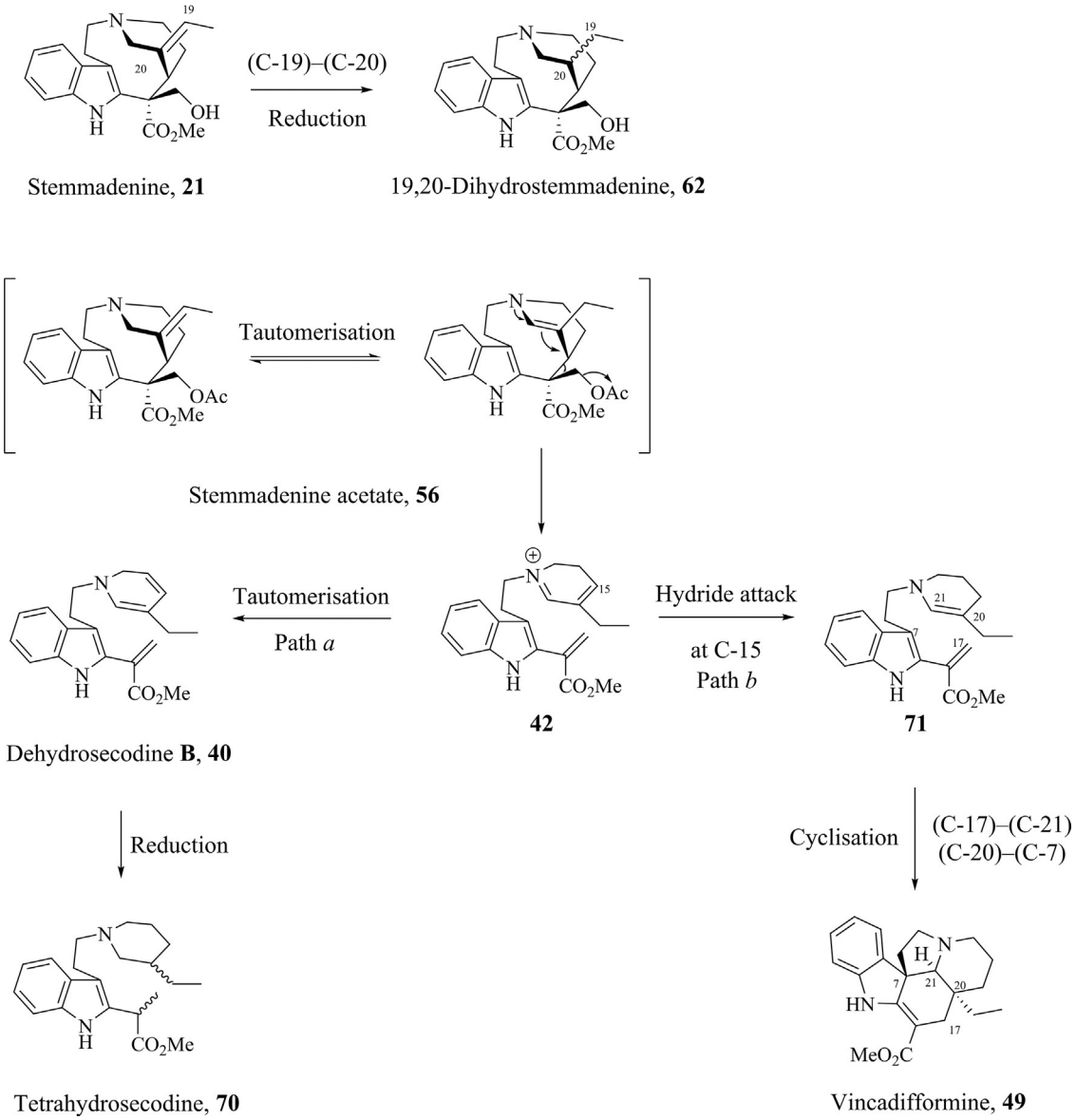

Scheme 9 Different fates for **21** and **56** illustrating the importance of the C-17 acetyl group (path *a*) and proposed explanation for formation of **49** (path *b*).[44,45]

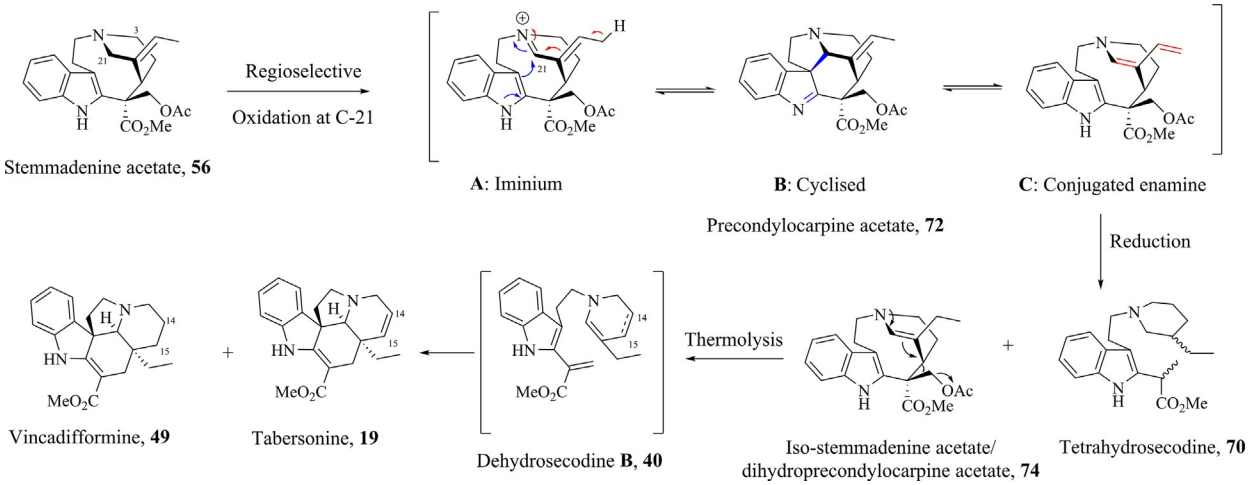

Scheme 10 Preferential oxidation at (C-20)–(C-21) to give the **72** and its reduction to generate unsaturation at (C-20)–(C-21) in isostemmadenine acetate (**74**). Subsequent thermolysis, presumably via **40**, led to cyclized **21** and **49**.[44,45]

reductive cyclization is favored over the direct approach to give **19** was not given. From previous experience with refluxing **21** in acetic acid,[22] it was known that regioselective oxidation of **21**, and hence **56**, at C-21 could be straightforwardly achieved to form pentacyclic **53** and **72**, respectively. It was envisaged that this step could be better controlled via platinum-catalyzed oxidation.[44,45]

Although it was never explicitly stated, presumably Scott's rationale in oxidizing these systems was to form iminium precondylocarpine acetate (**72A**), which may exist in equilibrium with the cyclized form **72B**, *blue* arrows, Scheme 10), or the conjugated enamine (**72C**, *red* arrows, Scheme 10); thus, **72C** now formally contains the desired double bond at (C-20)–(C-21) (Scheme 10). In the synthetic sequence depicted in Scheme 10, an explanation is required for the preferential hydride loss at C-21 over C-3. The most logical proposition for this regioselectivity is the extra tautomer enamine **72C**, afforded by presence of the 19,20-double bond. The alternative iminium/cyclized product, which may conceivably arise from dihydrostemmadenine acetate (**73**), may require a reversal of the redox steps: reduction of **21** (or **56**) followed by oxidation (Scheme 11).

Reduction of **72** yielded **70** and the dihydroacetate (**74**), the acetylated analog of the long-sought isostemmadenine (**41**).[44,45] Subsequent thermolysis of **74** generated (±)-**19**, and (±)-**49**, presumably via **40**. However, it was unexpected that no **20** could be detected in this instance. Moreover, this redox sequence, which was likely occurring in the earlier experiments in which **21** was refluxed in acetic acid, could be used to rationalize both the results from these early experiments and the Kunesch group's observation that **56** was the major product in their attempt to reproduce Scott's results. Stemmadenine (**21**) is first converted to **56**, which then undergoes sequential oxidation-reduction (which must have been facilitated by the vigorous reflux conditions) to generate the various cyclized products previously described.

Significantly, no trace of the cyclized products deriving from dehydrosecodine **A** (**75**), namely the isomeric pseudotabersonine (**43**) and allocatharanthine (**57**), which would have formed had selective C-3 oxidation occurred, was detected.[44,45] This realization called for analogous experiments with the 19,20-dihydro analogs of **21**. In order to complete the analogy with **56**, thermolysis of dihydrostemmadenine acetate (**73**) was carried out, which yielded (±)-**43** and its dihydro analog (**76**), and neither **19** nor **20** from the dehydrosecodine **B** (**40**) series was formed (Scheme 11).[44,57] This result is in agreement with the proposed mode of cyclization via **75**, analogous to the above series. Once again, the isomeric cyclized product, **57**, was not observed in this reaction. The alternative strategy to arrive at **43**, **57**, and their derivatives could be realized by formation of a double bond at the (C-3)–(C-14) position. Hence, regioselective oxidation of **73** was performed which indeed yielded the pentacyclic product of C-3 oxidation, dihydropreakuammicine acetate (**77**).[44,57]

Thermolysis of **77** led to (±)-**43**, whereas methanolysis of **77** yielded a diastereomeric mixture of the 15-methoxy derivatives (**79** and **80**).[44,57] The latter reaction would have proceeded via conjugate addition of methanol prior to cyclization and strongly supported the involvement of **75** as an intermediate *en route* to the cyclized products. Thus, it appeared that the precise control of the different classes of isomeric cyclized products is strongly reliant upon the timing of the oxidative and reductive steps to give either the precondylocarpine or preakuammicine scaffolds. From the above results, Scott concluded that interconversion between dehydrosecodines **A** and **B** could not have occurred, since each dehydrosecodine isomer leads only to unique cyclization product profile.

At first sight, this seemed inconsistent with the earlier results of Scott in which stemmadenine (**21**) or tabersonine (**19**) was reacted in hot acetic acid (Scheme 12). Whereas scrambling of products deriving from both dehydrosecodine **A** and **B** series is evident when **21** and **19** were subjected to reflux in acetic acid, direct thermolysis, as well as the sequential redox and thermolysis of **56** and its reduced analog (**73**) gave only the predicted cyclized products. Clearly, the use of acetic acid facilitated interconversion

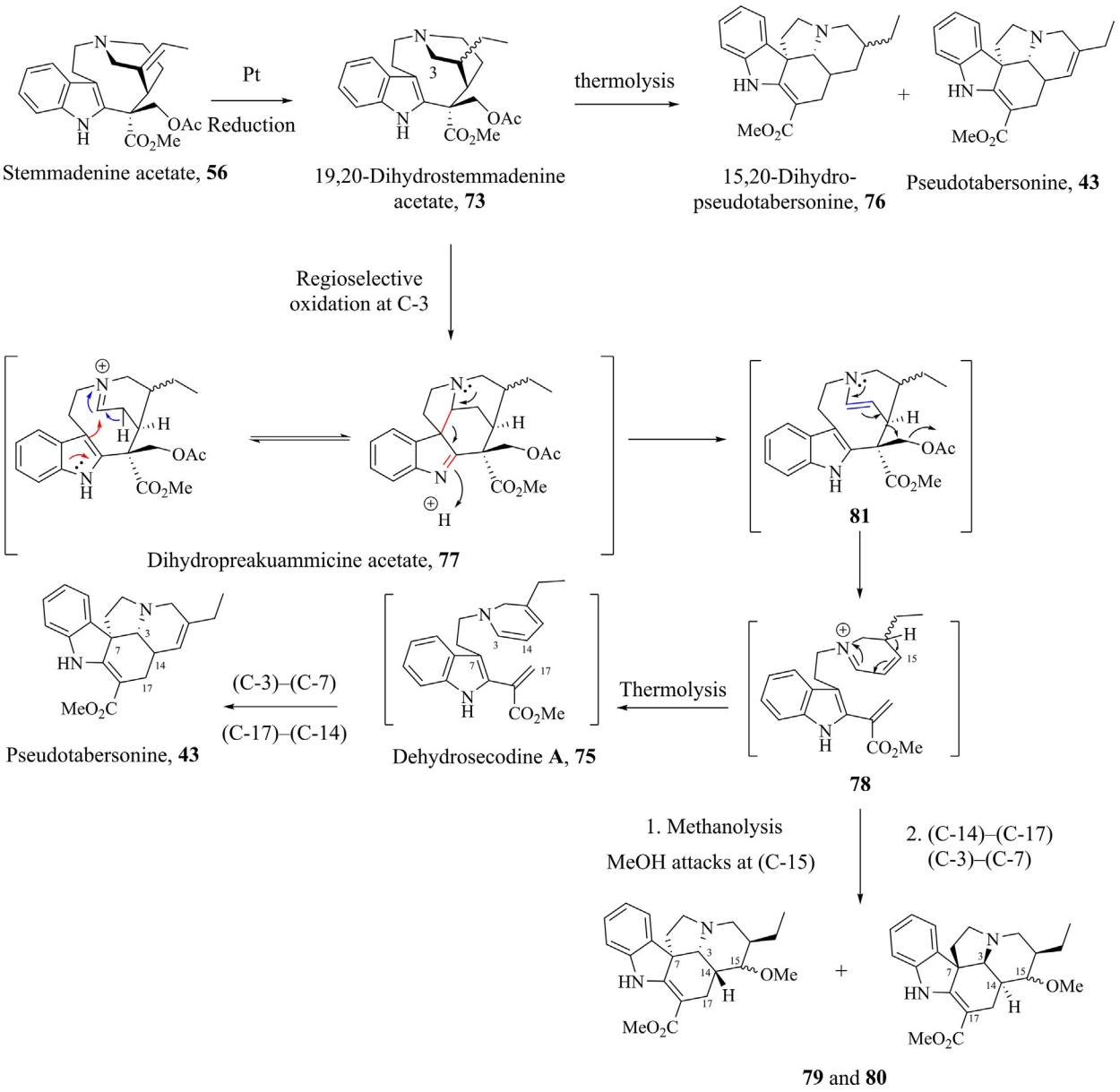

Scheme 11 The different products of **73** depending on reaction conditions, further corroborating Scott's dehydrosecodine hypothesis via **75**.[44,57]

between dehydrosecodines **A** and **B**, a realization which could explain for the anomalous formation of **43** when either **21** or **19** was refluxed in acetic acid.

The last point of contention concerned the conversion of **19** to **20** and **43**, which was previously reported by Scott et al. in 1968[22] and disputed by the Kunesch group a year later.[53] Kunesch and coworkers reported instead that only (+)-**57** and its derivatives were the thermolytic products.[53] Notably, Kunesch noted that this transformation would have followed a sequence as depicted in Scheme 8, and the absence of racemization would preclude cleavage of (C-17)–(C-20) bond to proceed via a dehydrosecodine-type intermediate.[53] In Scott's view, the reaction to form **20** and **43** would involve the rupture of both the (C-7)–(C-21) and (C-17)–(C-20) bonds, proceeding via **40** (Scheme 5).[22] On the other hand, Kunesch et al. proposed that the retro DAR occurred only as far as (C-7)–(C-21) cleavage. Isomerization of the resultant iminium intermediate (**60** to **61**) followed by cyclization of **61** would lead to (+)-**57**.[53]

*Re*evaluation of this reaction by thermolysis of (−)-**19** in acetic acid revealed that (+)-**57** was, in fact, a product of this reaction.[44,58] Thermolysis of (+)-**57** on a silica gel plate afforded (±)-**43** and optically pure (−)-**19**.[44,58] A consideration of the new results led Scott to conceive the pathway shown in Scheme 13, which could account for the absence of (±)-**19**, and is simply the reverse of Scheme 8, as previously proposed by Kunesch.[44,58] Furthermore, this result yet again supported lack of equilibration

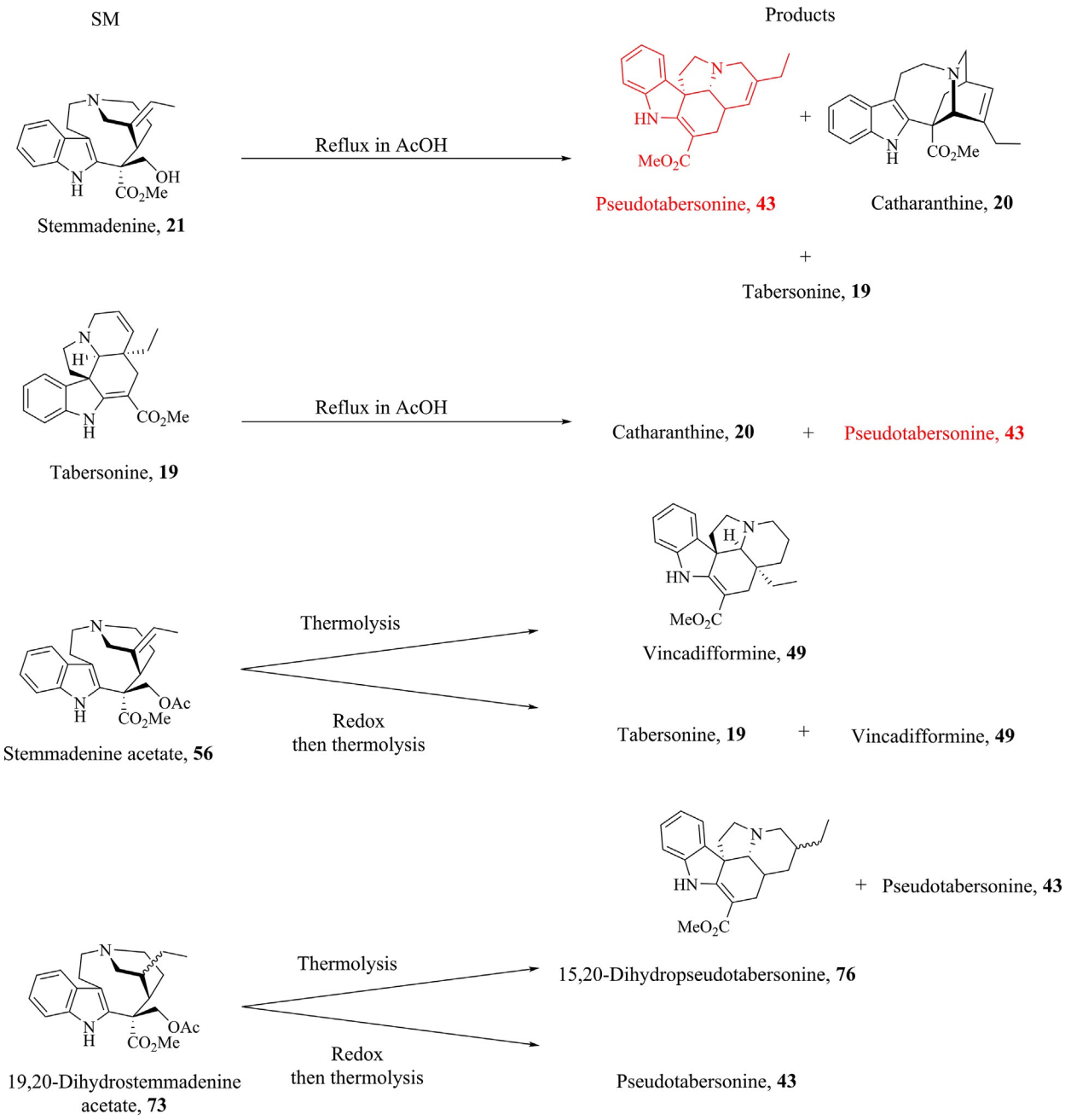

Scheme 12 Summary of the various in vitro experiments by Scott. *Red* entries denote unexpected cyclized products which must have derived from interconversion between the dehydrosecodine intermediates. Such a process was only observed in reactions with acetic acid.

between the two dehydrosecodine isomers, **A** and **B**, as only racemic **43** was observed, there being no racemization of **19**, which would have resulted from cyclization of **40**.[44,58]

At this stage, the existence of a dehydrosecodine intermediate was the only reasonable explanation to account for the experimental data. The next step was to isolate and structurally characterize this intermediate. Neither **75** (dehydrosecodine **A**) nor **40** (dehydrosecodine **B**) has ever been successfully synthesized/isolated, due to their instability. Isolation of related and more stable systems from indole alkaloid-producing plants such as the secamine **82** (*Rhazya stricta*, *Rhazya orientalis*),[59] presecamine **83** (*R. stricta*),[60] and secodine-type bases **84** and **85** (*R. stricta*) and **86–88** (*R. orientalis*)[61–63] had been reported by this time (Fig. 2). Importantly, Kutney demonstrated that synthesis of **84**, an acrylic ester which differs to the proposed dehydrosecodine intermediate only in the oxidation level at the piperidine ring, was possible.[19,64] Furthermore, Kutney showed that administration of tritium-labeled **84** to *C. roseus* led to low, but detectable, incorporation into **20** and **23**.[19,64] Altogether, these results are consistent with the presence of a secodine-type intermediate that plays a crucial role in the latter part of the vinblastine pathway.

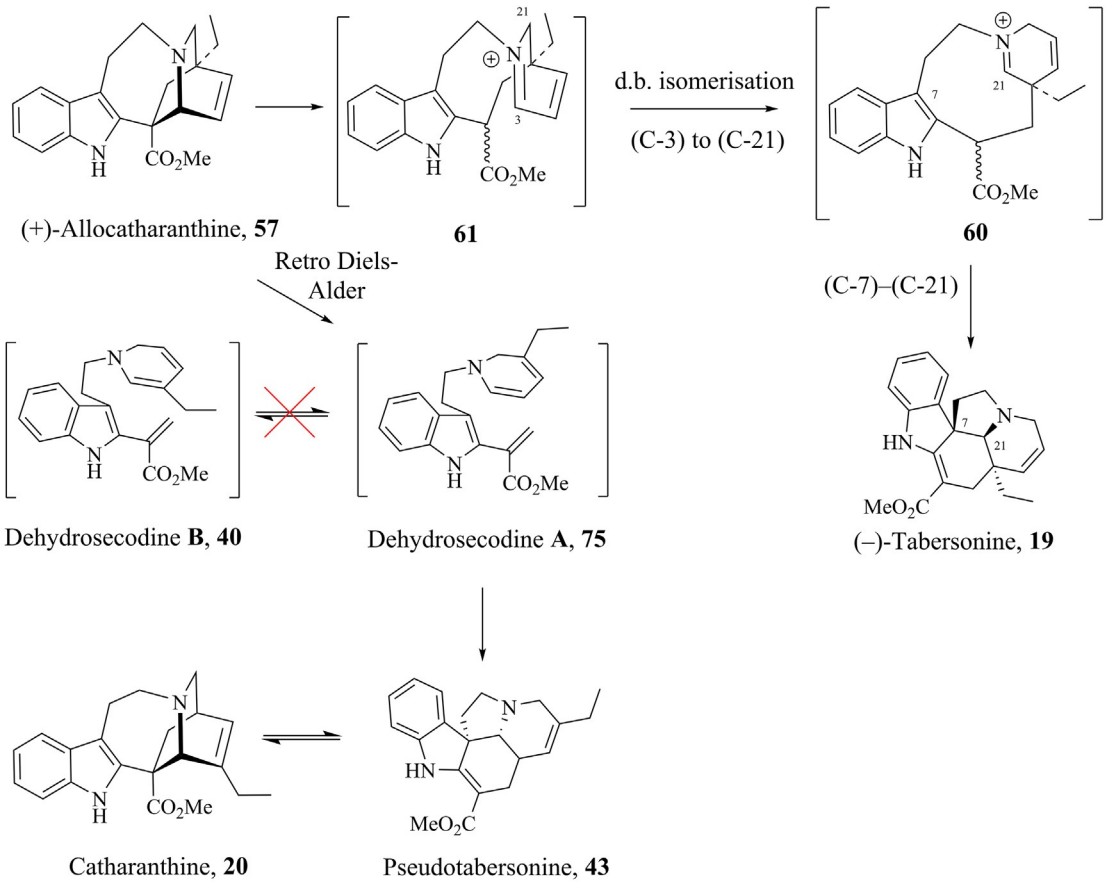

Scheme 13 Further evidence to support lack of equilibration between **40** and **75**, and to rationalize the relationships between the different cyclized products of the two dehydrosecodine series.[31,44]

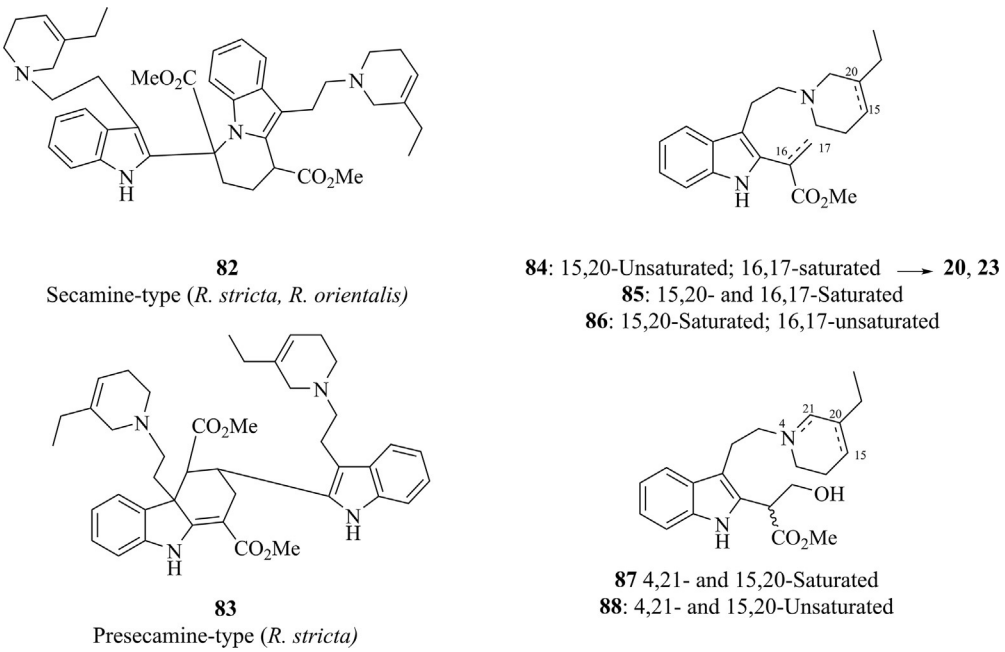

Fig. 2 The various secodine-like structures which have been isolated and synthesized. Collectively, these intermediates support the involvement of dehydrosecodine in the biosynthesis of vinblastine.[19,59–64]

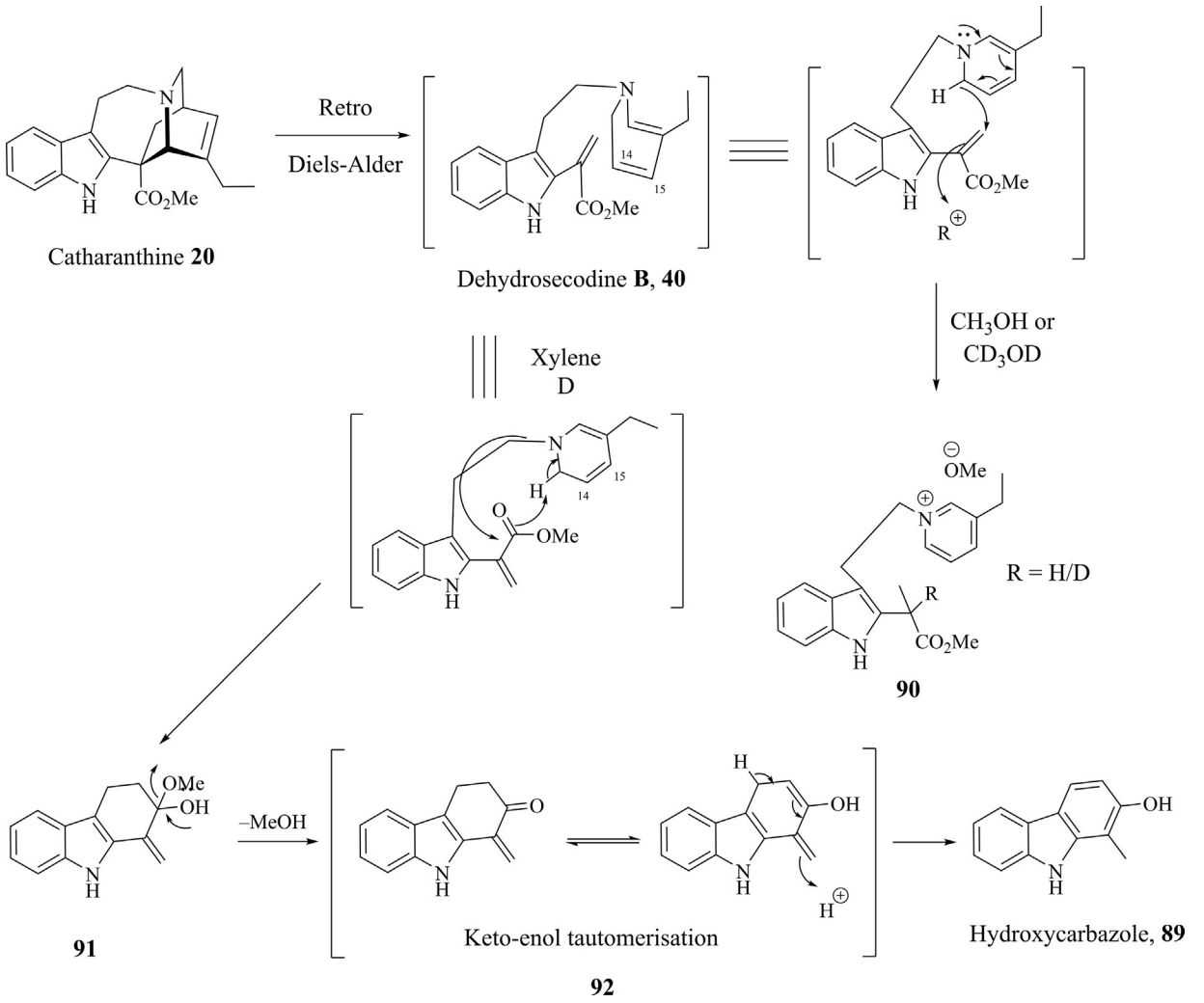

Scheme 14 Different products observed when **20** was heated in xylene versus methanol.[44,57]

Equally important was Scott's observation that when (+)-catharanthine (**20**) was heated in xylene, hydroxycarbazole (**89**) was formed, whereas when thermolysis was carried out in methanol, the pyridinium salt (**90**) was obtained (Scheme 13).[44,57] The former was hypothesized to proceed through a retro-DAR to initially give **40** followed by extrusion of pyridine to give the hemiacetal (**91**, note that in the corresponding scheme in reference 44, the authors mistakenly drew a structure with (C-14)–(C-15) reduced in the transformation from **20** to **40**).[44,57] Loss of methanol to form the carbonyl (**92**), which likely exists in equilibrium with the enol form, could go on to generate aromaticity via a proton transfer step. On the other hand, the protic methanol solvent seemed to trap the dehydrosecodine intermediate as the pyridinium salt **90**.[44,57] Lastly, when deuterated methanol was employed, the ^{1}H NMR spectrum no longer displayed a signal corresponding to R═H, and the CH_3 doublet was replaced by a singlet.[44] Collectively, these model chemical experiments demonstrate that the reactivity of these compounds is highly dependent on the specific reaction conditions. Furthermore, the above results only provided indirect evidence for the crucial role of **40** in the biosynthesis; however, the sensitivity of dehydrosecodine-like species may defy any attempt at isolation and characterization (Scheme 14).

2.24.2.3 Using Chemistry to Connect the Enzymatic Dots

2.24.2.3.1 Strictosidine-preakuammicine biosynthesis

The starting point for the majority of MIA pathways is strictosidine (**1**) deglycosylation. This enzyme, strictosidine glucosidase (*SGD*), was first reported by Zenk et al. in 1980.[65] However, the enzymes responsible for subsequent transformations of the deglycosylated product, strictosidine aglycone (**93**), which may exist as the isomeric 4,21-dehydrogeissoschizine (**94**), were not discovered until 2017 by the groups of O'Connor and De Luca. Virus-induced gene silencing (VIGS) was successfully employed by both groups to elucidate enzymes within this pathway. Briefly, VIGS requires infection of the plant with a virus vector carrying host

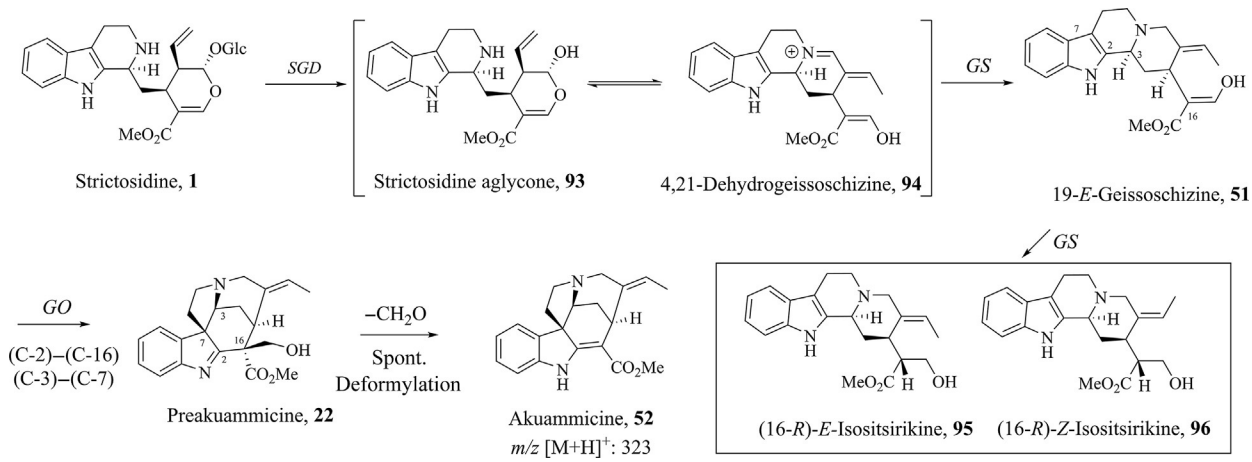

Scheme 15 O'Connor's identification of *GS* and *GO* for the conversion of dehydrogeissoschizine into akuammicine.[50] *SGD*, strictosidine glucosidase; *GS*, geissoschizine synthase; *GO*, geissoschizine oxidase.

gene sequences. The native plant's antiviral defense is exploited to transiently silence the expression of the gene of interest.[50] By comparing the metabolic profiles of the empty vector- and gene-silenced-plants, using targeted and untargeted mass spectrometry, the enzyme's role as well as its substrate(s) and/or product(s) may be simultaneously deduced.[50] Thus, geissoschizine synthase (*GS*, a medium chain alcohol dehydrogenase) and geissoschizine oxidase (*GO*, a cytochrome P450, *CYP71*), enzymes responsible for the formation of geissoschizine (**51**) from **93**, and its conversion into preakuammicine (**22**, Scheme 15), were identified by O'Connor, Courdavault et al.[50]

Notably, O'Connor et al. never observed the formation of **51** when the enzyme encoded by *GS* was purified from *Escherichia coli* and incubated with *SGD* and **1**;[50] only the over-reduced products (16-*R*)-*E*- and (16-*R*)-*Z*-isositsirikine (**95** and **96**, respectively) were observed.[50] Importantly, Courdavault's group noted that when they silenced the gene encoding *GO*, accumulation of a compound with *m/z* identical to that of **95** was observed.[50] This was a key observation that led to the hypothesis that the enzymatic reactions of *GS* and *GO* are linked. The authors hypothesized that *GS* initially reduces **94**–**51**, which, in the absence of the appropriate downstream enzyme (*GO*), *GS* could over-reduce **51** to the more stable isositsirikine isomers.[50] Surprisingly, when **1** was assayed with *SGD*, *GS*, and *GO*, the expected product **22** was not observed, although a decrease for both isomers of isositsirikine was detected. Instead, a compound with an *m/z* of 323, later revealed to be **52** by NMR analysis, was formed.[50] It is well-known that **22** can nonenzymatically deformylate to give **52**. Although the authors were not able to isolate and characterize the enzymatic products of *GS* and *GO*, detection of equimolar concentrations of **52** and formaldehyde, as well as colocalization of *GS*, *GO*, and related enzymes in the pathway in the leaf epidermis, provided key evidence for the roles of *GS* and *GO* in preakuammicine biosynthesis.[50]

Poupon et al. had first provided mechanistic speculations for the generation of the akuammicine scaffold from **51**,[51] which formed the basis for O'Connor and coworkers' proposal. Geissoschizine (**51**) was suggested to undergo an oxidative coupling to form rhazimal (**97**, Scheme 16).[50] Rhazimal (**97**), or its C-17 reduced derivative rhazimol (**98**), could rearrange to give either 16-*R*-dehydropreakuammicine (**99**), or preakuammicine (**22**), respectively.[50] The well-known nonenzymatic deformylation of **22** to give **52** accounts for the presence of this akuammilan-type alkaloid in plants.[50] In the context of their biosynthesis, O'Connor proposed that a reductase (*GS*) converts **94** into **51**.[50] The latter is then transformed into **97** by an oxidase (*GO*), which can rearrange to form **99**, and subsequently be reduced to **22**.[50] An analogous pathway could be envisaged whereby **97** is first reduced to give **98**, which then rearranges straightforwardly to preakuammicine.[50]

2.24.2.3.2 Preakuammicine-stemmadenine acetate biosynthesis

An independent study by De Luca et al. corroborated the roles of *GS* and *GO*; a year later an additional five enzymes leading to the biosynthesis of stemmadenine acetate (**56**) were also reported.[52] Notably, and unlike O'Connor's experience with *GS*, De Luca and coworkers were able to obtain and characterize **51** from enzyme assays with *GS* alone, or when the gene encoding *GO* was silenced by VIGS.[52] The next enzyme after *GS* and *GO* was a medium chain alcohol dehydrogenase named *Redox1*. Silencing of *Redox1* resulted in a decrease of **20** and vindoline (**23**) in *C. roseus* leaves, and an accumulation of **52** as well as a short-lived intermediate with an *m/z* of 369, which underwent spontaneous conversion to **52** (Scheme 17).[53] Interestingly, enzyme assay of **51** with *GO* microsomes and NADPH yielded the same products as those observed in VIGS-*Redox1* plants.[52] This suggests that the activities of these enzymes are coupled in the vinblastine pathway.

The authors hypothesized that the *m/z* increase of 16 relative to **51** (*m/z* 353) could mean that this intermediate is an oxidized product of *GO*.[52] This led De Luca et al. to propose a reaction sequence outlined in Scheme 17 to rationalize the presence of *m/z* 369 and **52**. While Schemes 16 and 17 both require initial oxidation of **51** to generate an indolenine/indoleninium motif, and the required (C-7)–(C-3) bond formation is, in part, mediated by the remote enol which overall results in the formation of the

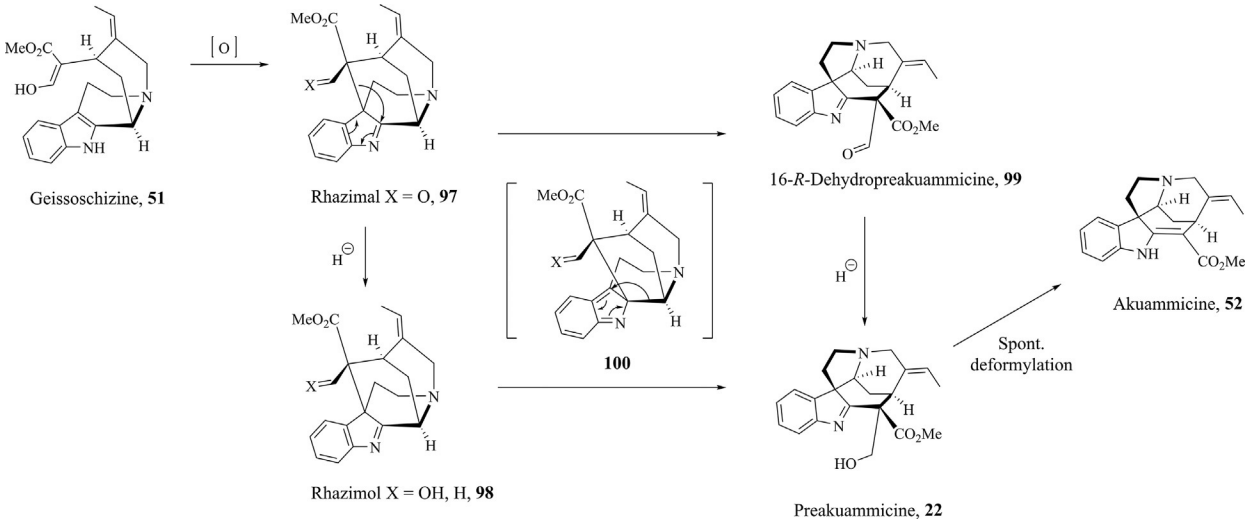

Scheme 16 Proposed mechanism for the formation of **52** from **51**.[50]

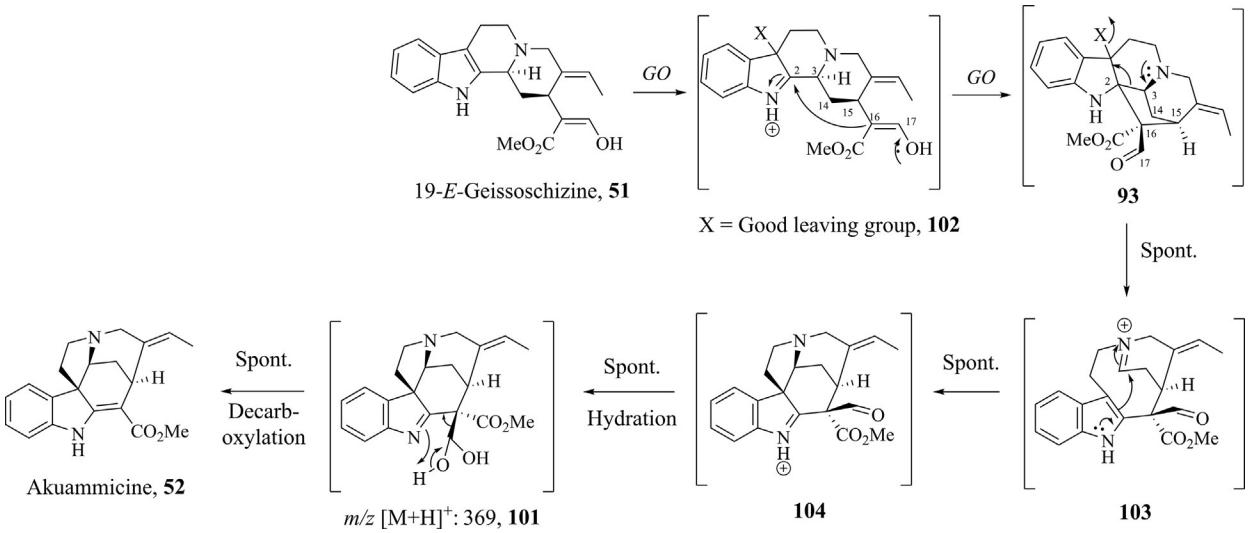

Scheme 17 De Luca's proposal to rationalize the formation of **52** from **51** via intermediate **101** (*m/z* 369).[52] *GO*, geissoschizine oxidase.

by-product **52**, it remains unclear how the important Corynanthe/Strychnos scaffold of **22** is generated. In fact, the latter proposal obviates the commonly reported vinblastine intermediate **22** entirely, choosing instead to lose formic acid from a C-17 hydrate derivative of preakuammicine (**101**, *m/z* 369). However, it must be noted that only Scott has ever reported the isolation of the reactive **22** intermediate,[46,47] a claim which has been challenged by Poupon et al.,[51] and indeed no complete characterization has been possible thus far. Hence, the exact mechanistic detail pertaining the transformation from **51** to **22**, or its derivative(s), requires further investigation. The propensity for **52** formation remains a problem to be addressed, which if successful, may enhance the yields of valuable downstream products.

The third gene discovered by VIGS in the De Luca study encodes another medium chain alcohol dehydrogenase named *Redox2*. When *Redox2* was suppressed, levels of **20** and **23** were lowered, whereas 16-*R*- and 16-*S*-deshydroxymethylstemmadenine (**105** and **106**, respectively, DHS) increased.[53] Furthermore, coupled assay with *GO* and *Redox1* converted **51** to both C-16 epimers of DHS. However, the loss of C-17 in DHS suggests that they may not be *Redox2* substrates to form **20** and **23** that would retain C-17. Instead, they are likely degradation products of unstable intermediate(s) (Scheme 18). This was confirmed when assays of both isomers of DHS with *Redox2* failed to give any new products.[52] Rewardingly, when *GO*, *Redox1*, and *Redox2* were assayed with **51**, stemmadenine (**21**) was recovered.[52]

Hydrolases *HL1* and *HL2* (annotated as isoflavonone dehydratases) were also subjected to VIGS. When *HL1* transcripts were reduced, **20** level decreased, whereas **23** level increased.[52] In contrast, when *HL2* was the silencing target, **23** declined, whereas **20**

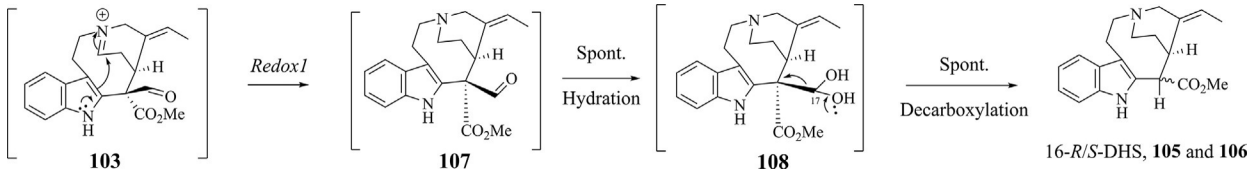

Scheme 18 De Luca's proposal for the formation of the by-products **105** and **106** by the coupled *GO*/*Redox1* assay with **51**.[52]

increased.[52] These results imply that **20** and **23** may be derived from the same precursor. Furthermore, the fate of this precursor would eventually diverge by the action of *HL1*, leading to **20**, or *HL2* to give **19** (and thereby **23** through the action of the enzymes in the well-established tabersonine-vindoline pathway, vide infra). Disappointingly, when yeast coexpressing *GO*, *Redox1*, *Redox2*, *HL1*, and *HL2* were administered with **51**, only **21** (stemmadenine) was obtained as the reaction product.[52] Thus, **21** cannot be the substrate for *HL1* and *HL2*, and it is likely that further modifications are required to convert **21** into a scaffold that can be utilized by *HL1* and *HL2* to form **20** and **19**, respectively.

When the assay was repeated with the above enzymes and crude *C. roseus* proteins, with and without acetyl CoA, only the reaction with acetyl CoA gave the desired compounds **19** and **20**.[52] This observation facilitated the identification of the next enzyme in this pathway, stemmadenine acetyltransferase (*SAT*), which catalyzes the acetylation of **21** to stemmadenine acetate (**56**).[52] When *GO*, *Redox1*, *Redox2*, and *SAT* were coexpressed in yeast, **56** accumulated. Curiously, silencing of the gene encoding *SAT* did not significantly alter the levels of **20** nor **23**, but low levels of **21**, the substrate of *SAT*, could be detected.[52] In contrast, **21** was absent in the negative empty vector control, which further supports the catalytic function of *SAT*. Last, the cofactor NADPH was reported to be a required component in the conversion of **56** into **19** and **20**, as enzyme assays of **56** and crude *C. roseus* protein extracts did not yield the pentacyclic products in the absence of NADPH.[52] When NADPH was present, **19** and trace quantity of **20** were formed. [52]

Although addition of *HL1* to the reaction mixture of substrate **51** and *GO*, *Redox1*, *Redox2*, *SAT*, and crude *C. roseus* proteins led to production of **20** at the expense of **19**, when *HL2* was added to the assay, the signal for **20** disappeared but no noticeable change to the amount of **19** could be detected.[52] Altogether, this led De Luca et al. to propose a pathway outlined in Scheme 19 to explain for the observations made when VIGS was performed on the above enzymes. Hypothesizing that the native *HL2* present in crude protein extracts may interfere with the outcomes of in vitro *HL2* assays, De Luca et al. circumvented this problem by employing crude leaf proteins from *Tabernaemontana litoralis*.[52] Although *T. litoralis* also produces **19**, when its protein extracts were assayed with **56**, NADPH and *HL2*, a 100% increase in **19** was observed relative to the negative control.[52] Furthermore, similar in vitro assays using *HL1* led to formation of **20**, and an 80% decrease in **19** relative to the negative control.[52]

Despite having to rely on crude leaf proteins, the requirement to add NADPH to the reaction mixture strongly suggested that a reduction is likely featured in the remaining steps in this pathway. It is clear that the above discoveries strongly reinforce the steps in Scott's dehydrosecodine hypothesis five decades ago, notably the importance of the acetoxy moiety that serves as both a protecting and leaving group to modulate the reactivity of the biosynthetic intermediates. Furthermore, it is reasonable to expect that aside from the missing reductase, an oxidase is also required. These redox enzymes could act in tandem to isomerize the exocyclic double bond to give a species prime for ring-opening with concomitant deacetoxylation and generation of **40**. The results of De Luca and coworkers along with Scott's proposal suggested that all that remained in the biosynthesis was the elucidation of the missing redox enzymes.

2.24.2.3.3 Stemmadenine acetate-tabersonine and catharanthine biosynthesis

Almost simultaneously, O'Connor et al. published a report which not only confirmed the roles of *HL1* and *HL2*, but also validated Scott's dehydrosecodine hypothesis.[66] Consistent with De Luca's report, VIGS treatment of the α/β hydrolases *HL1* (or catharanthine synthase, *CS*) and *HL2* (or tabersonine synthase, *TS*) led to substantial reduction of **20** and **19**, respectively.[66] Although enzyme-assay guided fractionation to isolate the substrate of *CS*/*TS* yielded fractions which were active for both enzymes, the rapid decomposition of this compound did not permit its structural characterization.[66] The product mixture instead contained tubotaiwine (**111**), presumably a degradation product of the substrate, as the major component.[66] Despite not being able to definitively ascertain the identity of the substrate of *CS*/*TS*, the fact that it decomposed into **111**, the reduced derivative of condylocarpine (**54**), led the authors to propose that dihydroprecondylocarpine (**112** or its acetate **74**) is the actual substrate for the hydrolases (the substrate was informally named "angry-line" by Caputi, given the propensity of this compound to degrade).[66] A mechanism analogous to the deformylation of **22** or **53** to give **52** and **54**, respectively, (cf. Schemes 7 and 20) could likely explain for the formation of **111**.

Taking inspiration from Scott and coworkers, the O'Connor group speculated that **112** (or **74**) could arise from an oxidation-reduction cascade from **21** (or **56**) to ultimately isomerize the double bond to the required (C-20)–(C-21) position.[66] A gene encoding reticuline oxidase, a class of enzymes capable of oxidizing an N–C bond, had a similar expression pattern to *TS* and was thus selected for VIGS studies.[66] When this enzyme was suppressed, **56** accumulated.[66] When this gene was expressed in *Nicotiana benthamiana*, *Pichia pastoris*, and Sf9 insect cells, **56** was converted into **72**, thus this enzyme was named precondylocarpine acetate synthase (*PAS*).[66] Furthermore, *PAS* failed to oxidize **21**, suggesting that the acetyl motif is vital for enzymatic recognition.[66]

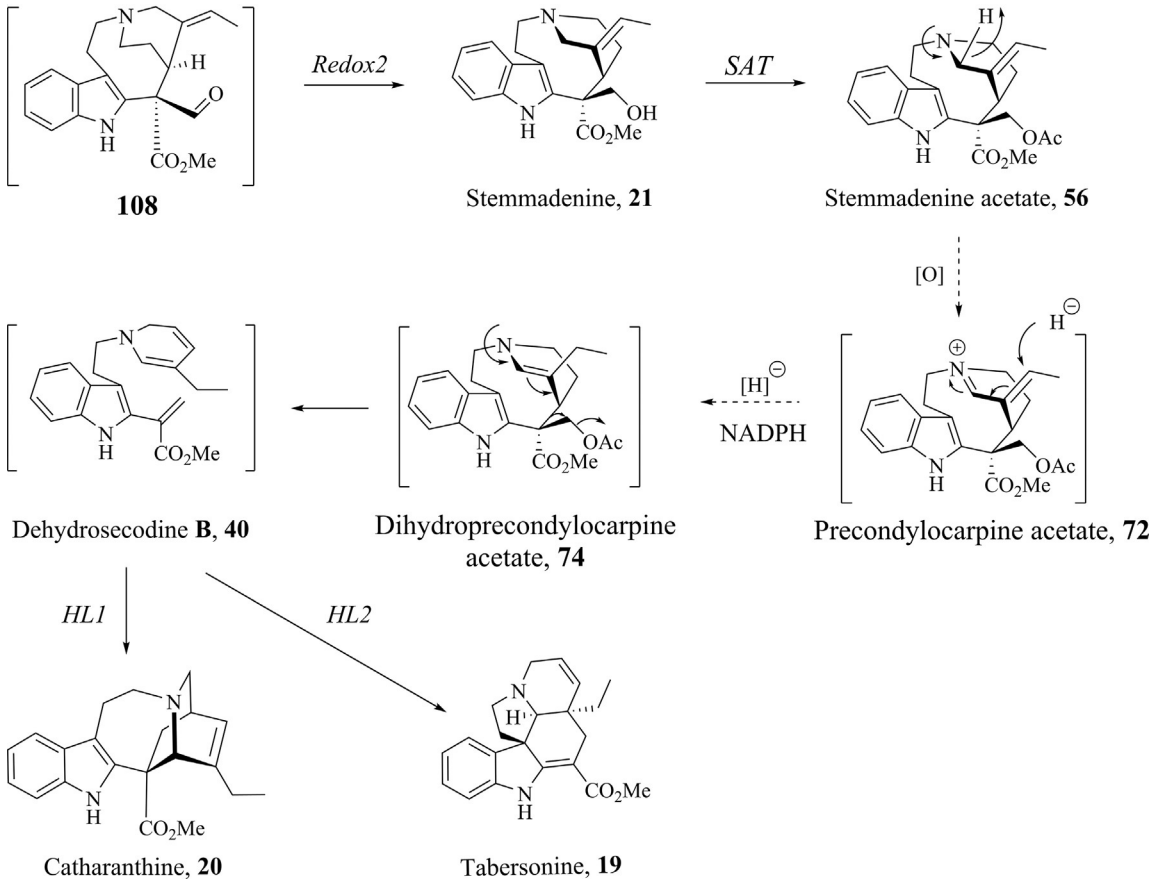

Scheme 19 De Luca's proposal for the formation of **19** and **20** via **40**. *Dashed arrows* denote transformations catalyzed by enzymes yet undetermined.[52] *SAT*, stemmadenine acetyltransferase; *HL1* and *HL2*, alpha/beta hydrolases.

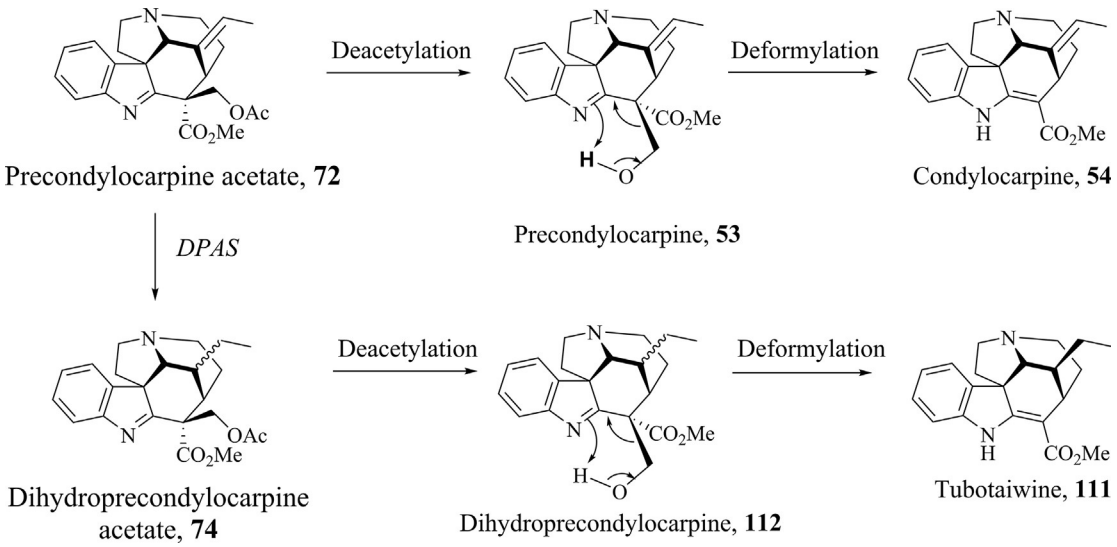

Scheme 20 Proposed mechanism to rationalize the formation of **111** from the proposed *CS*/*TS* substrate, dihydroprecondylocarpine acetate (**74**). *DPAS*, dihydroprecondylocarpine synthase; *CS*, catharanthine synthase; *TS*, tabersonine synthase.

Chemical oxidation of **21** formed the dead-end product **54** by deformylation from **53**; this implies that the acetyl functional group has a vital protecting role to prevent or slow deformylation.[66]

Silencing of a medium chain alcohol dehydrogenase resulted in accumulation of a compound with identical mass, retention time, and fragmentation pattern to **72**, thus this dehydrogenase was renamed dihydroprecondylocarpine acetate synthase (*DPAS*).[66] When *PAS*, *DPAS*, and *CS* or *TS* were transiently coexpressed in *N. benthamiana* in the presence of **56**, catharanthine (**20**, *PAS*/*DPAS*/*CS*), and tabersonine (**19**, *PAS*/*DPAS*/*TS*) were formed.[66] When semisynthetic **72**, prepared from stemmadenine acetate (**56**), was reacted with *DPAS* and *CS* or *TS*, **20** and **19** were formed, respectively.[66] Additionally, crude semisynthetic **74** was reacted with *CS* and *TS* to yield **20** and **19**, respectively.[66] Furthermore, this dihydroprecondylocarpine acetate (**74**) standard was also observed to deformylate to give **111**.[66] Altogether, the discoveries by O'Connor et al. not only consolidated Scott's hypothesis, but also formally completed the biosynthesis of **23** (the tabersonine derivative, vindoline) and **20**. These compounds **23** and **20** can be semisynthetically coupled to give the anticancer drug **17** (see "Chemical Synthesis of Anhydrovinblastine and Its Oxidation to Vinblastine" section).

It is still not clear at this stage whether the hydrolase enzymes *CS* and *TS* catalyze both the desacetoxylation of **74** and subsequent cyclization. It may be possible that desacetoxylation of dehydrosecodine **40** from **74** is spontaneous, and *CS*/*TS* only serve to orientate the diene/dienophile components into appropriate conformations for cyclization. Additionally, due to the reactivity of **40** and **74**, these compounds have not yet been isolated and structurally characterized. Moreover, two obvious questions arise from the discovery of *PAS*, *DPAS*, and *CS*, and *TS*. (1) Would a reversal of the redox steps, that is, reduction (*DPAS*) before oxidation (*PAS*) alter the fate of the cyclized products to give either pseudotabersonine (**43**) and/or allocatharanthine (**57**), analogous to the results from Scott's experiments long ago? (2) And if yes, would the same enzymes be capable of acting on these substrates? Or are there additional redox and hydrolase enzymes to be discovered? Nevertheless, the bio-chemical studies in recent years have confirmed many of the theories proposed in the 1960s and 1970s, and given credence to Scott's dehydrosecodine. Above all, the story of catharanthine (**20**) and tabersonine (**19**) illustrates how chemistry and biology must be effectively combined to reveal the intricate networks of natural product biosynthesis.

2.24.2.4 Tabersonine–Vindoline Biosynthesis

The elaboration of **20** into vindoline (**23**), one half of the dimeric vinblastine (**17**) and vincristine (**18**), was fully characterized over the last several years (Scheme 21). The seven-step biosynthetic sequence starts with regiospecific hydroxylation of **19** at the C-16 position by a cytochrome P450 monooxygenase (tabersonine 16-hydroxylase, *T16H*).[68] This hydroxylation step could be catalyzed by two distinct isoforms of *T16H*. The first, *T16H1*, was first cloned from cell suspension cultures in 1999 by Schröder et al.[69] However, among all tested *C. roseus* organs, young leaves possessed the highest activity of *T16H*, and its expression correlates well with **23** accumulation.[70] In contrast, *C. roseus* cell cultures are not able to produce **23**, despite displaying high levels of *T16H* activity.[68] Moreover, the expression profile of the gene encoding *T16H1* did not follow those of other vindoline biosynthetic genes.[68] These discrepancies prompted Courdavault et al. to clone *T16H* using *Catharanthus roesus* leaves, which led to the identification of *T16H2*.

Both enzymes were expressed separately in *Saccharomyces cerevisiae* and both successfully hydroxylated **19** at the C-16 position.[68] Further proof for the role of *T16H2* in vindoline biosynthesis was demonstrated when the corresponding gene was silenced. This resulted in a marked decrease of **23**, along with known vindoline pathway intermediates (16-hydroxytabersonine [**113**],

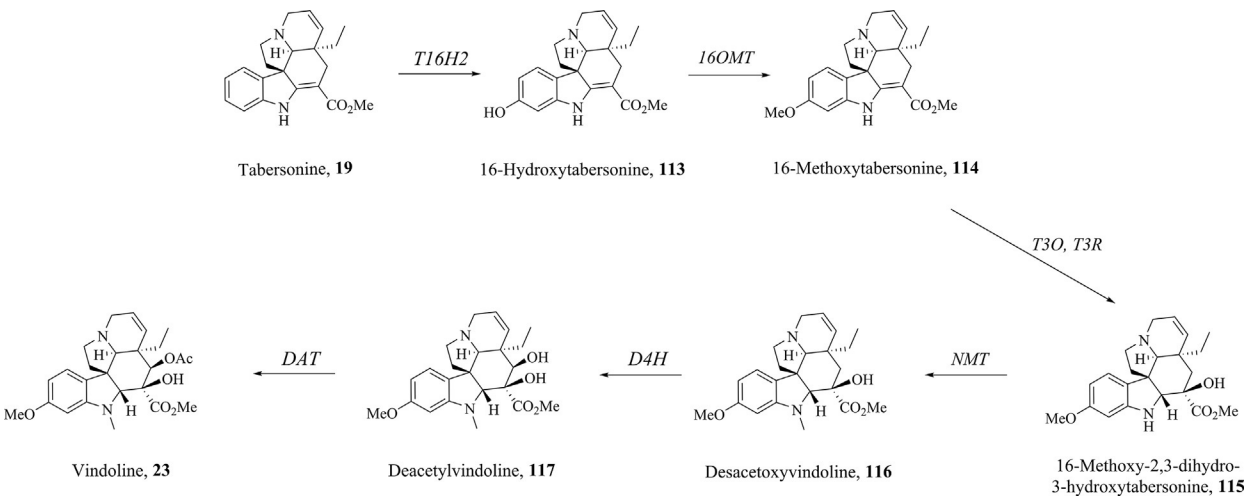

Scheme 21 The 7-step biosynthesis of **23** from **19** and the corresponding enzymes.[67] *T16H2*, tabersonine 16-hydroxylase 2; *16OMT*, tabersonine 16-*O*-methyltransferase; *16T3O*, 16-methoxytabersonine 3-oxygenase; *T3R*, tabersonine 3-reductase; *NMT*, *N*-methyltransferase; *D4H*, desacetoxyvindoline-4-hydroxylase; *DAT*, deacetylvindoline-4-*O*-acetyltransferase.

desacetoxyvindoline [**116**], and deacetylvindoline [**117**]).[68] Transcripts of the gene encoding *T16H1* were minimal in young leaves, but are instead localized to *C. roseus* flowers.[68] Floral biosynthesis of **23** is only 6% relative to that in leaves, and only low expression levels of other vindoline biosynthetic genes were recorded.[68] In contrast, expression of the gene responsible for *T16H2* production was very low in flowers, but high in leaves (particularly in young leaves), where the highest *T16H* activity was recorded.[70] These results suggest that *T16H2*, rather than its isoform *T16H1*, is the dedicated 16-hydroxylase in vindoline biosynthesis in *C. roseus* leaves.

16-hydroxytabersonine (**113**) is subsequently methylated by the enzyme 16-hydroxytabersonine-16-*O*-methyltransferase (*16OMT*), which was identified by De Luca and coworkers from a transcriptome derived from *C. roseus* leaf epidermal cells. *E. coli* expressing *16OMT* produced 16-methoxytabersonine (**114**) when fed with **113**.[71] This enzyme was reported to be highly substrate-specific, as it failed to methylate other MIAs, flavonoids, and aromatic substrates in in vitro assays.[71] Notably, **19**, and tabersonine derivatives such as 2,3-dihydro-3-hydroxytabersonine (**118**), lochnericine (**119**), and hörhammericine (**120**), and their corresponding C-16 hydroxylated analogs (**121–123**) were not accepted by *16OMT* (Fig. 3, not all tested compounds shown).[71] The authors emphasized that the inability of *16OMT* to methylate **118** supported the proposed biosynthetic order in Scheme 21, thus this reaction must occur prior to C-3 hydroxylation.[71]

Although the enzymes catalyzing the subsequent hydroxylation and reduction at the C-2 and C-3 positions of **114** are known, the instability of the intermediates involved hinders our complete understanding of the underlying mechanism. From the literature,[72–75] it was hypothesized that hydroxylation at the C-3 position could involve initial epoxidation at the (C-2)–(C-3) double bond to give **124**. A spontaneous opening of the epoxide could then be mediated by the electron lone pair on the indole nitrogen follows to give a β-hydroxyindolenine (**125**). Reduction of **125** should give the desired vindoline pathway intermediate: 16-methoxy-2,3-dihydro-3-hydroxytabersonine (**115**, Scheme 22). Thus, Courdavault, O'Connor and coworkers hypothesized that the biosynthetic pathway likely involved an oxidase to form the intermediate epoxide/indolenine, and a reductase to reduce the imine double bond.[76]

Initial screening of an RNA-seq dataset for cytochrome P450 genes with similar expression profiles to known MIA genes and/or increased expression in response to the elicitor methyl jasmonate yielded five potential candidates.[76] VIGS silencing of these genes in *C. roseus* showed that downregulation of one of these genes led to a marked decrease in levels of **23**; in addition, a compound with identical *m/z* and retention time to **114**, the proposed substrate for this oxidase, accumulated in the silenced tissue compared to the negative control.[76] The corresponding enzyme was thus named 16-methoxytabersonine-3-oxidase (*16T3O*).[76] However, large scale in vivo assay of a yeast strain harboring *16T3O* and *C. roseus* cytochrome P450 reductase (*CPR*, enzyme enabling proper functioning of P450 enzymes) with **114** and subsequent NMR characterization of the product revealed that this compound was in

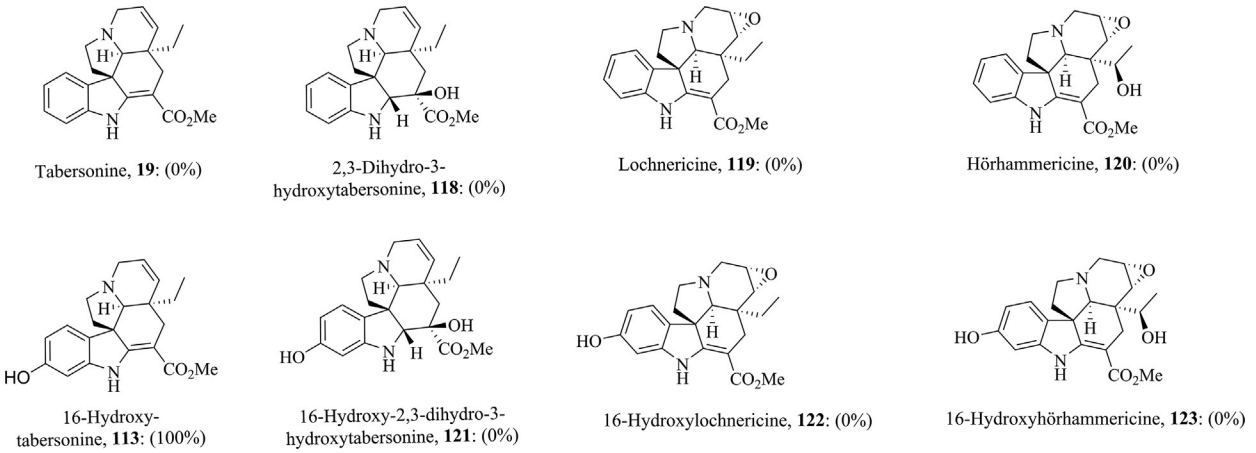

Fig. 3 Selection of compounds assayed with *16OMT* illustrating its high substrate specificity (100% = specific activity).[71]

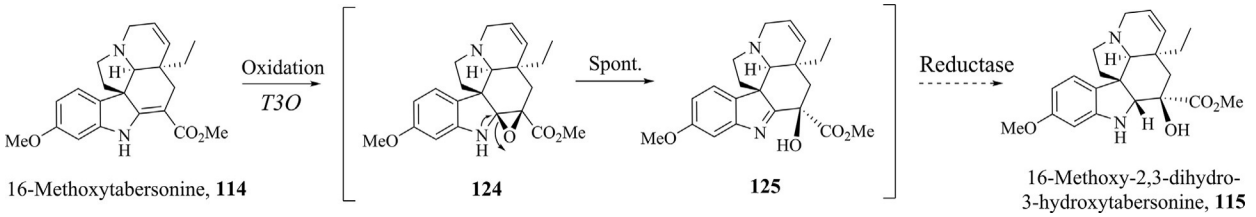

Scheme 22 Courdavault and O'Connor's proposed biosynthetic two-step conversion of **114–115**.[76] *16T30*, 16-methoxytabersonine 3-oxygenase.

fact not the expected **124** or **125**, but a derivative of vincamine which formed via an extensive rearrangement process after initial oxidation.[76] As hydroxyindolenine analogs of **19** had been proposed to undergo such rearrangements in the presence of acid to give vincamine scaffolds,[48,77–79] the authors concluded that *16T3O* catalyzes initial epoxidation of **114**, which, in the absence of the downstream reductase enzyme, could readily rearrange to give vincamine-related alkaloids.[76] This observation provides further evidence for a biosynthetic link between the structurally distinct vindoline and vincamine.

Although a previous report had suggested that *N*-methyltransferase (*NMT*), a downstream enzyme involved in the vindoline pathway, was localized in the leaf mesophyll cells,[80] reverse transcription quantitative PCR (RT-qPCR) analyses showed that *NMT* expression is three times higher in the leaf epidermis than in whole leaf tissues, consistent with the localization of upstream enzymes *T16H2* and *16OMT* in the leaf epidermis.[67] Based on this evidence, De Luca et al. inferred that the enzymes immediately preceding *NMT*, namely the aforementioned oxidase and reductase, might also be localized in the leaf epidermis.[67] Screening an EST database enriched in *C. roseus* transcripts for "hydratase" enzymes revealed two potential candidates: a cytochrome P450 and an alcohol dehydrogenase-type gene.[67] Suppression of the P450 gene led to analogous results with those reported by Courdavault and O'Connor for their *16T3O*, thus solidifying the role of this enzyme in the vindoline pathway.[67] On the other hand, silencing of the alcohol dehydrogenase did not lead to a decrease in the levels of **23**, but desacetoxyvindoline (**116**), a downstream product in the vindoline pathway, was reduced by 69%.[67] This reduction was accompanied by accumulation of three isomeric MIAs (*m/z* 383).[67]

Importantly, when yeast containing *16T3O* was assayed with NADPH, oxygen and *CPR* and **114** (*m/z* 367), 16-hydroxytabersonine (**113**, *m/z* 353), or tabersonine (**19**, *m/z* 337), three isomeric alkaloids resulted in each case, and structures were proposed for these compounds (Scheme 23).[67] Unexpectedly, when recombinant *ADHL1* was assayed with the MIAs assigned as **124**, **126** or **131**, **132**, no new products were obtained.[67] However, *ADHL1* assays with all isomeric products deriving from *16T3O* oxidation of **114** (MIAs assigned as **124**, **126,** and **127**), or tabersonine (MIAs assigned as **131–133**) yielded low levels of the respective 2,3-dihydro-3-hydroxylated products (16-methoxy-2,3-dihydro-3-hydroxytabersonine [**115**] and 2,3-dihydro-3-hydroxytabersonine [**118**]).[67] The production of these hydroxylated products was accompanied by reduction of the respective products from the *16T3O*-catalyzed oxidation of **114** and **19**. Thus this reductase was renamed tabersonine-3-reductase (*T3R*).[67] From these data, the authors concluded that the substrates for *T3R*, namely MIAs **127**, **130**, and **133**, are unstable intermediates, which, in the absence of *T3R*, may spontaneously be converted into diastereomeric epoxide mixtures unsuitable for *T3R* (Scheme 24).[67] De Luca et al. also proposed that initial oxidation of **19** (or its 16-substituted analogs) would yield a peroxide (**136**) which may exist in an equilibrium with the zwitterions **127**, **130**, or **133**, which could then be reduced by *T3R* to give the 2,3-dihydro-3-hydroxylated products.[67] However, in the absence of *T3R*, De Luca proposed that both the peroxide and the zwitterionic species could undergo spontaneous epoxide ring formation (Scheme 24).[67]

The exact mechanistic details pertaining to the C-3 hydroxylation of **19** and its derivative require further studies. Nevertheless, it is clear that the β-hydroxyindolenine **125** (drawn as a zwitterion [**133**] in Scheme 24) is the real substrate of *T3R*.

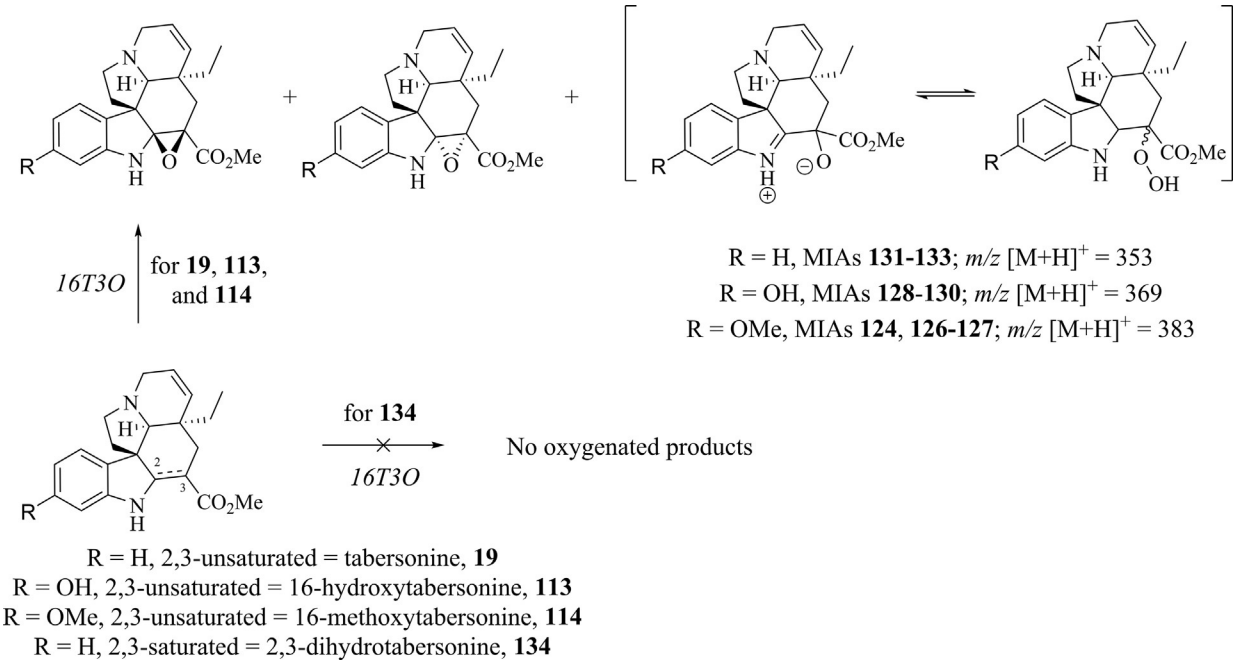

Scheme 23 Proposal for monooxygenation of **19**, **113**, and **114** by *16T30*. When **134** lacking the (C-2)–(C-3) double bond was assayed with *16T30*, no reaction occurred, illustrating the regiospecificity of this enzyme.[67] *16T30*, 16-methoxytabersonine 3-oxygenase.

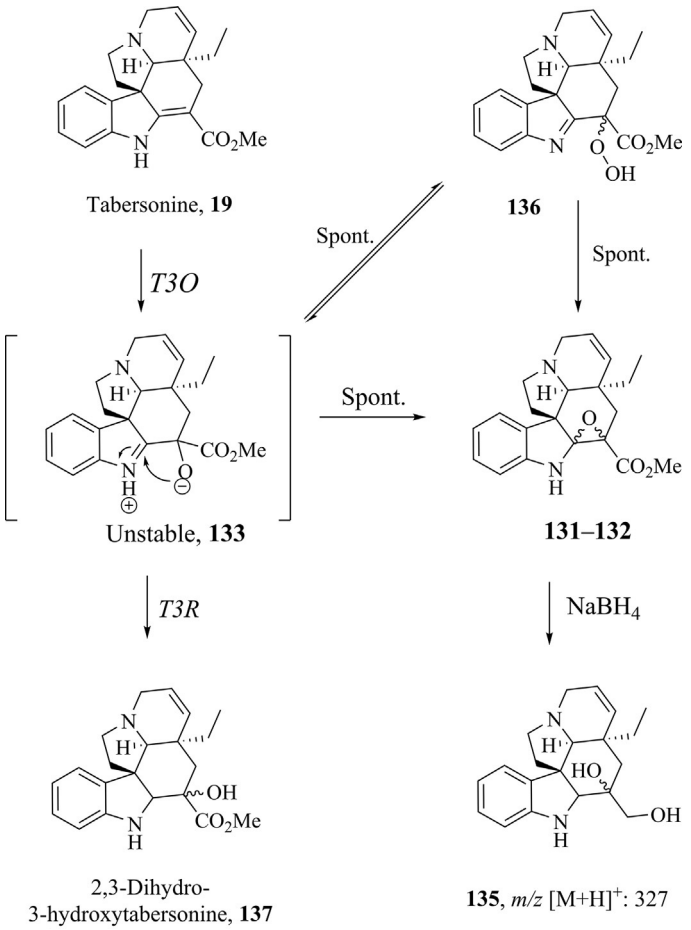

Scheme 24 Formation of the 2,3-dihydro-3-hydroxylated products require coupled action of *16T30* and *T3R*. Absence of *T3R* results in spontaneous formation of the diastereomeric epoxide products. Here, only compounds deriving from **19** are shown, but analogous processes could be envisaged for **113** and **114**.[67] *16T30*, 16-methoxytabersonine 3-oxygenase; *T3R*, tabersonine 3-reductase.

The next step in vindoline biosynthesis is methylation of the indole nitrogen by the enzyme *NMT*. It is well known that *NMT* activity is associated with thylakoid membranes of the chloroplast.[80–82] In addition, vindoline production primarily occurs in leaf tissues. Altogether, this information was exploited by Liscombe, O'Connor et al. to generate a list of potential methyltransferase candidates that may be involved in the vindoline pathway.[83] Known plant *NMT* sequences were used as queries and compared against a *C. roseus* EST library using tBLASTn.[83] This yielded an initial list which was then manually censored by removing methyltransferases with known function.[83] From this master list, three candidate proteins were purified and used for enzymatic assays.[83] Since it has been reported that *NMT* is only active against tabersonine-derived substrates where the (C-2)–(C-3) double bond is reduced,[80,82] the candidate enzymes were assayed with the model substrate 2,3-dihydrotabersonine (**134**), as this compound could be easily accessed by borohydride reduction of commercially available **19**.[83]

Of the three enzymes, only one was able to methylate **134** in the presence of the methyl group donor *S*-adenosyl-L-methionine (SAM).[83] The product of this enzymatic reaction coeluted with a synthetic standard of *N*-methyl 2,3-dihydrotabersonine (**138**) on LC-MS.[83] Of note is the failure of *NMT* to methylate **19** that still retains the double bond at (C-2)–(C-3).[80,83] A previous report by De Luca et al. confirmed this finding and further illustrated the substrate specificity of this enzyme.[80] No methylation occurred when the tabersonine derivatives lacked the (C-6)–(C-7) double bond (2,3-dihydro-3-hydroxyvincadifformine, [**139**], Fig. 4, not all tested compounds shown).[80] Likewise, when 4-acetoxylated (**140**) or 4-hydroxylated (**141**) was assayed with this *NMT*, the corresponding *N*-methylated products were not observed.[80] The best conversion was obtained for 2,3-dihydro-3-hydroxytabersonine (**137**),[80] suggesting that the hydroxyl group at C-3 also allows substrate recognition by *NMT*. These evidence support the sequence of events in Scheme 21, namely methoxylation and reduction of the (C-2)–(C-3) double bond must precede *N*-methylation, whereas C-4 acetoxylation is a downstream event. O'Connor et al. proposed that the absence of the double bond at this critical position would break conjugation with the ester functional group, making the indole nitrogen more electron rich, and therefore more susceptible to methylation.[83]

To definitively prove the role of *NMT* in the vindoline pathway, the proposed substrate, 16-methoxy-2,3-dihydro-3-hydroxytabersonine (**115**), would need to be assayed with this enzyme. However, access to this compound via chemical

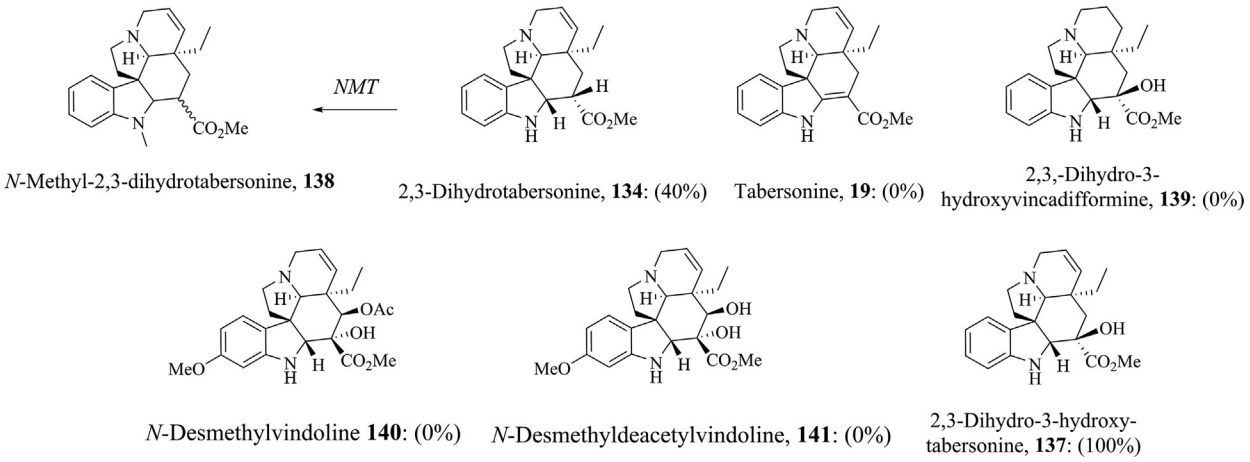

Fig. 4 Selection of compounds tested with *NMT*. Percent yields are relative to that of **137**.[80] *NMT* = *N*-methyltransferase.

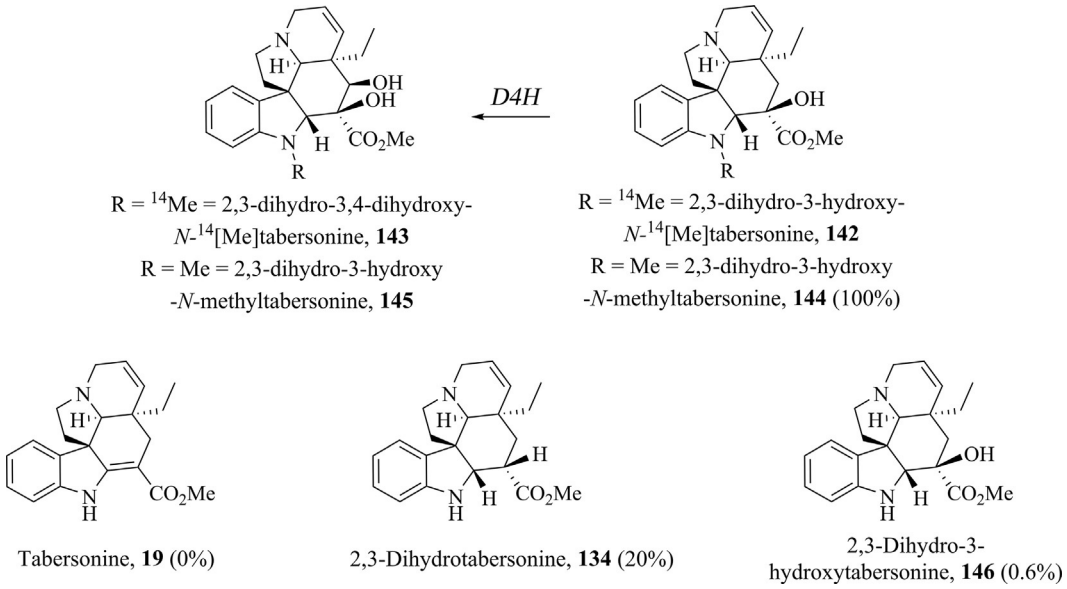

Fig. 5 Various compounds tested with *D4H*. Percent yields are relative to that of **144**.[84] *D4H* = desacetoxyvindoline-4-hydroxylase.

synthesis would be laborious, and isolation from plants would give insufficient quantities for characterization.[83] However, it was determined that crude *C. roseus* seedling extracts contained a compound with identical mass to the proposed substrate.[83] Indeed, assay of these extracts with *NMT* in the presence of SAM cofactor led to consumption of the starting material and formation of a new signal with an *m/z* ratio corresponding to addition of a methyl group, as observed by LC-MS.[83] Last, when the MIA inducer methyl jasmonate was used to up-regulate vindoline biosynthetic gene expression, it was found that all vindoline pathway genes, including the proposed *NMT*, were up-regulated relative to the controls.[83] Taken together, these evidence strongly solidify this methyltransferase as the *NMT* in the vindoline pathway in planta.

The penultimate step in the vindoline pathway is a hydroxylation at the C-4 position catalyzed by the nonheme iron dioxygenase desacetoxyvindoline-4-hydroxylase (*D4H*). The presence of the cofactor 2-oxoglutarate was reported to be essential for hydroxylase activity, as only assays containing 2-oxoglutarate converted 2,3-dihydro-3-hydroxy-*N*-[$^{14}CH_3$]tabersonine (**142**) to the 4-hydroxylated product (**143**).[84] In contrast, the cofactor ascorbic acid enhances the reaction but is not a required component, while removal of oxygen completely abolished product formation.[84] Fe^{II} ions also appeared to improve *D4H* activity, as *D4H* activity rapidly diminished after chromatographic purification; addition of Fe^{II} was able to reactivate the enzyme after short periods of incubation at 4°C.[85]

When *D4H* was heterologously expressed in *E. coli*, enzyme assays successfully converted alkaloid substrate (not specified) into the hydroxylated product.[86] When *D4H* was assayed with the proposed substrate, desacetoxyvindoline (**116**), the 4-hydroxylated derivative (**117**) was obtained.[86] Like other vindoline pathway enzymes, *D4H* also exhibited remarkable substrate specificity, and only hydroxylates at the C-4 position (Fig. 5).[84] Notably, *N*-methylation (**144** vs. **146**) and C-3 hydroxylation (**144** vs. **134**)

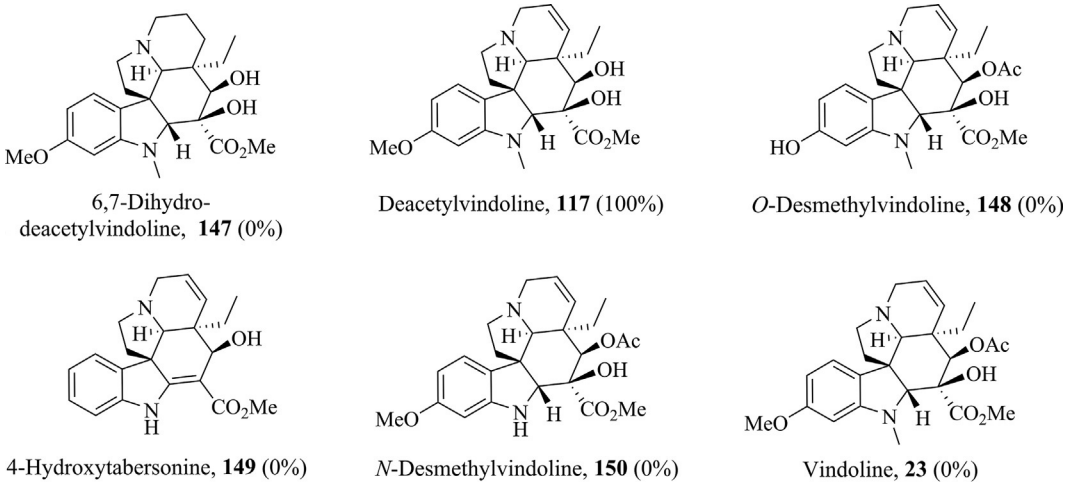

Fig. 6 Various compounds tested with *DAT*. Percent yields are relative to that of **117**.[87,88] *DAT* = deacetylvindoline-4-*O*-acetyltransferase.

appeared to be absolutely crucial for reaction efficiency, whereas the presence of a methoxy group at C-16 appeared to have no effect in this regard.[84]

The last enzyme in vindoline biosynthesis is deacetylvindoline-*O*-acetyltransferase (*DAT*) and was independently discovered by De Luca and Stöckigt in 1985.[87,88] In the presence of acetyl CoA, *DAT* completely converted **117** into **23**, whereas no product was observed in the absence of either *DAT* or the acetyl group donor.[87,88] The reversible nature of this reaction was also demonstrated when assay of *DAT*, CoA and the **23** yielded **117**; once again, no reaction took place when either the aceyltransferase or the coenzyme was absent.[87,88] This enzyme also exhibits high substrate specificity, particularly for the double bond at (C-6)–(C-7) (**117** vs. **147**, Fig. 6).[87] Additionally, all posttabersonine modifications appeared to contribute to enzyme-substrate recognition, as any tabersonine derivative lacking any of these modifications decreased *DAT*'s activity.[88] Importantly, the acetylation reaction is chemospecific, as no acetylation takes place on the hydroxyl group at C-3, even when OH at C-5 is already acetylated (**148**), or C-4 (**149**).[88] The substrate specificity of *DAT* strongly supports that acetylation of **117** is the last step in vindoline biosynthesis.[87,88]

The discovery of the reductase *T3R*, an alcohol dehydrogenase responsible for the formation of 16-methoxy-2,3-dihydro-3-hydroxytabersonine, by De Luca et al. in 2015 formally completed the tabersonine-vindoline pathway.[67] With the identities of all vindoline biosynthetic genes in hand, they were able to reconstitute the entire pathway in yeast.[67] When yeast containing all seven vindoline pathway genes was fed with starting tabersonine substrate (**19**), the expected product **23** along with other pathway intermediates was formed.[67] Over 95% of the assay products were secreted to the growth medium, which could then be recovered by ethyl acetate extraction, making the yeast system a promising route toward commercial production of **23** and vindoline-derived compounds.[67]

2.24.2.5 Anhydrovinblastine Biosynthesis

Anhydrovinblastine (**151**), the dimeric alkaloid resulting from the coupling of catharanthine (**20**) and vindoline (**23**), has long been recognized to be the direct precursor of vinblastine (**17**). However, the realization of the precursory role of **151** was not straightforward. It is obvious that while the "bottom half" of **17** is the vindoline motif, the velbamine unit is slightly different to **20**. First, the bond connecting C-16 and C-21 is cleaved (Fig. 7A). Second, the double bond in the tetrahydropyridine ring is reduced, and a hydroxyl group is installed at (C-20) to create a new stereogenic center with *R* chirality. Last, the coupling occurs at C-16 of velbamine, and C-10′ of vindoline; importantly, the stereochemistry at C-16 is retained upon coupling (*S*). Nonetheless, due to the structural similarity between **20** and **23** to the top and bottom halves of **17**, these compounds, or their closely related derivatives, were suspected to constitute the monomers of **17**.

The first piece of evidence to indirectly support this hypothesis came in 1974 from Hutchinson et al. through feeding studies of labeled loganin (**13**), an early pathway precursor, and subsequent isolation of labeled **17**, **20**, and **23**.[89] However, early feeding studies of labeled **20** and **23** to intact *C. roseus* plants gave negligible incorporation into **17**.[90,91] Nonetheless, it was known that the metabolic turnover of **20** and **23** was faster in apical cuttings than in intact plants,[92] which led Hutchinson to reinvestigate earlier feeding experiments. When the labeled monomers were fed to apical cuttings, labeled **17** was observed.[91] While this datum supports the precursor role of **20**, it does not rule out the possible involvement of catharanthine derivatives such as cleavamine (**152**) and 15,20-dihydro-20-hydroxycatharanthine (**153**, Fig. 7B).

Early attempts to synthesize **17** yielded the unnatural compound that differs to **17** at the stereochemistry at C-16, which drastically reduces its antitumor activity.[93] Potier and Langlois were the first to successfully couple **20** and **23** to yield **151** via a Polonovski reaction (Fig. 7C, see also *2vi*).[94] Importantly, aside from the hydroxyl group at C-20, **151** resembles **17** in every

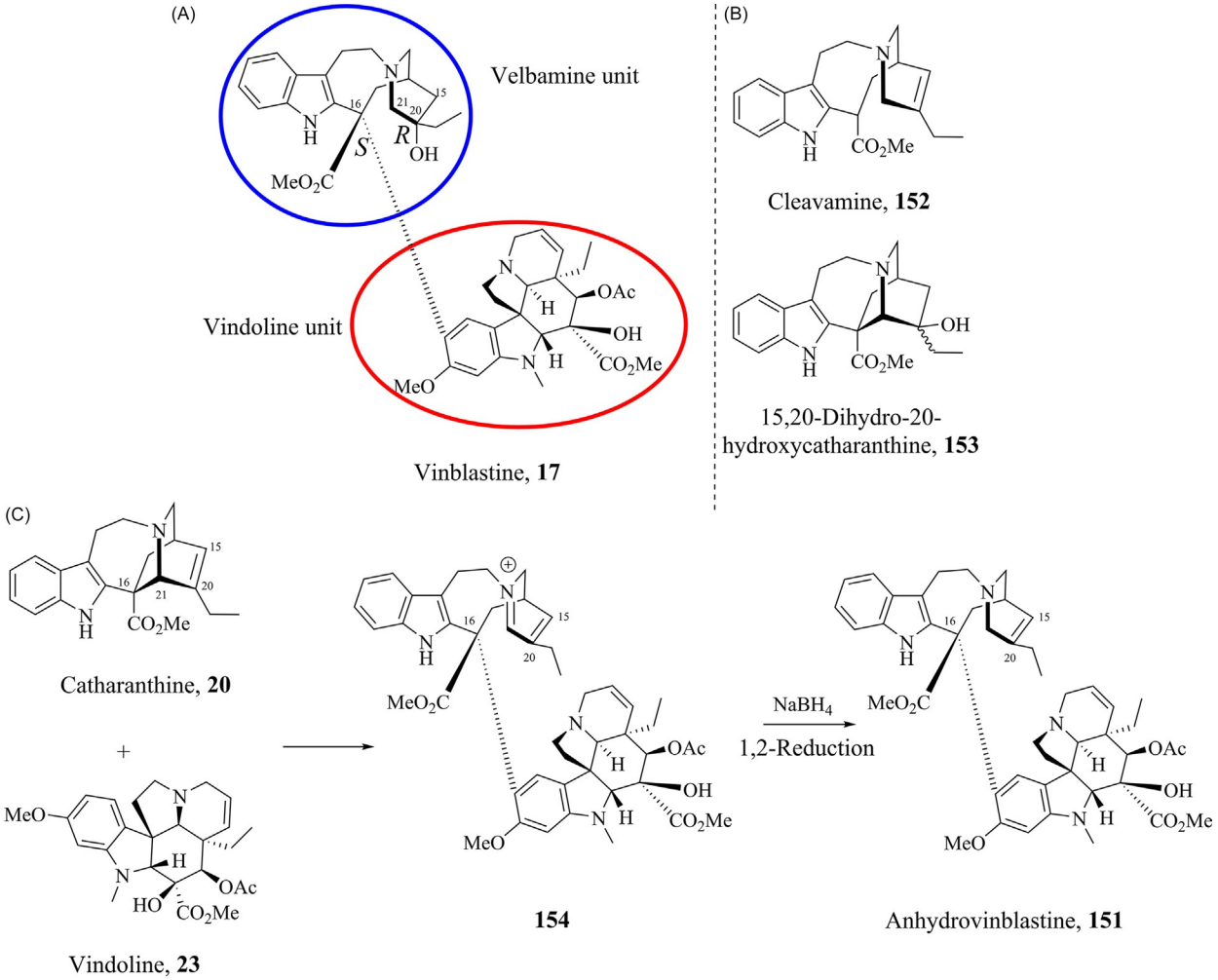

Fig. 7 (A) Structure of vinblastine with labeled velbamine and vindoline units; (B) other possible structures that may act as intermediates for the velbamine unit in the vinblastine pathway; (C) coupling of **20** and **23** to give **151** via the iminium **154**.

respect, including the orientation of the substituents at C-16 in the velbamine unit. An important breakthrough was made by Scott when he isolated labeled **151** when isotopically labeled **20** and **23** were fed to *C. roseus* plants; this was the first instance whereby anhydrovinblastine (**151**) had been isolated from plants and provided strong evidence for its role as a productive intermediate in the vinblastine pathway.[95]

However, in the same report, Scott also noted that administration of labeled **151** to *C. roseus* did not yield the correspondingly-labeled **17**, although he proposed that this might have been due to the instability of **151** or the compartmentalization of vinblastine biosynthetic enzymes.[95] In an ensuing communication, Scott successfully circumvented this problem by administering labeled **151** to cell-free extracts of *C. roseus*, from which labeled **17** was recovered.[96] When an analogous experiment with boiled enzyme was performed, a lowered, but still significant incorporation of **151** into **17** was observed. However, controlled experiments without enzymes failed to give any **17**.[96] This confirms that the conversion from **151** into **17** does not occur spontaneously, and also suggests the enzyme(s) responsible for this transformation is somewhat stable with respect to thermal elevation.[96] Other studies by Scott as well as the groups of Misawa and Kutney to further optimize the coupling and the transformation from **151** to **17** established the involvement of **20** and **151** in this pathway.[97–100]

Misawa et al. were the first to propose that a peroxidase enzyme was responsible for the coupling of **20**–**23** to give **151** in 1988.[101] This transformation was initially carried out using the commercially available horseradish peroxidase (*HRP*) in the presence of either flavin mononucleotide and manganese dichloride, or hydrogen peroxide as oxidants, and sodium borohydride as the reducing agent.[101] As expected, no **151** was detected in reactions with inactivated enzyme or without the enzyme, and yield of **151** was reduced significantly in boiled-enzyme experiments.[101] The omission of borohydride also failed to give any **151**. Notably, the nonspecific *HRP* appeared to catalyze a stereoselective dimerization, as the resultant purified product exhibited Cotton effects similar to those of an authentic **151** standard by circular dichroism (CD), whereas CD of the 16-*R* epimer was vastly different.[101]

In a subsequent report, Misawa was able to partially purify five isoenzymes from *C. roseus* cell suspension cultures.[102] They showed that the coupling activities of these enzymes closely mirrored their peroxidase activities.[102] Moreover, the yields between different isoenzyme were similar, ranging from 43% to 50%, which were higher than that displayed by *HRP*.[102] The authors proposed that these enzymes catalyzed a peroxidation of **20**.[102] The activated **20** could then proceed to couple with **23** nonenzymatically to give an iminium intermediate **154**, which could then be reduced by sodium borohydride to form **151** (Fig. 7C).[102] That no **151** could be detected when the reduction step was omitted supported the intermediacy of **154**. However, as the activated form of **20** has never been detected in plants, it is difficult to ascertain the exact mechanism of the reaction.[102]

Notwithstanding the important discovery of the involvement of a peroxidase, it was not until 1996 that Sottomayor et al. identified this enzyme.[103] Initial search for the crucial peroxidase focussed on the leaves of *C. roseus*, since it was known that the MIAs involved in the vinblastine pathway, including the monomeric **20** and **23**, as well as **151** and other anhydrovinblastine-derived dimeric alkaloids were localized to the aerial parts of the plant.[103] This yielded partially purified protein extracts containing a single peroxide-dependent isoenzyme which successfully coupled **20** and **23** to give **151** and was tentatively named anhydrovinblastine synthase (*CrPrx1*).[103] The enzyme was later purified to homogeneity,[104] rigorously characterized and identified as a high spin ferric haemprotein that is part of the plant peroxidase superfamily (class III peroxidases).[104–106]

As with other peroxidases, *CrPrx1* is promiscuous, and has been reported to display peroxidase activity against 4-methoxy-α-naphthol, ascorbic acid, and several other phenolic and alkaloid substrates.[105] Furthermore, plant genomes contain a large and diverse number of isoforms of class III plant peroxidases, as has been previously demonstrated for *Arabidopsis thaliana* and *Oryza sativa*.[107–110] However, it is common for one of these genes to be predominantly expressed in different plant tissues, at different developmental stages, despite many having a common substrate profile.[105] The vast diversity of class III plant peroxidases coupled with the inherent lack of specificity hampers unambiguous functional assignment for these peroxidases. Ideally, the in planta role for *CrPrx1* should also be validated by silencing experiments. However, the plants used for VIGS are too young to accumulate **151**, and **151** or **17** do not accumulate in cell cultures, making in planta functional characterization of this enzyme challenging.

Several pieces of evidence were thus used to solidify the role of *CrPrx1* in vinblastine biosynthesis. As previously mentioned, the leaves of *C. roseus* contained a high level of MIA, with the main constituents being **20**, **23**, and **151**, making up 75% of the total alkaloids detected, which suggests that *C. roseus* leaves retain a high activity for anhydrovinblastine synthesis.[105] Furthermore, both the substrates, product, and the proposed anhydrovinblastine synthase, of which only one isoenzyme was detected, have been shown to localize to the leaf vacuoles.[103] The strict peroxide-reliance for anhydrovinblastine synthase activity could only be attributed to this single peroxidase isoenzyme, since anhydrovinblastine synthase activity was copurified with the peroxidase.[104] Additionally, the transcript expression of *CrPrx1* in mature leaves is similar to the expression patterns of other MIA pathway genes.[106] Enzyme levels in the same leaf samples also followed a similar pattern of their corresponding *CrPrx1* transcript levels.[106]

However, when the authors attempted to determine the alkaloid levels in these samples, no meaningful conclusion could be drawn as individual alkaloid levels were variable between different samples.[106] They addressed this problem by analyzing leaves of young plants instead, since MIA levels are often higher here.[106] The results demonstrated that anhydrovinblastine synthase activity increased with leaf age, and was accompanied by an increase in **151**, as well as a decrease in the levels of **20** and **23**.[106] Unexpectedly, in mature leaves, *CrPrx1* level displayed an increase with concomitant decrease of **20** and **23** as observed before, but **151** level decreased.[106] The authors hypothesized that this might be due to overoxidation of **151** into leurosine (**155**, Scheme 25, path *a*), since **155** has been detected as a by-product in previous peroxidase-catalyzed coupling of **20** and **23**, and of direct oxidation of **151**.[95,97,113–115] This proposal was substantiated when a time-course analysis of the in vitro assay with *CrPrx1* and the substrates showed that prolonged incubation led to a decrease in **151** levels after a maximum has been reached.[106] Last, the authors proposed a channeling model involving other enzymes/carriers to aid the diffusion of the monomeric substrates to the inner tonoplast membrane, where the proposed anhydrovinblastine synthase resides, to rationalize the high levels of **151** detected in *C. roseus* leaves, despite the broad range of substrate specificity.[105]

The mechanism for the coupling reaction was first studied for the *HRP*-catalyzed coupling of **20** and **23**, and Sottomayor et al. proposed that this reaction follows that of a previously reported *HRP* peroxidation of **23** and acetylvindoline.[112] The ferric peroxidase is initially oxidized by hydrogen peroxide to give compound 1 (CoI, Eq. 1).[111] CoI proceeds to undergo two sequential one-electron reduction by the alkaloid (R_3N) to give at first CoII (Eq. 2), then regenerated ferric peroxidase (Eq. 3).[111]

$$Fe_p^{III} + H_2O_2 \rightarrow CoI + H_2O \; k_1 \tag{1}$$

$$CoI + R_3N \rightarrow CoII + R_3N^{\cdot+} \; k_2 \tag{2}$$

$$CoII + R_3N^{\cdot+} \rightarrow Fe_p^{III} + R_3N^{+} \; k_3 \tag{3}$$

For the coupling reaction of **20** and **23** by *HRP*, it was found that the reduction of CoII (Eq. 3) was the rate-limiting step.[111] The addition of the alkaloid substrates (**20** and **23**) completely reduced CoII to give the native ferric peroxidase, and a time-course investigation revealed that CoII disappearance closely correlated with Fe_p^{III} regeneration, consolidating the roles of these alkaloids in the reduction of CoII.[111] Next, the ability of either substrate to reduce CoII was investigated. The k_3 for the reduction of CoII by **23** was higher than that for **20**, suggesting that **23** is a better substrate for *HRP*; nonetheless, when both substrates were present, k_3 was equal, within the experimental errors, to the sum of CoII reduction by each individual substrate.[111]

Moreover, while incubation of both substrates with *HRP* led to **151** as the main product, alongside a small amount of **155**; when **20** was the sole substrate, a mixture of products was observed. The presence of two antiparallel bonds with respect to the tertiary

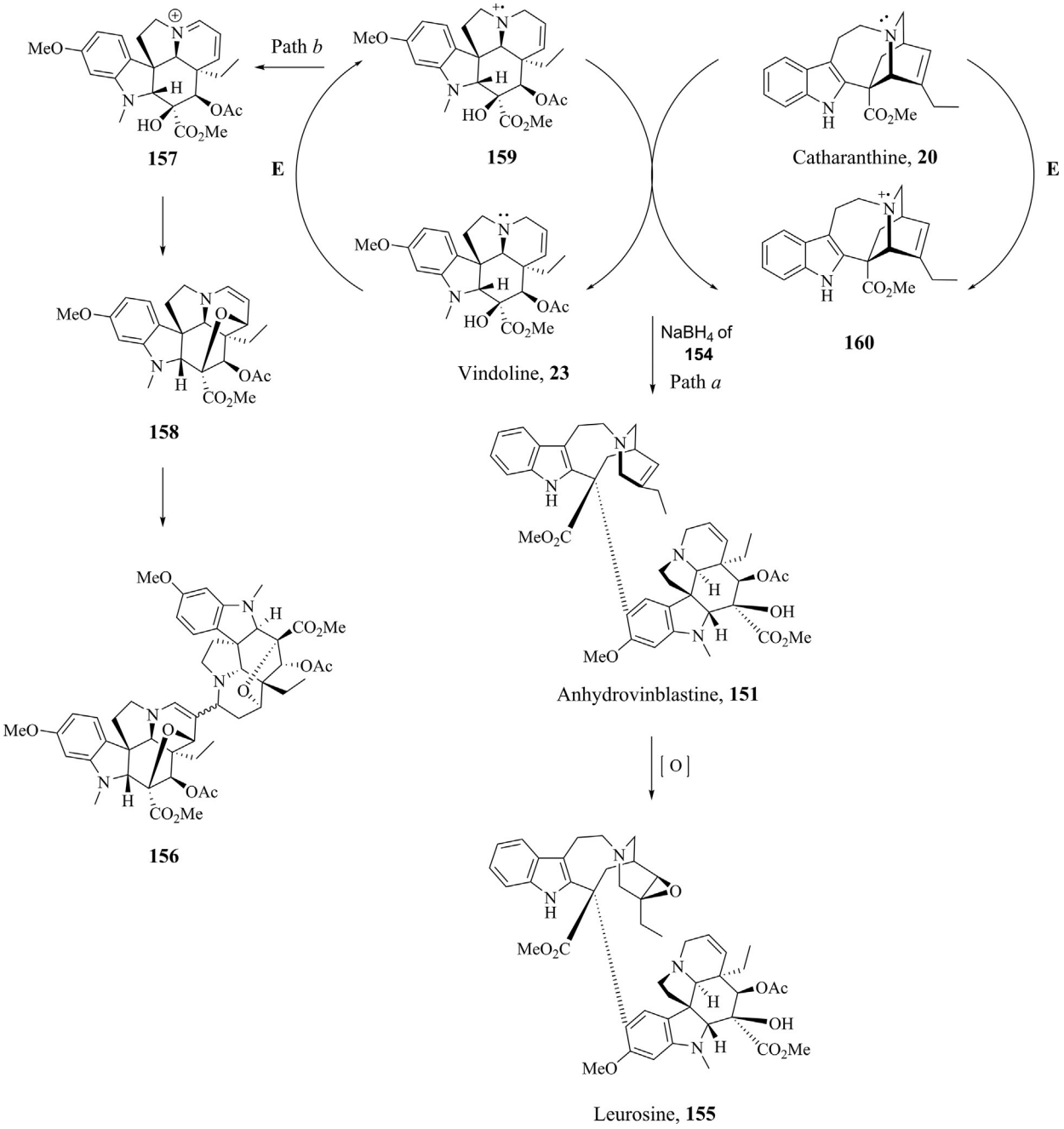

Scheme 25 *HRP* catalyzes the formation of the vindoline homodimer (**156**) in the absence of **20** (path *a*) and **151** and **155** in the presence of **20**. *E*, enzyme-catalyzed oxidations.[111,112] *HRP*, horseradish peroxidase.

nitrogen [(C-5)–(C-6) and (C-16)–(C-21)] in **20** makes it especially susceptible to oxidative fragmentation and this could partly explain the formation of multiple products when **20** was the sole alkaloid substrate.[111] In contrast, only one product formed in the presence of **23** alone.[111] The vindoline-reaction product was proposed to be the homodimer of vindoline, which had been reported prior (**156**, Scheme 25, path *b*).[112] Importantly, when both alkaloids were present, **156** was observed, which signifies the pathway leading to the vindoline dimer is completely blocked when **20** was present.[111] Last, HPLC analysis of the coupling reaction showed that **23** disappearance was accompanied by a stoichiometric formation of **151**, while consumption of **20** was much more rapid, once again possibly due to oxidative breakdown catalyzed by *HRP*.[111]

Collectively, these results suggested that the reaction would initiate with a one-electron oxidation of **23** by CoI to give an iminium radical cation (**159**).[111] In the absence of **20**, two vindoline radicals could couple to form the observed homodimer **156**. However, when **20** was present in the reaction mixture, **23** is reformed through a one-electron transfer to give a catharanthine

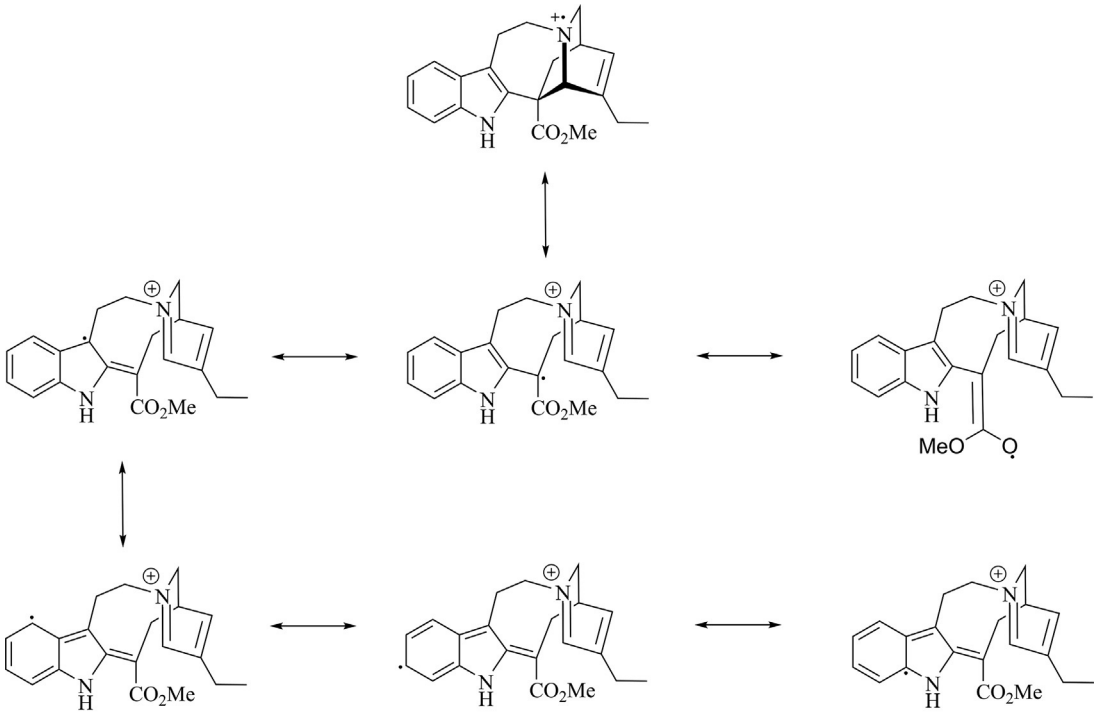

160

Fig. 8 Resonance structures of the catharanthine radical cation (**160**).[111]

radical intermediate (**160**).[111] The authors also reasoned that the oxidation of **20** by **159** occurred due to the formation of the resonance-stabilized **160** (Fig. 8).[111] This radical cation would undergo fragmentation and further oxidation, and could then be nucleophilically attacked by **23** to form the coupled iminium intermediate (**154**, Scheme 25, path *a*).[111] A final borohydride reduction then yielded **151**, which, if left exposed to oxidizing conditions, could give the by-product leurosine (**155**).[111] Thus, one molecule of **23** is required to initiate the reaction to give one molecule of **151**. However, this mechanism does not preclude the side-reactions, but rather, these reactions probably occur to some extent, which would also explain the observation that excess **20** is required in the reaction.[111]

Subsequent studies on the catalytic mechanism of *CrPrx1*-mediated coupling of **20** and **23** showed that this reaction possesses many similarities to *HRP*-mediated coupling,[104,105] namely:

1. The three-step catalytic cycle involving initial two-electron oxidation of the ferric haem by hydrogen peroxide followed by two consecutive one-electron reduction by the tertiary amine (NR_3).
2. The reduction of CoII (Eq. 3) was determined to be the rate-determining step.
3. Although both **20** and **23** were able to act as one-electron donors to reduce CoI and CoII to produce homodimers, k_3 for the **23** reduction of CoII was higher than that for **20**, indicating a preference for **23** as substrate for CoII.
4. When both substrates were present, k_3 was, within experimental errors, the sum of the rate constants of CoII reduction by **20** or **23** alone.
5. **20** Disappears much more rapidly, once again indicating that oxidative cleavage is also taking place; on the other hand, **23** is consumed stoichiometrically in the presence of **20**.

On this basis, the authors concluded that the mechanism for *CrPrx1* coupling to give **151** would also likely be radical-facilitated.[104,105]

Novel methods to prepare **151** using enzymes not derived from *C. roseus* have also been reported. By noting that the haem group, which contains a ferric center, plays an important role in the active site of peroxidase enzymes, Misawa investigated the possibility of various haemproteins catalyzing the **20**/**23** coupling.[113] All of the haems tested contain ferric iron, except for hemoglobin which contains a mixture of ferrous and ferric haem.[113] Microperoxidase effectively coupled the monomers to give **151** with yields similar to *HRP*.[113] Haemin, cytochrome *C* and lactoperoxidase were not active at 0.5 μM, but assays with increased concentrations of each of these haemproteins led to an increase in the **151** product formed.[113] To ascertain the importance of ferric haem, cytochrome C and *HRP* were reduced and examined for peroxidase activity. Although the yield of **151** in each case was reduced, peroxidase activity was not abolished.[113] The authors hypothesized that the lack of complete inhibition may be due to in situ reoxidation of the haem.[113]

Interestingly, when microperoxidase and haemin were incubated with the substrates in the absence of hydrogen peroxide, coupling still proceeded, albeit with lower yields.[113] This was unexpected, since hydrogen peroxide is a requirement for the *HRP*-catalyzed peroxidation, and suggests that a different mode of coupling is possible that does not require peroxide.[113] A similar observation had been reported previously whereby a haemprotein was shown to oxidize the alkaloids arecoline and atropine to their *N*-oxides in the absence of hydrogen peroxide, and such a reaction may be happening here with **20**.[116] If this were true, then the enzymatic coupling mechanism utilized by these haems may be analogous to that proposed by Potier in the Polonovski reaction, in which **20** is initially converted to its *N*-oxide (**161**) prior to coupling with **23** (vide infra).

An alternative method to enzymatically couple **20** and **23** was devised by Riva et al., this time using laccases.[117] These are oxido-reductases which contain a copper center and are widely found in nature.[117] A screen of several commercially available laccases identified the laccase derived from *Trametes pubescens* (*Tp*) and *Trametes versicolor* (*Tv*) as the most efficient coupling enzymes.[117] Under optimized conditions, incubation of the alkaloid substrates with *Tv* in a preparative-scale reaction led to 56% isolated yield of the **151** coupled product.[117] If these enzymes were immobilized prior to the reaction, then they could be simply recovered and reused for five reaction cycles with minimal impact to reaction yield.[117] The stability of these enzymes, simple and mild reaction protocol (only oxygen was required as the oxidant), and high yield offered by the *Tv* laccase relative to previous enzymatic protocols offers an attractive method to access **151**.[117]

2.24.2.6 Chemical Synthesis of Anhydrovinblastine and Its Oxidation to Vinblastine

Despite the identification of *CrPrx1* and other enzymes capable of coupling the two halves of **151**, the current method to access this compound still relies on semisynthetic approaches.[66,118] Here we shall discuss specifically three of these methods and their mechanisms, namely: the Polonovski-Potier reaction, the Kutney Fe^{III} approach, and finally the Boger Fe^{III} approach. For a thorough treatment of the multiple methods to chemically couple **20** and **23** and their elaboration to **17**, reference 119 is highly recommended.[119] Since Potier was the first to develop a method that not only successfully coupled the velbamine and vindoline units, but also ensured the crucial *S* stereochemistry at the C-16 position, it would be most appropriate that our discussion should start here. To generate the velbamine half of **151**, it was necessary to cleave the (C-16)–(C-21) bond, and it was envisaged that such a process could occur by initial oxidation of the tertiary amine followed by a Polonovski reaction (Scheme 26).

Formation of **161** could be achieved by reacting **20** with *p*-nitroperbenzoic acid.[120] Fragmentation ensued when the *N*-oxide was exposed to trifluoroacetic anhydride (Scheme 26, path *a*). In the presence of vindoline and sodium borohydride, **151** and its 16-*R* epimer (**162**) were obtained.[94] It must be noted that the rigid conformation of the polycyclic velbamine unit enables fragmentation of either the (C-16)–(C-21) or (C-5)–(C-6) bond, as both bonds are antiparallel to N^+-OX; and the propensity for fragmentation of the latter to give **165** was reported to be dependent on the nucleophilicity of the leaving group (OX^-, Scheme 26, path *b*).[120] However, the presence of the conjugating double bond at (C-15)–(C-20) should favor the fragmentation of the (C-16)–(C-21) bond over (C-5)–(C-6).[119] As expected, the major component of the product mixture were often the (C-16)–(C-21) fragmentation products, while a small amount of the (C-5)–(C-6) cleavage product was usually reported.[120]

Two mechanisms were proposed for this reaction: one involving a concerted approach whereby cleavage of the (C-16)–(C-21) bond in **161** and formation of the (C-16)–(C-10) bond between **20** and **23** occur simultaneously (Scheme 27).[119] The second involves a stepwise approach in which initial fragmentation of the (C-16)–(C-21) bond leads to diiminium intermediate **166**.[119] This species could then be attacked by **23** to give the dimer with the natural 16′*S* configuration (**151**) or its epimer (**162**).[119] With regard to the former approach, stereoelectronic requirements necessitate that **23** must attack from the α face to produce **151**.[119–121] On the other hand, the alternative stepwise approach could draw on the various possible conformations of the initially formed **166** intermediate to rationalize the different stereochemical outcomes when different reaction conditions were employed.

Molecular modeling suggested that if **166** could maintain its conformation before conformational fluctuation could occur, then the nucleophilic **23** would preferentially attack from the α face (Scheme 27, path *a*).[119] However, if reaction conditions (temperature, solvent, etc.) permitted, then intermediate **166** could form conformation **167** (Scheme 27, path *b*).[119–121] The β face becomes more accessible, and **23** approaching from this trajectory and borohydride reduction would lead to the unnatural 16-*R* isomer (**162**).[119–121] The conformation **167** was suggested to be the energetically more stable, while **166** could be trapped by appropriate reaction conditions before its relaxation to **167**.[121,122] A detailed study of the effects of reaction conditions on these parameters was conducted by Kutney et al., which also shed light on the mechanism at play.[119,123] The mechanism in Scheme 27 is briefly discussed below, and a more detailed account of the mechanistic studies has been previously reported.[119,122,124]

Temperature is a key factor in this dimerization reaction. Kutney reported an increased amount of the unnatural dimeric product being observed at higher temperatures ($> -10°C$), while only **151** was obtained when reactions were conducted at $-50°C$[119] (although Potier reported that a temperature of $-70°C$ was required for exclusive formation of the natural configuration, while a 5:1 of natural: unnatural was obtained at $-50°C$, presumably with slight variations in other parameters).[121] Obviously, conformational mobility would be promoted at elevated temperatures to give a higher percentage of conformation **167** and consequently more of the 16-*R* isomer being observed, a result which is supportive of the stepwise mechanism.[119,121]

Other evidence in support for the mechanism outlined in Scheme 27 is the lowered yields obtained for the coupling products when the double bond in the tetrahydropyridine ring is reduced (catharanthine (**20**) versus dihydrocatharanthine (**168**), or allocatharanthine (**57**) versus dihydroallocatharanthine (**169**), Fig. 9).[119,120] This observation could be rationalized by considering the enhanced stability of the iminium **154** afforded by the presence of the conjugating double bond.[119] In other words, for **19**, the developing pi orbital at C-21 (or C-3 for **57**) could interact with the adjacent π bond of (C-20)–(C-15) (or [C-14]–[C-15] for **57**),

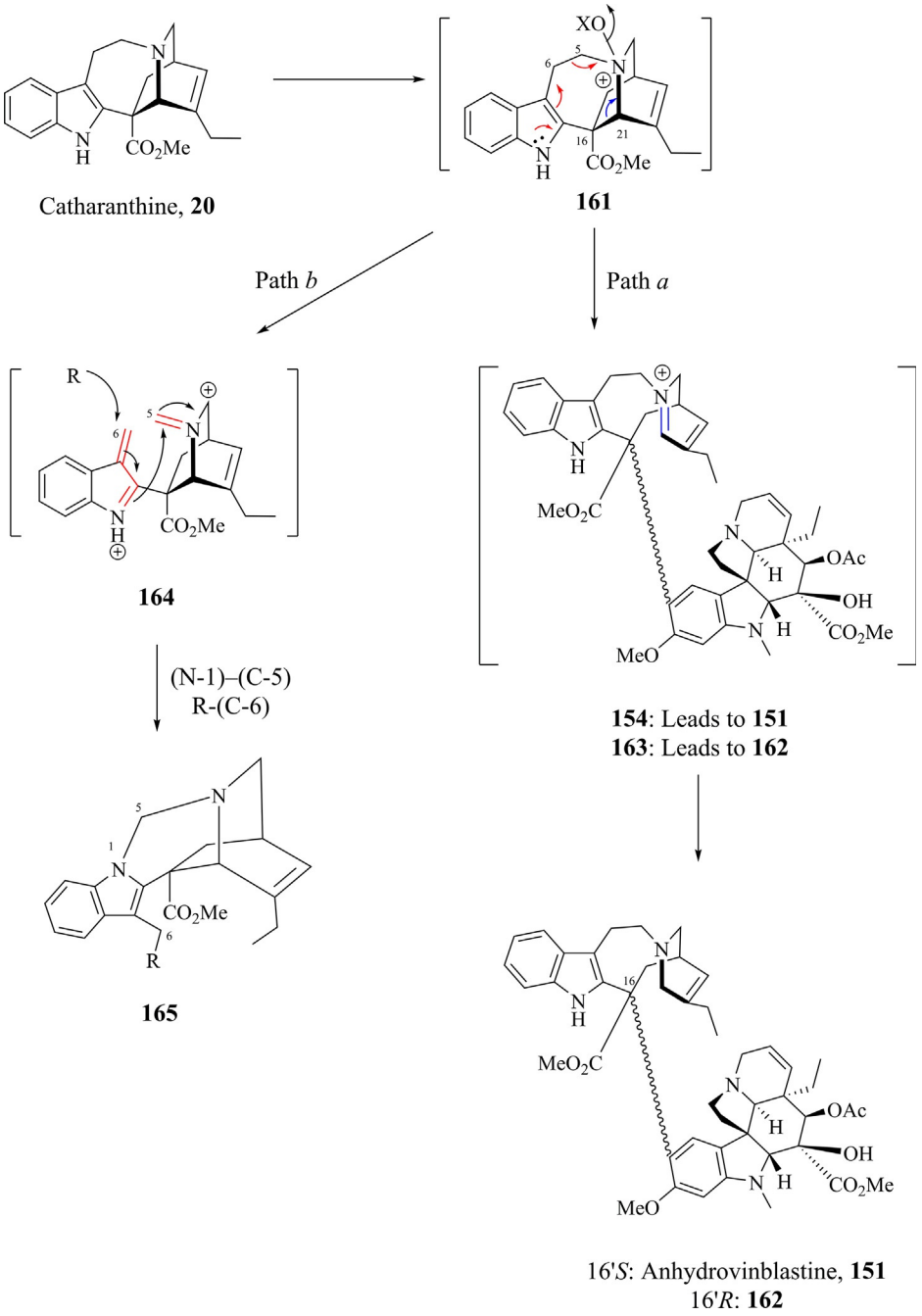

Scheme 26 Fragmentation of **161** via cleavage of the (C-16)–(C-21) bond to give **151** and **162** (path *a*), or (C-5)–(C-6) bond to give **165** (path *b*) via the Polonovski reaction.[119,120]

thus lowering the kinetic barrier.[119] Expectedly, when the reactions for **168** were conducted at temperatures between −50 and −30°C, only two products were formed: the C-14 isomers (*S* and *R*, **170** and **171**, respectively, Scheme 28) of the 16-*S* dimers.[119] In contrast, the reaction carried out at −10°C yielded the aforementioned 16-*S* dimers, as well as their 16-*R* diastereomers (*S* and *R*, **172** and **173**, respectively),[119] illustrating the effect that temperature has on the stereochemistry at C-16 extends beyond the catharanthine system.

Additionally, dimerization of catharanthine derivatives lacking the ester group, such as decarbomethoxycatharanthine, occurred less readily and often lower yields of the coupled products were obtained.[119] This result is also in line with the proposed mechanism, since charge build-up at C-16 would be expected upon fragmentation, and this would be stabilized by the electron-withdrawing ester group.[119] Indeed, unlike the coupling of **20** which could be effected at −50°C, the reaction with decarbomethoxycatharanthine only proceeded at elevated temperatures, whereby the formation of the 16′*R* isomer could not be prevented.[119]

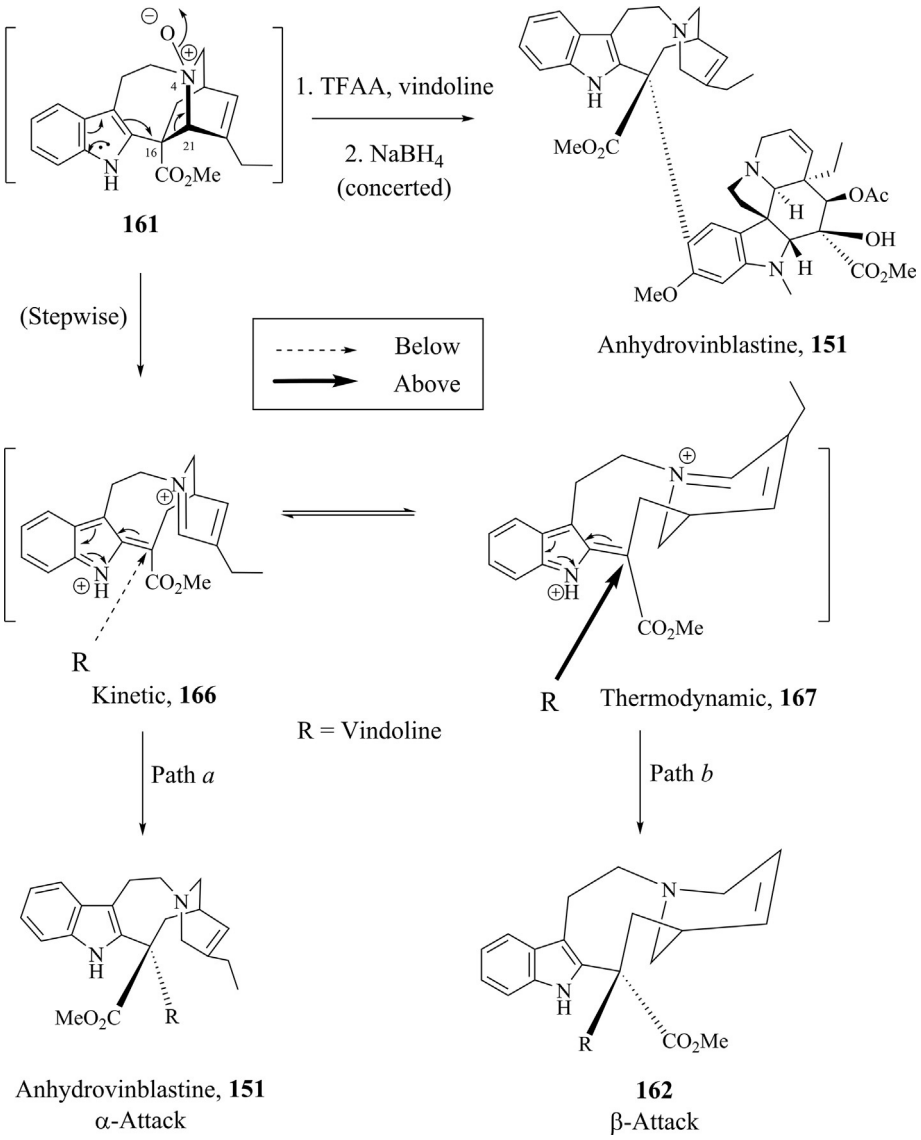

Scheme 27 Comparison of the proposed concerted and stepwise mechanisms for the coupling of **20** and **23** via the Polonovski reaction.[119,121] TFAA, trifluoroacetic anhydride.

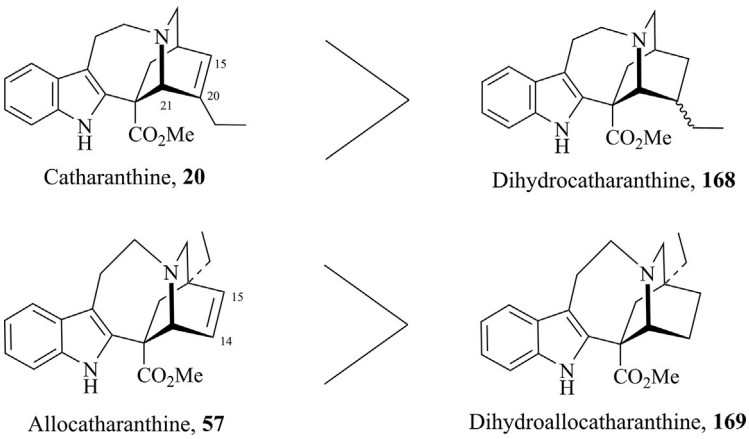

Fig. 9 Increased yields for the coupling reaction when the velbamine unit retains the double bond adjacent to the site of fragmentation (**20** and **57**), illustrating the stabilizing effect of the double bond.[119,120]

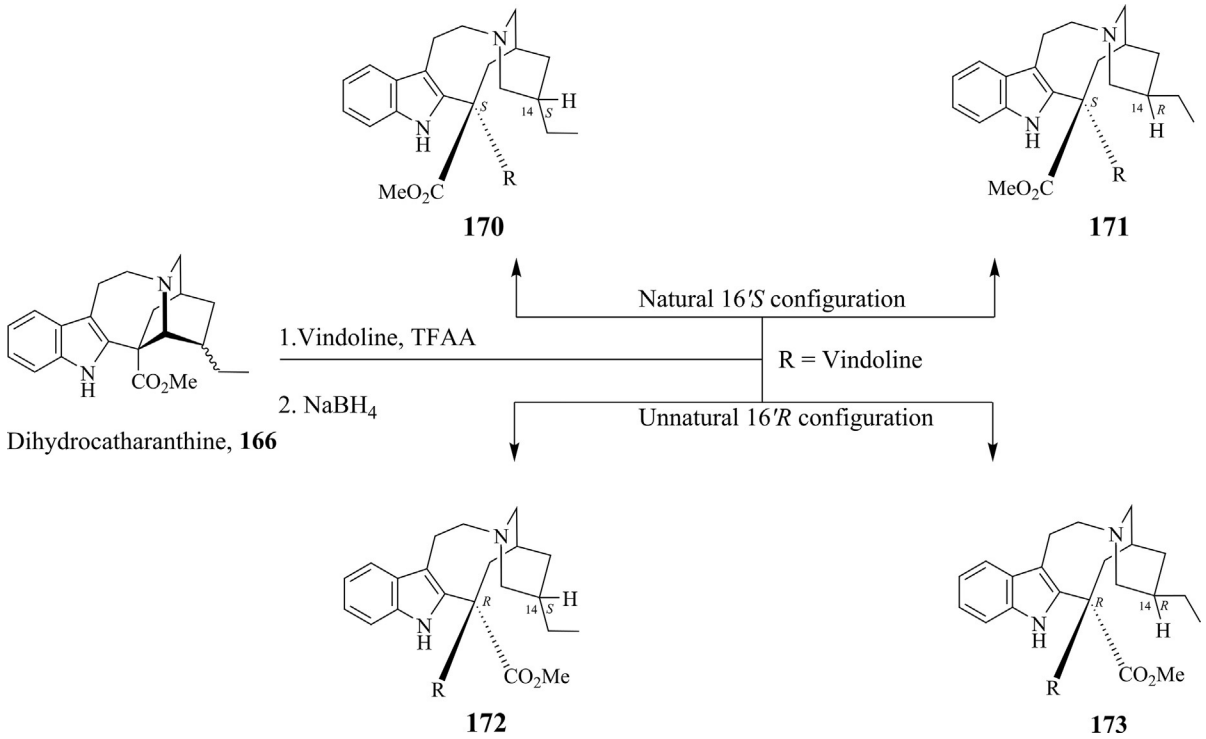

Scheme 28 Between −50 and −30°C, only the natural 16-*S* diastereomers (**170** and **171**) were obtained. Above −10°C, all four diastereomers (**170**–**173**) were produced.[119] *TFAA*, trifluoroacetic anhydride.

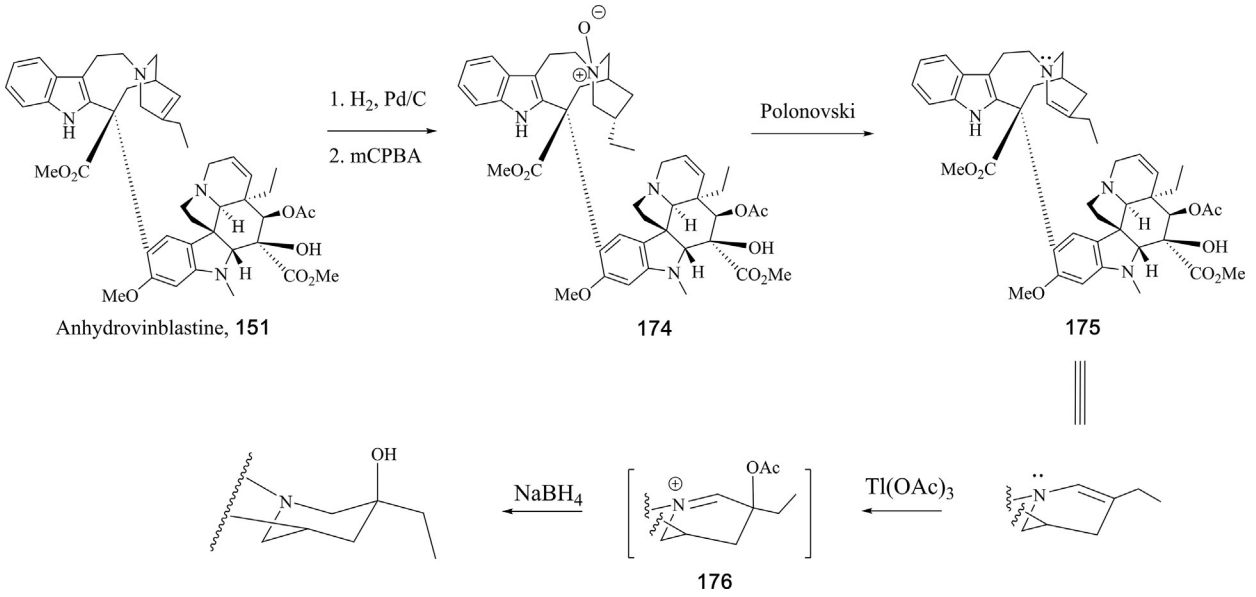

Scheme 29 Potier's semi-synthesis of **17** via a Polonovski reaction on the enamine **175**.[125] *mCPBA*, *m*-chloroperoxybenzoic acid.

Having established an efficient route to access **151** via the Polonovski reaction, Potier et al. exploited this reaction once more to obtain the anti-tumor compound **17**.[125] Thus, the double bond at (C-15)––(C-20) was reduced and the *N*-oxide of the tertiary amine (**174**) was reformed and subjected to a 2nd Polonovski reaction to yield the expected enamine (**175**).[125] Oxidation of **175** with thallium triacetate to give **176** followed by 1,2-borohydride reduction afforded vinblastine (**17**, Scheme 29).[125] Potier rationalized that the configuration at C-20 was dictated by the rigid configuration of the N-4 lone pair, which presumably serves to orientate the acetoxy motif at the β face of the π bond.[125]

Kutney et al. later improved upon this synthesis by varying the reducing and oxidizing agents.[126] Thus, catharanthine *N*-oxide (**161**) and **23** were coupled in the usual manner via a Polonovski reaction to give the iminium intermediate **154**.[126] This time, instead of using sodium borohydride, the crucial enamine **175** was obtained by 1,4-reduction with NADH derivative **177** (Scheme 30).[126] Exposure of the enamine to $FeCl_3$ in air followed by borohydride reduction led to a mixture of **17** and the 4-α-hydroxy epimer leurosidine (**178**).[126] Optimization of this reaction sequence gave a 40% overall yield of **17** from the monomeric precursors, which was considerably higher than Potier's previous semi-synthesis of **17** (10%).[126] Conveniently, Kutney noted that their semisynthetic sequence could be performed in one-pot.[126] The use of ferric chloride also obviated the need for the toxic thallium triacetate.[126]

Kutney further incorporated ferric chloride in his preparation of **17** by using this reagent as the coupling mediator to form **151**.[127] Under optimized conditions, this one-pot reaction gave a conversion of 77%.[127]He proposed that the ferric chloride could facilitate the (C-16)–(C-21) bond cleavage via two radical abstraction steps to give iminium **178** (Scheme 31).[127] Analogous to the mechanisms proposed for the coupling of **20** and **23** using trifluoroacetic anhydride (Scheme 27), a stepwise (Scheme 31A) and concerted process (Scheme 31B) were also suggested for the Fe^{III}-mediated coupling. Kutney noted that the excess of the 16-*S* dimer upon nucleophilic attack of **23** would suggest a concerted reaction mechanism where **23** approaches from the α face, the reasoning being the same as that for the "original" Polonovski reaction.[127]

Additionally, it was also thought that for this modified Polonovski reaction, an equilibrium may also exist to give two possible diiminium intermediates (**166** and **167**) for the stepwise mechanism.[127] In the previous reaction, enhanced formation of the natural coupled product was achieved at low temperatures. However, in the case of the modified Polonovski reaction, the use of ferric ions provides an appropriate conformation at temperatures conducive for production of the unnatural 16-*R* product (**162**).[127] Thus, to account for the propensity of **151** formation, this "freezing" effect may originate from a coordinating interaction between the ferric ions with **166**.[127] This hypothesis was supported by the observation that the coupling reaction could only be effected when the oxidant was uncomplexed.[127]

A landmark in total synthesis was recently presented by Boger et al. in their preparation of the bisindole alkaloid **17** in 12 steps.[128,129] Of significance is Boger's adopted use of Kutney's and Sakamoto's ferric ion approaches to produce **151**, and

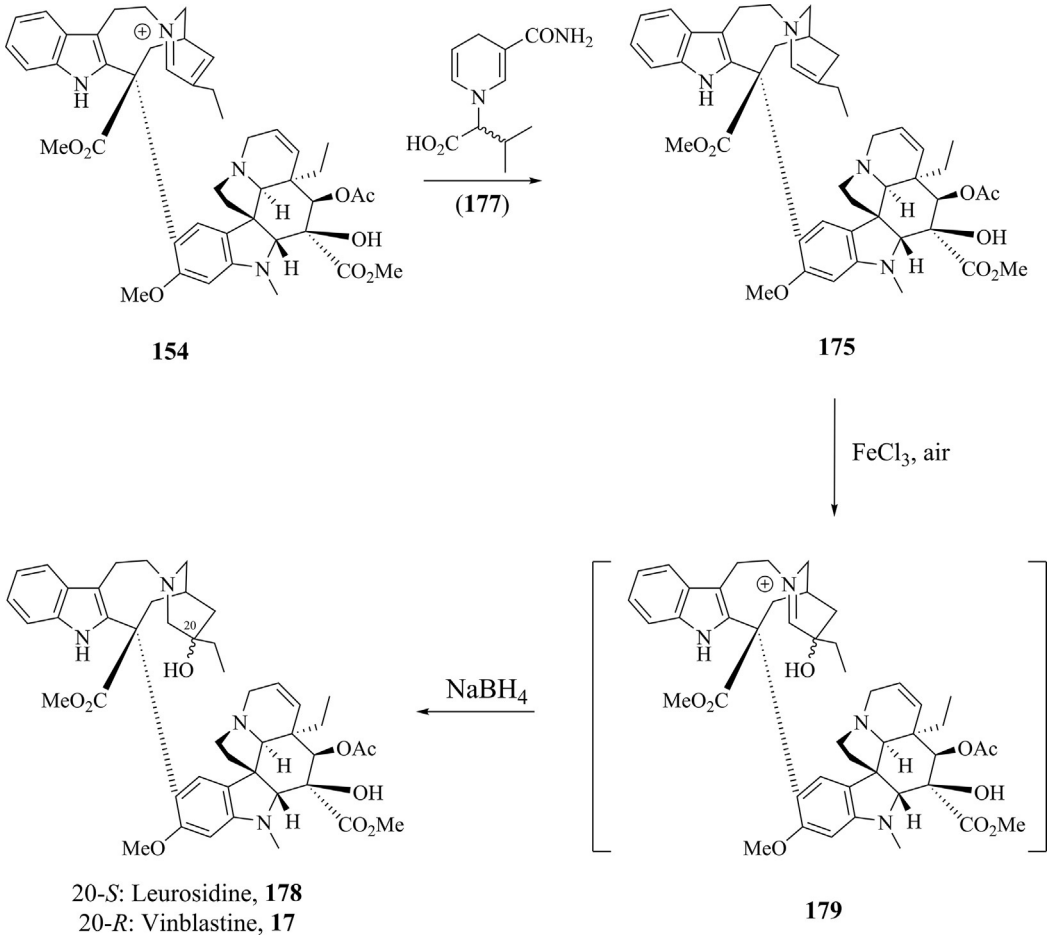

Scheme 30 Kutney's improved semi-synthesis of **17** by use of ferric chloride.[126]

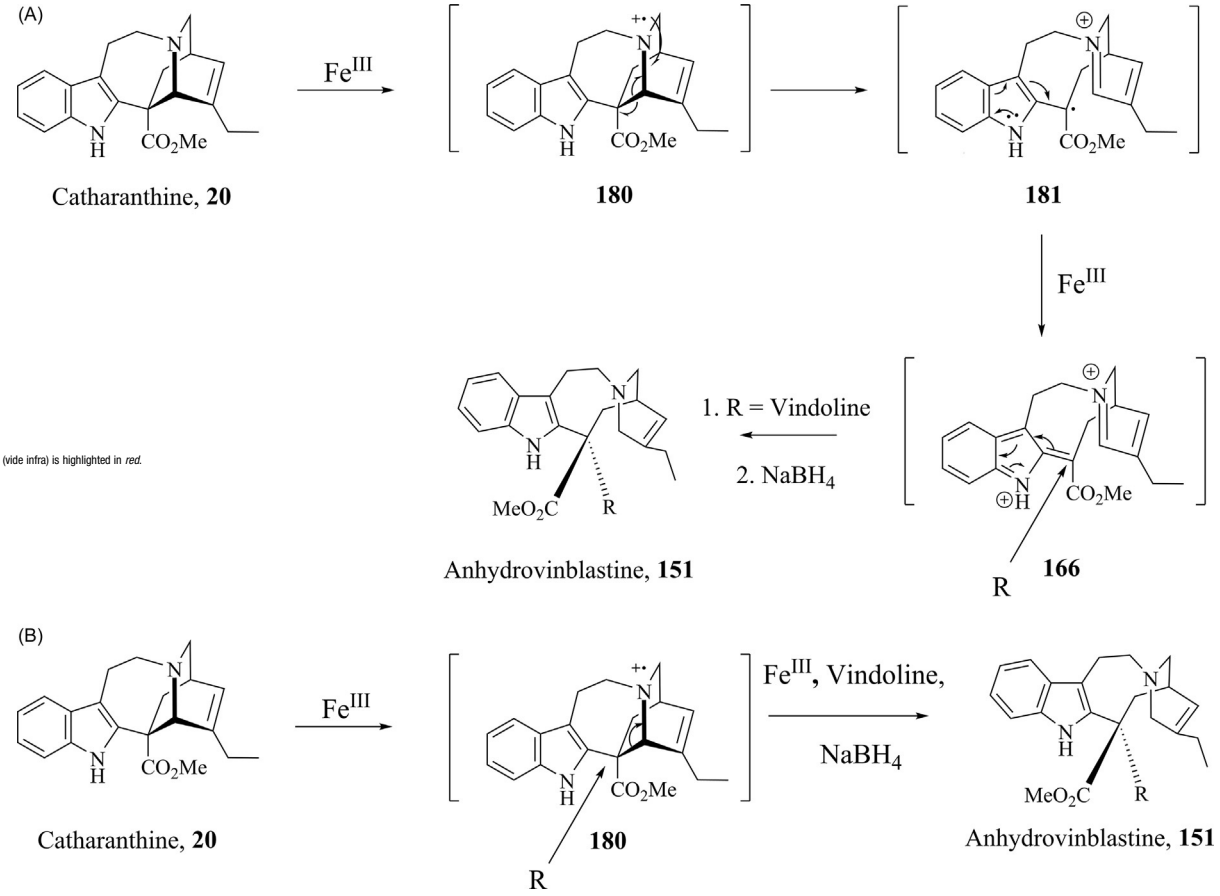

azabenzfulvene motif (vide infra) is highlighted in *red*.

Scheme 31 (A) The stepwise and (B) concerted mechanisms proposed by Kutney for the formation of **151** via the modified Polonovski reaction.[127] The

subsequently **17**.[128,129] In addition to the impressive synthetic design, Boger's explorations of the underlying mechanism has challenged Kutney's own mechanistic proposal and provided crucial insight into the aspects controlling the stereoselectivity of these reactions. A detailed comparison of the findings of the two groups has recently emerged,[130] and is summarized below. Notably, aspects of Boger's mechanism are proposed to occur in the in planta biosynthesis of **17**.[131]

Using a modified protocol based on Kutney's ferric chloride construction of **151**, Boger was able to achieve the desired coupling with exclusive selectivity for the 16-*S* dimer product in 90% yield when the iminium **154** was reduced with sodium borohydride (Scheme 32, path *a*).[128,129] Alternatively, it was possible to combine the coupling and subsequent installment of the hydroxyl group at C-20 in a two-step one-pot synthesis by direct aeration of **154** with $Fe_2(ox)_3$-$NaBH_4$ (Scheme 32, path *b*).[128,129] Overall, this reaction afforded a 66% yield of the hydroxylated products with a 2:1 preference for the 4′-β alcohol compound. Notably, $Fe_2(SO_4)_3$ was suitable for both the coupling and oxidation reaction, unlike ferric chloride which could only effect the former, or $Fe_2(ox)_3$ that only mediated the latter; this discovery, although offering a lower yield of 71% (unoptimized) for production of **151**, further simplified the synthetic protocol. Additionally, improvement in yield and diastereoselectivity was reported in the presence of an organic base, suggesting further optimization is possible and potential for industrial application.[128,129]

In the previous results from the groups of Kutney and Sundberg, first, Sundberg et al. noted that *N*-methylcatharanthine was consumed but did not couple with **23**, whereas in the absence of **23**, it was recovered unchanged.[124] This observation led them to conclude that **20** (with free-indole) was necessary to realize the desired coupling. Furthermore, **23** may act as a base in this reaction by removal of the indole (or indolium) proton to facilitate the bond cleavage process.[124] Altogether, this implied the involvement of an azabenzfulvene motif (e.g., structure **166**, highlighted in *red*, Scheme 31A) upon fragmentation and subsequent nucleophilic attack by **23** onto an sp^2 C-16. Second, an important element in Kutney's proposal is the requirement of 2 one-electron oxidations of **20** necessary to generate azabenzfulvene (Scheme 31).[127] The first electron abstraction was proposed to occur at the tertiary amine while the second to convert the C-16 secondary radical into a resonance-stabilized cation.[127]

However, when Boger reacted **20** with ferric chloride in the absence of **23**, the recovery of **20** was unexpected and inconsistent with the requirement of an azabenzfulvene intermediate, which initiated Boger's efforts to reexamine this reaction in more details.[132] Moreover, Boger's experience with *N*-methylcatharanthine was different to that of Sundberg: *N*-methylcatharanthine was consumed regardless whether or not **23** was present under Kutney's conditions, and no **151** was formed in these reactions.[129]

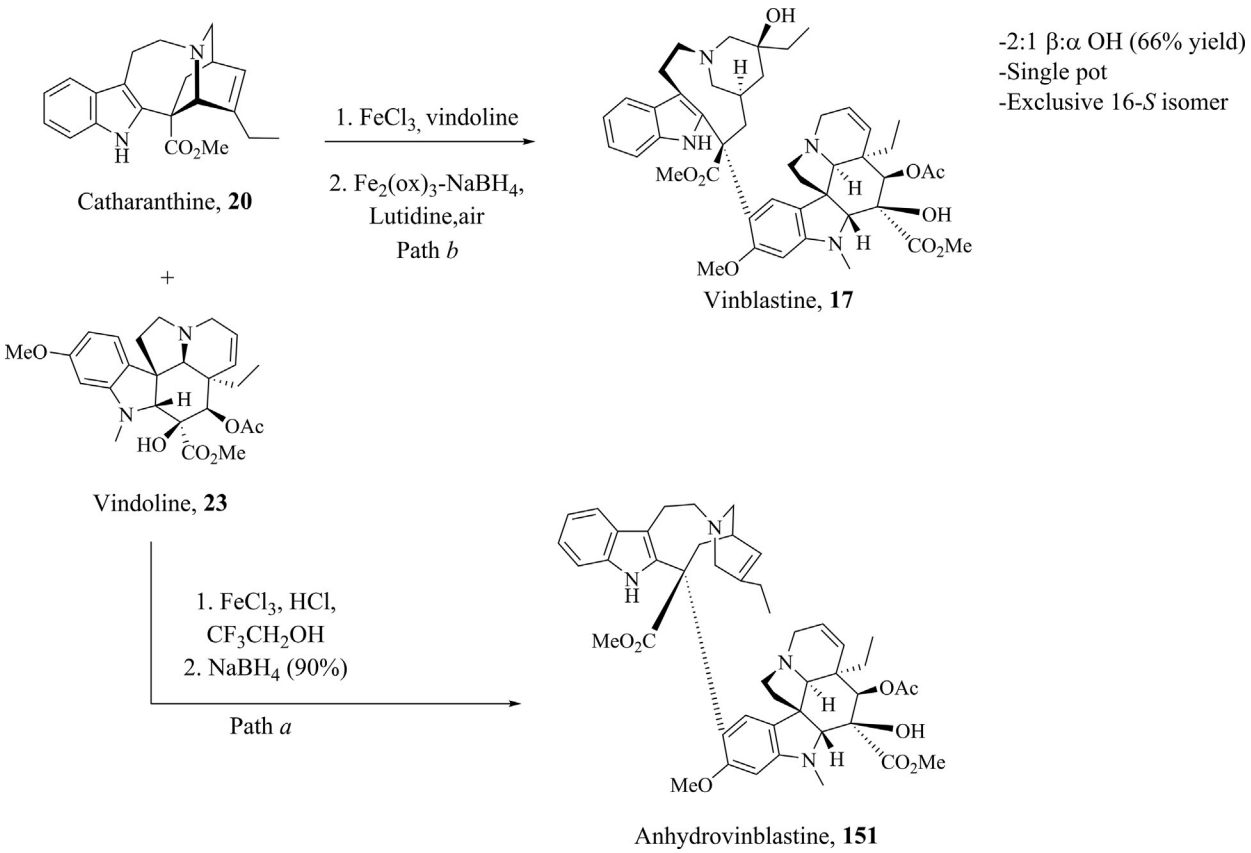

Scheme 32 Boger's modified coupling of **20** and **23** to give **151** (path *a*), and a two-step one-pot synthesis of **17** (path *b*).[128,129]

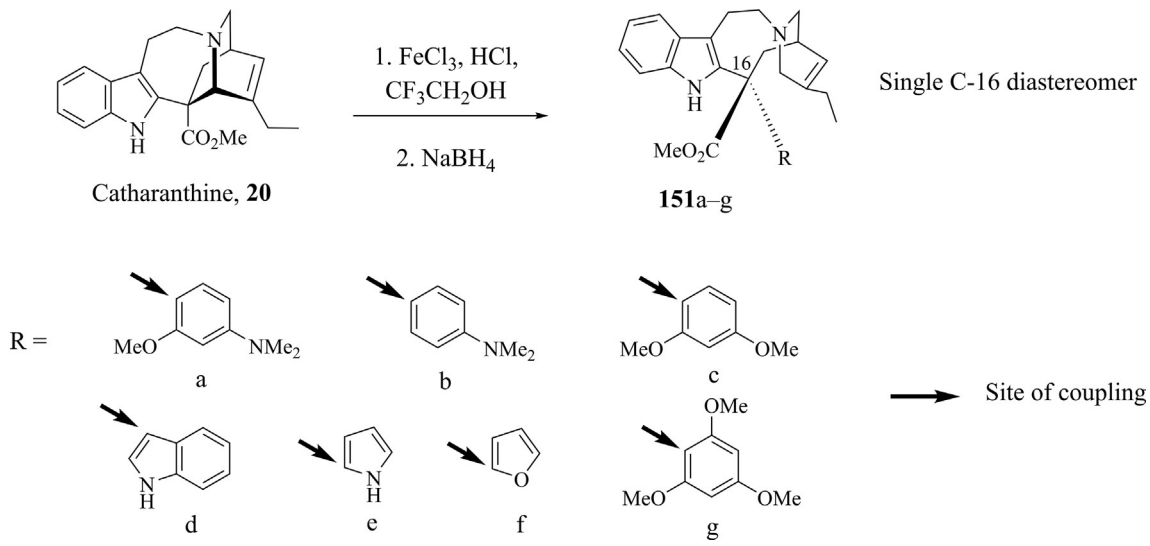

Scheme 33 Coupling of **20** with aromatic substrates illustrating **20**'s ability to direct regio- and stereoselectivity.[132]

Finally, under the aqueous conditions of the Fe^{III}-promoted coupling, the lack of incorporation of a nucleophilic solvent such as water by trapping of reaction intermediates was noted.[132] The following describes a series of experiments to determine the essential requirements for the coupling substrates.

First, the nature of the nucleophilic reagent (vindoline substitutes a–g, Scheme 33) was investigated. Simple substrates bearing electron-donating and -withdrawing substituents were examined under the $FeCl_3$-$NaBH_4$ conditions. It was determined that electron-rich systems (indole, pyrrole, *N*,*N*-dimethyl-3-methoxyaniline, etc.) participated in the reaction readily and gave yields comparable to that with the vindoline reaction.[132] On the other hand, less electron-rich, neutral or electron-poor substrates such

(A)

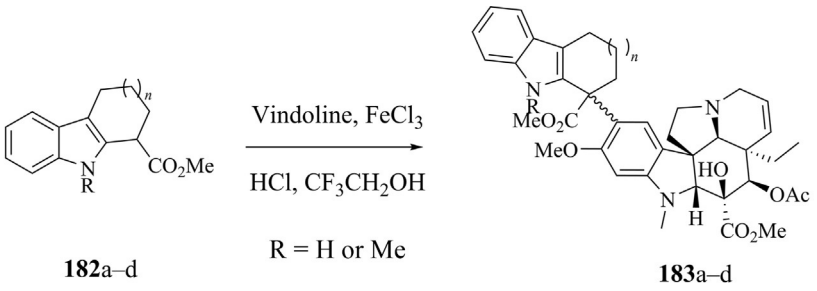

182a–d

183a–d

Entry	n	R	Percentage yield/%	dr
a	0	H	63	1:1.5
b	0	Me	64	≥4.3:1
c	1	H	86	1:1.3
d	3	H	24	Single

(B)

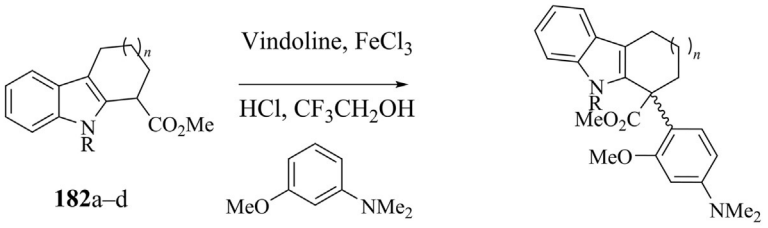

182a–d

R = H or Me

184a–d

Entry	N	R	Percentage yield/%
a	0	H	74
b	0	Me	41
c	1	H	58
d	3	H	50

Scheme 34 (**A**) Coupling of **23** with various indolic substrates illustrating that neither indolic proton nor tertiary amine were required for the coupling reaction and (B) Successful replacement of **20** and **23** illustrating the generality of the coupling reaction.

as benzene, thiophene, or anisole failed to couple with **20**.[132] When coupling occurred, then the 16′*S* diastereomer was formed exclusively, indicating that **20** alone dictated the regio- and stereochemistry for this reaciton.[132]

Kutney et al. had initially proposed that the tertiary nitrogen was the initial site of radical formation;[127] whereas Sundberg had emphasized the importance of the free-indole which was an essential aspect if the reaction were to proceed via a neutral azabenzfulvene.[124] To validate these hypotheses, a series of simplified substrates (catharanthine substitutes, **182**a–d, Scheme 34A) were examined where the tertiary nitrogen was removed and the substituent on the indole nitrogen was either H or Me. The results were clear: both of the aforementioned requirements were not necessary, as coupling proceeded smoothly with a range of substrates lacking the tertiary nitrogen; and the replacement of H by Me (**182**b) did not hinder the reaction.[132] However, the reaction generally afforded a mixture of diastereomers, which once again supported the role of **20** in controlling the configuration at C-16.[132] Successful replacement of **20** and **23** with alternative coupling substrates (Scheme 34B) illustrated the generality of this reaction: neither **20** nor **23** was required to effect the coupling.[132] Notably, no participation of water or Cl^- counteranion took place despite the acidic reaction conditions, which was at odds with any mechanism involving a cationic or neutral azabenzvulvene.[132]

Two studies examining the role of the C-16 substituent in **20**, as well as the C-10 and C-12 substituents, also proved insightful. Compounds possessing an electron-withdrawing group (**185**a–c, Scheme 35A) at C-16 gave superb yields, whereas electron-donating (**185**e–g) or neutral substituents (**185**d) all failed to couple with **23**.[133] With regard to variations to the indole ring, it was found that both C-10 and C-12 substituents had the same effects. Generally, neutral or electron-donating groups (**187**d–f, Scheme 35B) coupled well with **23**, whereas electron-withdrawing substituents (**187**a–c, j–l) either slowed or precluded coupling altogether.[134] Notable exceptions included OH (**187**g) and amine derivatives (**187**h–i, m), which participated in competitive oxidation instead.[134] These results are supportive of initial radical abstraction occurring at the catharanthine indole nitrogen and not the previously thought tertiary amine (Scheme 36).[134]

Accordingly, Boger suggested that the coupling occurred between the resonance-stabilized **181** (Scheme 36), generated by a single-electron oxidation of the indole nitrogen.[132] This is consistent with the requirement for a C-16 electron-withdrawing group and the ability for an electron-donating group at C-10/C-12 to promote the coupling reaction. This radical coupling mechanism was

(A)

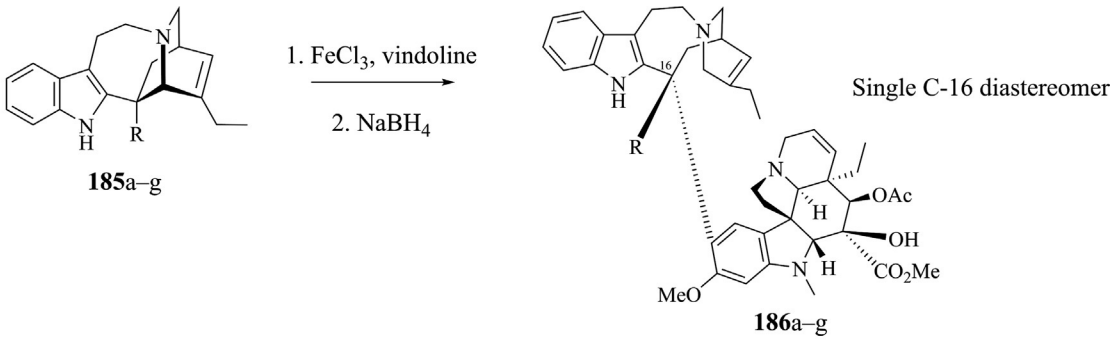

Entry	R	Percentage yield/%
A	CO_2Me	90
B	CO_2Et	82
C	CN	95
D	H	0
E	OH	0
F	CH_2OH	0
G	CH_3	0

(B)

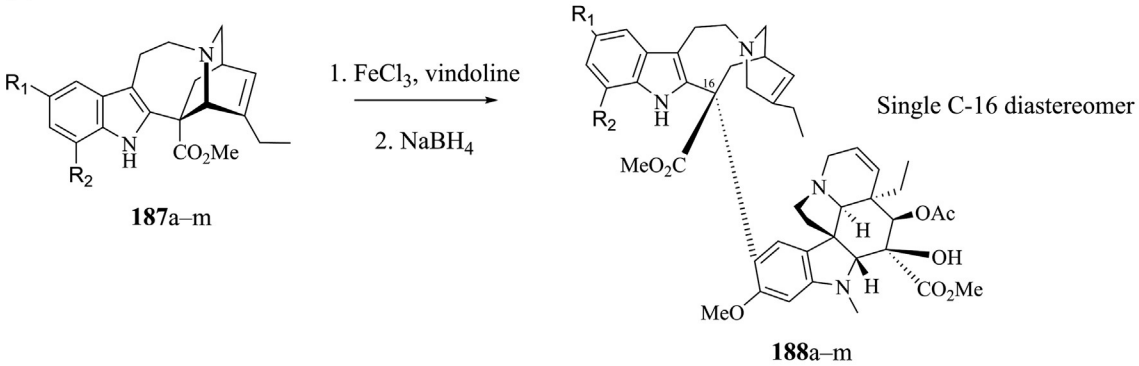

Entry	R_1	R_2	Percentage yield/%
a	NO_2	H	0
b	CN	H	<5
c	I	H	29
d	SMe	H	70
e	Me	H	95
f	OMe	H	62
g	OH	H	0
h	NH_2	H	0
i	NMe_2	H	0
j	H	NO_2	0
k	H	I	33
l	H	Br	44
m	H	NH_2	0

Scheme 35 (**A**) Catharanthine derivatives with varying C-16 substituents illustrating the importance of an electron-withdrawing group at this position and (B) Catharanthine derivatives with varying C-10 or C-12 substituents illustrating the importance of an electron-donating group at these positions.[133,134]

consolidated when coupling occurred between **23** and an electrophilic carbon radical derived from ICH_2CO_2Et and $BrCH(CO_2Et)_2$ (Scheme 37).[132]

Furthermore, Boger suggested that the captodatively stabilized intermediate **181** could be reversibly formed from intermediate **189**, which would explain for the observation that **20** was recovered in the absence of **23** after a reductive workup.[132] The alternative azabenzfulvene intermediate would not be expected to regenerate **20** following workup.[132] Additionally, the one-electron-two-center exhibited by the resonance forms of **181** could rationalize the high stereoselectivity of this reaction at room temperature by stabilizing a conformation which blocks incoming nucleophilic attack from the upper face.[132] We can see from Schemes 31 and 36

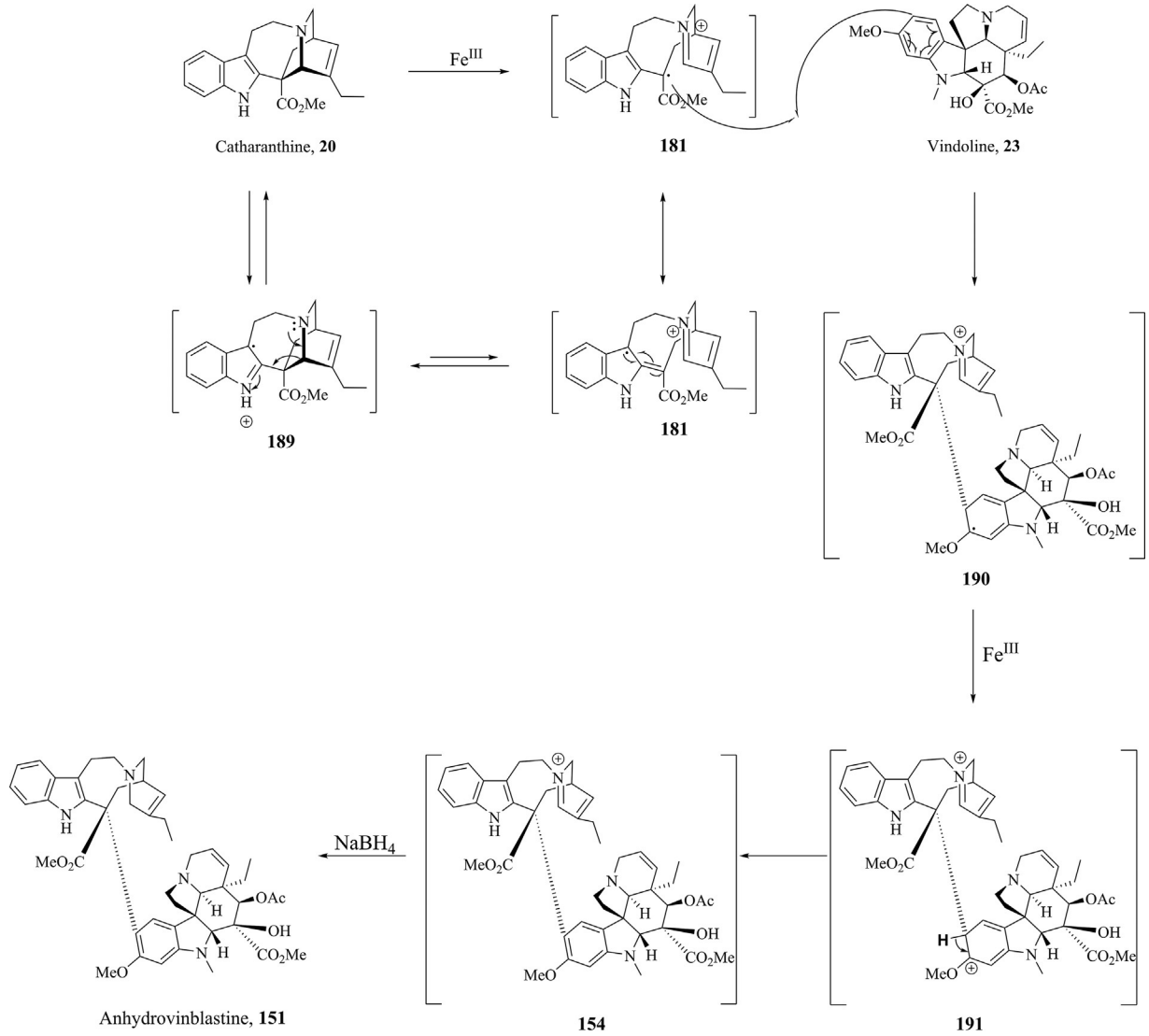

Scheme 36 Boger's proposed mechanism for the Fe^{III}-mediated coupling of **20** and **23**.[132]

that despite the different initial sites of radical formation (tertiary amine vs. indole amine), both the Kutney and Boger mechanisms lead to the same radical cation **181**.[130] From the available evidence provided by Boger's thoughtful experiments, we can conclude that the azabenzfulvene intermediate **166** is not involved in the pathway and thus we could forgo Kutney's second Fe^{III}-mediated oxidation to give the dication **166** in favor of Boger's postcoupling oxidation step.[130]

To probe the mechanism for the oxidation of **151** to **17** and leurosidine (**178**, vinblastine 20′ epimer) a series of detailed labeling studies using $NaBD_4$, D_2O, and $^{18}O_2$ were conducted on the various reactions previously discussed to eliminate otherwise attractive mechanistic possibilities.[129] The coupling to give **151** using the Fe^{III}-$NaBD_4$ conditions led to a single D incorporation at C-21, as expected (**195**, Scheme 38A).[129] When unlabeled **151** was oxidized to **196**, once again using the Fe^{III}-$NaBD_4$ conditions, a single D incorporation at C-15 was observed (Scheme 38B). When this reaction was performed with Fe^{III}-$NaBH_4$ but in D_2O, no deuterium was incorporated (Scheme 38C).[129] Oxidation using $^{18}O_2$ revealed that the C-20 alcohol is derived from oxygen (**197**) and that water does not play a role in the installation of this hydroxyl group.[129] In the absence of oxygen, no oxidation occurred, but instead the (C-15)–(C-20) double bond was reduced by borohydride, as revealed when clean incorporation of deuterium atoms across the double bond was observed when $NaBD_4$ was employed (**198** and **199**).[129] Last, when the coupling and oxidation reactions were combined, both C-15 and C-21 were deuterated (**200**, Scheme 38D).[129]

From the labeling study, we could conclude that this reaction is effected without the intermediacy of iminium **179**, and it also dismissed the possibility of an Fe-catalyzed isomerization of the double bond in **151** to give the enamine (**175**) followed by C-20 hydroxylation due to the lack of deuterium incorporation at C-21.[129] Combined, Boger proposed that these results suggested an initial radical hydrogen, whose presence resulted from sodium borohydride treatment of an Fe^{III} source, addition to C-15 to give the tertiary radical **201** (Scheme 39), thus accounting for the single deuterium incorporation to C-15 in the

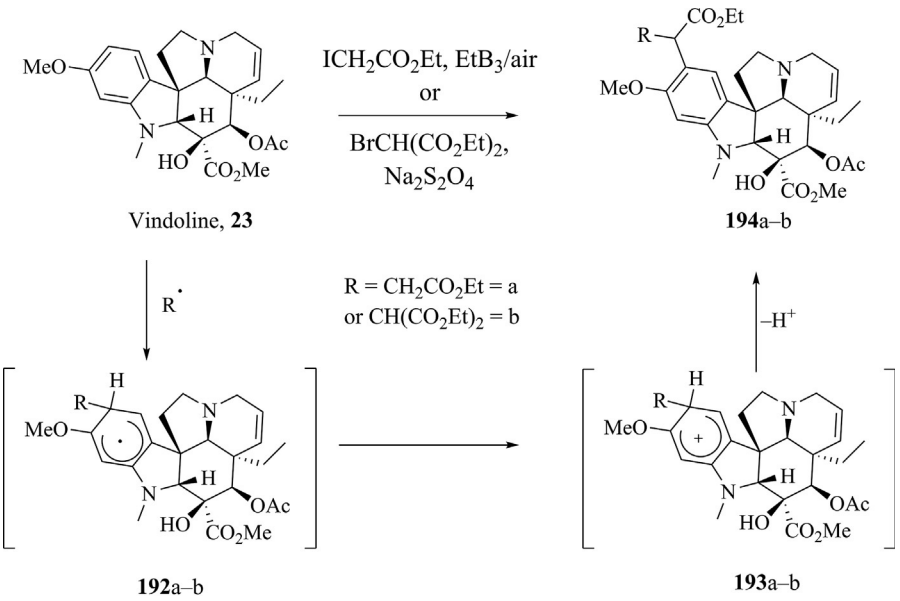

Scheme 37 Radical coupling of **23** with $\cdot CH_2CO_2Et$ or $\cdot CH(CO_2Et)_2$ radicals, consolidating direct coupling of **23** with the single-electron indole oxidation intermediate **181** in Scheme 36.[132]

labeling studies.[129] **201** could proceed to react with oxygen to yield a hydroperoxide radical (**202**), reduction of which would give the 4′-hydroxylated products.[129] In the one-pot coupling and oxidation, sodium borohydride initially reduced iminium **154** to give **151**, and subsequently provided the hydrogen radical to promote C-20 oxidation (double D incorporation at C-15 and C-21).[129]

In efforts to increase the diastereoselectivity of the oxidation reaction to favor for formation of **17**, Boger and coworkers prepared the *exo*-catharanthine analog (**203**).[129] This derivative differs from **20** in the placement of the double bond, but still retains the prerequisites for selective coupling at C-16 and subsequent radical-mediated oxidation (Scheme 40).[129] The unoptimized two-step reaction produced hydroxylated products with little difference in diastereoselectivity when compared to that for **20** (exclusive 16-*S* but 2:1 β:α diastereomers).[129] Oxidation of the unsaturated 19,20-anhydrovinblastine (**204**) derivative using the $Fe_2(ox)_3$-$NaBH_4$ conditions did not alter the stereoselectivity.[129] These results suggested that the conversion of **20** and **203**, to **151** and **204** likely proceeded through a common intermediate and/or mechanism.[129] Finally, Boger et al. noted that their ferric ion coupling and oxidation reproduced the relative abundance of **17** and **178** in plants. This and the discovery of the distinct localization of **20** and **23** in different parts of plant leaf[135] led Boger to make the provocative suggestion that the dimerization and subsequent functionalization of these monomers may be due to stress-induced mixing of the two compounds in the presence of an Fe^{III} source and air.[131]

2.24.3 Conclusion

The family of MIAs may have received more ingenious mechanistic speculations than any other class of natural products.[47] The chemical complexity of the MIA family may initially appear daunting, and the scarcity and reactivity of these compounds further complicates experimental investigations. In the words of Professor Ian Scott, "...the manipulation of microgram quantities in biomimetic experiments is an art which, in our experience, has oft-times required *several hundred trials before declaring a negative result.*"[56]

However, as approaches for identifying genes in plant metabolism have improved, modern researchers could capitalize on the early work of these chemists to assemble the genetic basis of this pathway.[136] Our present knowledge of the biosynthesis of these compounds is undeniably owed to the laborious studies on these systems by the myriad of research groups over the past six decades (Fig. 10). The insights and perseverance of Wenkert, Scott, Kutney, and many other researchers are responsible for our knowledge of the intricate and beautiful chemistry encoded by the biosynthetic pathway of this life-saving drug. We also highlight Ms. Halina Czajkowski Robinson, who was the first to note the effect of *C. roseus* oral extracts to the white blood cell count of rats, and whose contribution has so often been overlooked whenever the vinblastine story is recounted.[2] Collectively, this work has culminated in the recent complete biosynthesis of anhydrovinblastine (**151**) which could be semisynthetically oxidized to give vinblastine (**17**).

Scott wrote "In spite of the many frustrations and experimental difficulties encountered by the investigators of biogenetic-type synthesis in the field of indole alkaloids, there is emerging the most satisfying viewpoint that many of Nature's processes can be

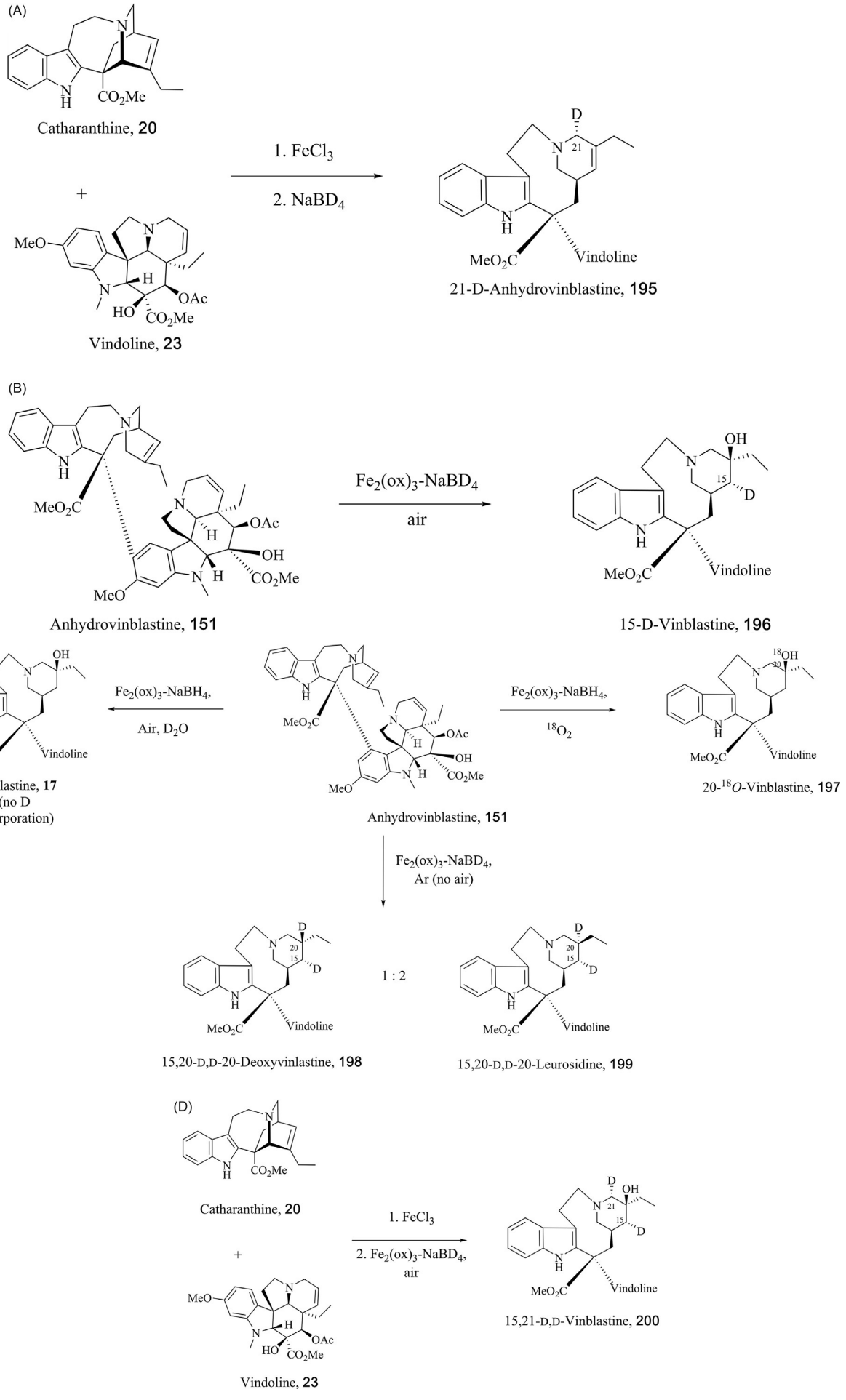

Scheme 38 (A) Coupling of **20** and **23** using $NaBD_4$ led to single D incorporation at C-21, (B) Oxidation of **151** with $Fe_2(ox)_3$-$NaBD_4$ led to single D incorporation at C-15, (C) Various oxidation conditions illustrating that the hydroxyl group at C-20 in **17** is derived from oxygen, and (D) One-pot coupling of **20** and **23** and subsequent oxidation led to double D incorporation at C-15 and C-21.[129]

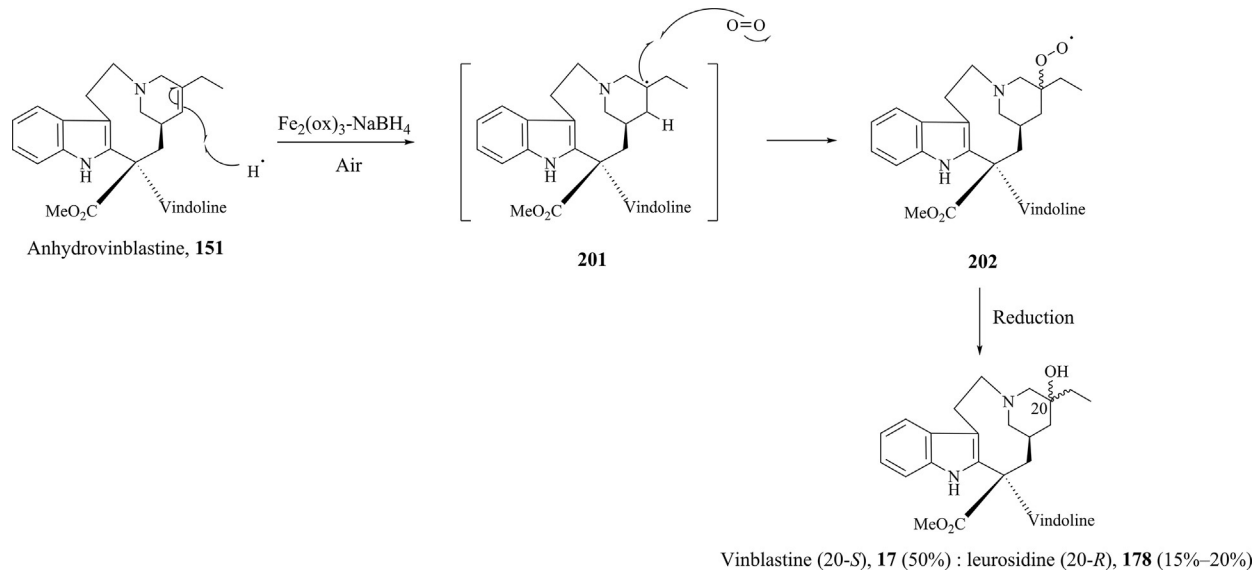

Scheme 39 Boger's proposed mechanism for the oxidation of **151** to **17** and **178**.[129]

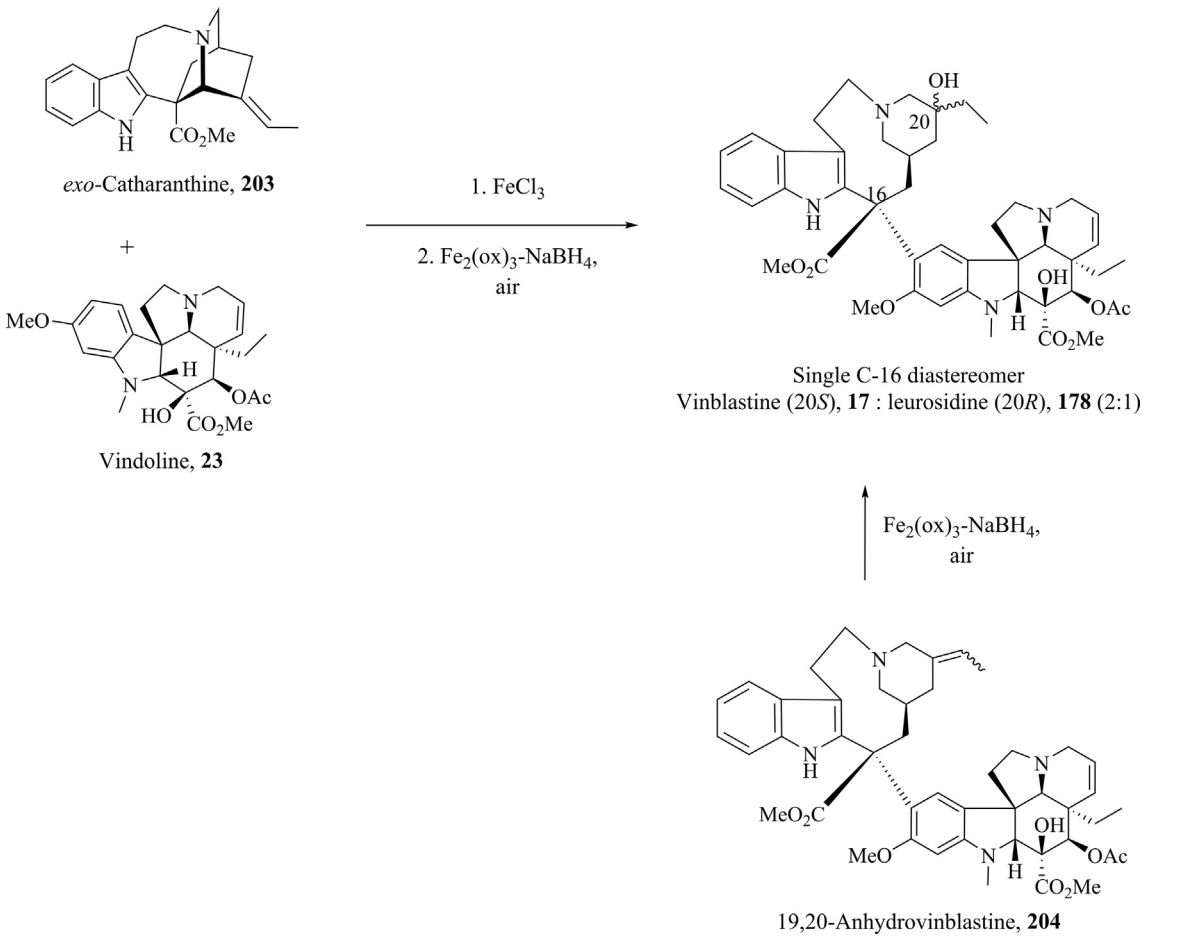

Scheme 40 Boger's attempt to improve diastereoselectivity (β vs. α C-20 OH group) by coupling of **203** and **23** and subsequent oxidation, or oxidation of **204** to **17** and **178**.[129]

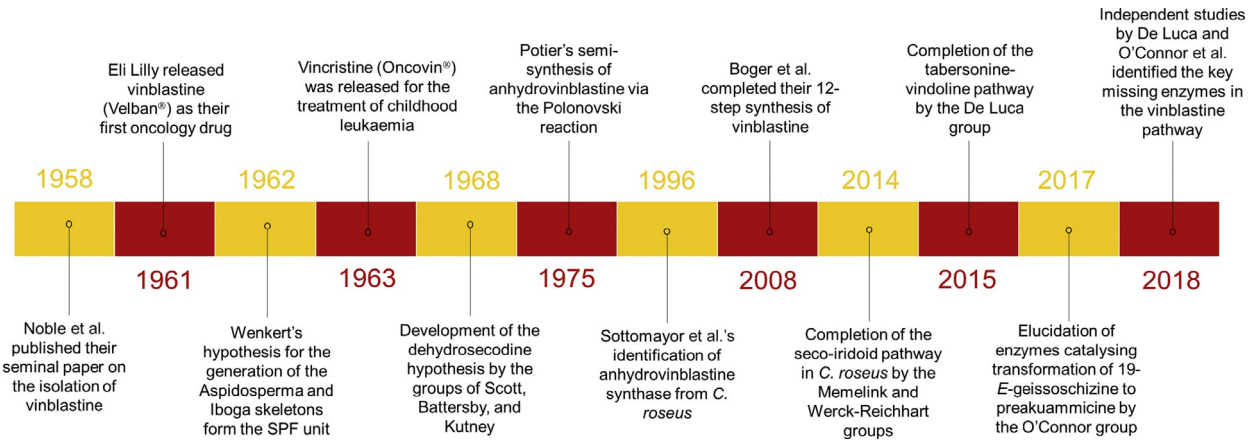

Fig. 10 Timeline of the major events in the vinblastine story, starting with Noble's seminal paper on the isolation of **17**.

simulated in a significant way."[44] Vinblastine and vincristine are gifts from Nature, and the biosynthetic insights described in this article now enable the next phase of research in these compounds. For example, synthetic biology and metabolic engineering efforts can be used to generate *C. roseus* plants with improved levels of anti-cancer agents. Alternatively, pathway enzymes can be reconstituted in fermentable host organisms, such as baker's yeast, to potentially allow better access to these compounds. Knowledge of the biosynthetic enzymes, along with a fundamental understanding of the chemistry catalyzed by these enzymes, may also enable strategies to biosynthetically prepare new vinblastine derivatives, and even to use these enzymes to generate new-to-nature scaffolds. The coming years will demonstrate how Nature's catalysts can be used to harness the chemical potential of these medicinal plants.

References

1. Noble, R. L.; Beer, C. T.; Cutts, J. H. *Ann. N. Y. Acad. Sci.* **2006**, *76*, 882–894.
2. Duffin, J. *Can. Bull. Med. Hist.* **2000**, *17*, 155–192.
3. Dewick, P. M. *Medicinal Natural Products.* John Wiley & Sons, Ltd: New Jersey, 2009; pp 311–420.
4. O'Connor, S. E.; Maresh, J. J. *Nat. Prod. Rep.* **2006**, *23*, 532–547.
5. Miettinen, K.; Dong, L.; Navrot, N.; Schneider, T.; Burlat, V.; Pollier, J.; Woittiez, L.; van der Krol, S.; Lugan, R.; Ilc, T.; Verpoorte, R.; Oksman-Caldentey, K.-M.; Martinoia, E.; Bouwmeester, H.; Goossens, A.; Memelink, J.; Werck-Reichhart, D. *Nat. Commun.* **2014**, *5*, 3606.
6. Kutchan, T. M.; Hampp, N.; Lottspeich, F.; Beyreuther, K.; Zenk, M. H. *FEBS Lett.* **1988**, *237*, 40–44.
7. McKnight, T. D.; Roessner, C. A.; Devagupta, R.; Scott, A. I.; Nessler, C. L. *Nucleic Acids Res.* **1990**, *18*, 4939.
8. Luca, V. D.; Marineau, C.; Brisson, N. *Proc. Natl. Acad. Sci.* **1989**, *86*, 2582–2586.
9. Vetter, H.-P.; Mangold, U.; Schröder, G.; Marner, F.-J.; Werck-Reichhart, D.; Schröder, J. *Plant Physiol.* **1992**, *100*, 998–1007.
10. Irmler, S.; Schröder, G.; St-Pierre, B.; Crouch, N. P.; Hotze, M.; Schmidt, J.; Strack, D.; Matern, U.; Schröder, J. *Plant J.* **2000**, *24*, 797–804.
11. Collu, G.; Unver, N.; Peltenburg-Looman, A. M. G.; van der Heijden, R.; Verpoorte, R.; Memelink, J. *FEBS Lett.* **2001**, *508*, 215–220.
12. Geu-Flores, F.; Sherden, N. H.; Courdavault, V.; Burlat, V.; Glenn, W. S.; Wu, C.; Nims, E.; Cui, Y.; O'Connor, S. E. *Nature* **2012**, *492*, 138–142.
13. Salim, V.; Yu, F.; Altarejos, J.; Luca, V. D. *Plant J.* **2013**, *76*, 754–765.
14. Salim, V.; Wiens, B.; Masada-Atsumi, S.; Yu, F.; De Luca, V. *Phytochemistry* **2014**, *101*, 23–31.
15. Asada, K.; Salim, V.; Masada-Atsumi, S.; Edmunds, E.; Nagatoshi, M.; Terasaka, K.; Mizukami, H.; Luca, V. D. *Plant Cell* **2013**, *25*, 4123–4134.
16. Thamm, A. M. K.; Qu, Y.; Luca, V. D. *Phytochem. Rev.* **2016**, *15*, 339–361.
17. Wenkert, E. *J. Am. Chem. Soc.* **1962**, *84*, 98–102.
18. Battersby, A. R.; Brown, R. T.; Kapil, R. S.; Plunkett, A. O.; Taylor, J. B. *Chem. Commun.* **1966**, 46–47.
19. Kutney, J. P.; Beck, J. F.; Ehret, C.; Poulton, G.; Sood, R. S.; Westcott, N. D. *Bioorg. Chem.* **1971**, *1*, 194–206.
20. Kutney, J. P.; Chan, K. K.; Failli, A.; Fromson, J. M.; Gletsos, C.; Nelson, V. R. *J. Am. Chem. Soc.* **1968**, *90*, 3891–3893.
21. Battersby, A. R.; Byrne, J. C.; Kapil, R. S.; Martin, J. A.; Payne, T. G.; Arigoni, D.; Loew, P. *Chem. Commun.* **1968**, 951–953.
22. Qureshi, A. A.; Scott, A. I. *Chem. Commun.* **1968**, 945–946.
23. Laschat, S. *Angew. Chem. Int. Ed. Engl.* **1996**, *35*, 289–291.
24. Tang, M.-C.; Zou, Y.; Watanabe, K.; Walsh, C. T.; Tang, Y. *Chem. Rev.* **2017**, *117*, 5226–5333.
25. Minami, A.; Oikawa, H. *J. Antibiot. (Tokyo)* **2016**, *69*, 500–506.
26. Lin, C.-I.; McCarty, R. M.; Liu, H. *Angew. Chem. Int. Ed.* **2017**, *56*, 3446–3489.
27. Oikawa, H.; Katayama, K.; Suzuki, Y.; Ichihara, A. *J. Chem. Soc., Chem. Commun.* **1995**, 1321–1322.
28. Oikawa, H.; Suzuki, Y.; Naya, A.; Katayama, K.; Ichihara, A. *J. Am. Chem. Soc.* **1994**, *116*, 3605–3606.
29. Kennedy, J.; Auclair, K.; Kendrew, S. G.; Park, C.; Vederas, J. C.; Hutchinson, C. R. *Science* **1999**, *284*, 1368–1372.
30. Kim, H. J.; Ruszczycky, M. W.; Choi, S.; Liu, Y.; Liu, H. *Nature* **2011**, *473*, 109–112.
31. Oikawa, H.; Watanabe, K.; Yagi, K.; Ohashi, S.; Mie, T.; Ichihara, A.; Honma, M. *Tetrahedron Lett.* **1999**, *40*, 6983–6986.
32. Watanabe, K.; Oikawa, H.; Yagi, K.; Ohashi, S.; Mie, T.; Ichihara, A.; Hornma, M. *J. Biochem.* **2000**, *127*, 467–473.
33. Qureshi, A. A.; Scott, A. I. *Chem. Commun.* **1968**, 947–948.
34. Qureshi, A. A.; Scott, A. I. *Chem. Commun.* **1968**, 948–950.
35. Kutney, J. P.; Cretney, W. J.; Hadfield, J. R.; Hall, E. S.; Nelson, V. R.; Wigfield, D. C. *J. Am. Chem. Soc.* **1968**, *90*, 3566–3567.

36. Kutney, J. P.; Ehret, C.; Nelson, V. R.; Wigfield, D. C. *J. Am. Chem. Soc.* **1968**, *90*, 5929–5930.
37. Battersby, A. R.; Burnett, A. R.; Hall, E. S.; Parsons, P. G. *Chem. Commun.* **1968**, 1582–1583.
38. Battersby, A. R.; Burnett, A. R.; Parsons, P. G. *J. Chem. Soc. C* **1969**, 1193–1200.
39. Battersby, A. R. The Alkaloids. Royal Society of Chemistry, 1972; vol. 1.
40. Battersby, A. R.; Saxton, J. E. In *The Alkaloids*; Saxton, J. E., Ed.; The Royal Society of Chemistry: London, 1971; vol. 1, pp 31–47.
41. Scott, A. I.; Cherry, P. C.; Qureshi, A. A. *J. Am. Chem. Soc.* **1969**, *91*, 4932–4933.
42. Battersby, A. R.; Hall, E. S. *J. Chem. Soc., Chem. Commun.* **1969**, 793–794.
43. Scott, A. I.; Reichardt, P. B.; Slaytor, M. B.; Sweeny, J. G. *Bioorg. Chem.* **1971**, *1*, 157–173.
44. Runeckles, V. *Recent Advances in Phytochemistry*, 1st edn.; Springer: New York, 1975; vol. 9.
45. Scott, A. I.; Wei, C. C. *J. Am. Chem. Soc.* **1972**, *94*, 8264–8265.
46. Scott, A. I.; Qureshi, A. A. *J. Am. Chem. Soc.* **1969**, *91*, 5874–5876.
47. Scott, A. I. *Acc. Chem. Res.* **1970**, *3*, 151–157.
48. Wenkert, E.; Wickberg, B. *J. Am. Chem. Soc.* **1965**, *87*, 1580–1589.
49. Battersby, A. R. *Pure Appl. Chem.* **1967**, *14*, 117–136.
50. Tatsis, E. C.; Carqueijeiro, I.; de Bernonville, T. D.; Franke, J.; Dang, T.-T. T.; Oudin, A.; Lanoue, A.; Lafontaine, F.; Stavrinides, A. K.; Clastre, M.; Courdavault, V.; O'Connor, S. E. *Nat. Commun.* **2017**, *8*, 316.
51. Benayad, S.; Ahamada, K.; Lewin, G.; Evanno, L.; Poupon, E. *Eur. J. Org. Chem.* **2016**, *2016*, 1494–1499.
52. Qu, Y.; Easson, M. E. A. M.; Simionescu, R.; Hajicek, J.; Thamm, A. M. K.; Salim, V.; Luca, V. D. *Proc. Natl. Acad. Sci.* **2018**, *115* (12), 3180–3185.
53. Brown, R. T.; Hill, J. S.; Smith, G. F.; Stapleford, K. S. J.; Poisson, J.; Muquet, M.; Kunesch, N. *J. Chem. Soc., Chem. Commun.* **1969**, 1475–1477.
54. Joule, J. A. *Annu. Rep. Prog. Chem., Sect. B: Org. Chem.* **1969**, *66*, 469–490.
55. Rahman, A.-U.; Basha, A. *Biosynthesis of Indole Alkaloids*, 1st edn.; Oxford University Press: Oxford, 1983; vol. 7.
56. Scott, A. I. *J. Am. Chem. Soc.* **1972**, *94*, 8262.
57. Scott, A. I.; Wei, C. C. *J. Am. Chem. Soc.* **1972**, *94*, 8263–8264.
58. Scott, A. I.; Wei, C. C. *J. Am. Chem. Soc.* **1972**, *94*, 8266–8267.
59. Evans, D. A.; Smith, G. F.; Smith, G. N.; Stapleford, K. S. J. *Chem. Commun.* **1968**, 859–861.
60. Cordell, G. A.; Smith, G. F.; Smith, G. N. *J. Chem. Soc., Chem. Commun.* **1970**, 191–192.
61. Cordell, G. A.; Smith, G. F.; Smith, G. N. *J. Chem. Soc., Chem. Commun.* **1970**, 189–190.
62. Brown, R. T.; Smith, G. F.; Stapleford, K. S. J.; Taylor, D. A. *J. Chem. Soc., Chem. Commun.* **1970**, 190–191.
63. Battersby, A. R.; Bhatnagar, A. K. *J. Chem. Soc., Chem. Commun.* **1970**, 193–194.
64. Kutney, J. P.; Beck, J. F.; Eggers, N. J.; Hanssen, H. W.; Sood, R. S.; Westcott, N. D. *J. Am. Chem. Soc.* **1971**, *93*, 7322–7324.
65. Hemscheidt, T.; Zenk, M. H. *FEBS Lett.* **1980**, *110*, 187–191.
66. Caputi, L.; Franke, J.; Farrow, S. C.; Chung, K.; Payne, R. M. E.; Nguyen, T.-D.; Dang, T.-T. T.; Carqueijeiro, I. S. T.; Koudounas, K.; de Bernonville, T. D.; Ameyaw, B.; Jones, D. M.; Vieira, I. J. C.; Courdavault, V.; O'Connor, S. E. *Science* **2018**, *360* (6394), 1235–1239.
67. Qu, Y.; Easson, M. L. A. E.; Froese, J.; Simionescu, R.; Hudlicky, T.; Luca, V. D. *Proc. Natl. Acad. Sci.* **2015**, *112*, 6224–6229.
68. Besseau, S.; Kellner, F.; Lanoue, A.; Thamm, A. M. K.; Salim, V.; Schneider, B.; Geu-Flores, F.; Höfer, R.; Guirimand, G.; Guihur, A.; Oudin, A.; Glevarec, G.; Foureau, E.; Papon, N.; Clastre, M.; Giglioli-Guivarc'h, N.; St-Pierre, B.; Werck-Reichhart, D.; Burlat, V.; Luca, V. D.; O'Connor, S. E.; Courdavault, V. *Plant Physiol.* **2013**, *163*, 1792–1803.
69. Schröder, G.; Unterbusch, E.; Kaltenbach, M.; Schmidt, J.; Strack, D.; Luca, V. D.; Schröder, J. *FEBS Lett.* **1999**, *458*, 97–102.
70. St-Pierre, B.; Luca, V. D. *Plant Physiol.* **1995**, *109*, 131–139.
71. Levac, D.; Murata, J.; Kim, W. S.; Luca, V. D. *Plant J.* **2008**, *53*, 225–236.
72. Kuboyama, T.; Yokoshima, S.; Tokuyama, H.; Fukuyama, T. *Proc. Natl. Acad. Sci. U. S. A.* **2004**, *101*, 11966–11970.
73. Danieli, B.; Lesma, G.; Palmisano, G.; Riva, R. *J. Chem. Soc., Chem. Commun.* **1984**, 909–911.
74. Kobayashi, S.; Ueda, T.; Fukuyama, T. *Synlett* **2000**, *2000*, 883–886.
75. Kuehne, M. E.; Podhorez, D. E.; Mulamba, T.; Bornmann, W. G. *J. Org. Chem.* **1987**, *52*, 347–353.
76. Kellner, F.; Geu-Flores, F.; Sherden, N. H.; Brown, S.; Foureau, E.; Courdavault, V.; O'Connor, S. E. *Chem. Commun.* **2015**, *51*, 7626–7628.
77. Danieli, B.; Lesma, G.; Palmisano, G.; Gabetta, B. *J. Chem. Soc., Chem. Commun.* **1981**, 908–909.
78. Calabi, L.; Danieli, B.; Lesma, G.; Palmisano, G. *J. Chem. Soc., Perkin Trans. 1* **1982**, 1371–1379.
79. Kutney, J. P.; Beck, J. F.; Nelson, V. R.; Sood, R. S. *J. Am. Chem. Soc.* **1971**, *93*, 255–257.
80. DeLuca, V.; Balsevich, J.; Tyler, R. T.; Kurz, W. G. W. *Plant Cell Rep.* **1987**, *6*, 458–461.
81. Luca, V. D.; Cutler, A. J. *Plant Physiol.* **1987**, *85*, 1099–1102.
82. Dethier, M.; De Luca, V. *Phytochemistry* **1993**, *32*, 673–678.
83. Liscombe, D. K.; Usera, A. R.; O'Connor, S. E. *Proc. Natl. Acad. Sci.* **2010**, *107*, 18793–18798.
84. Carolis, E. D.; Chan, F.; Balsevich, J.; Luca, V. D. *Plant Physiol.* **1990**, *94*, 1323–1329.
85. Carolis, E. D.; Luca, V. D. *J. Biol. Chem.* **1993**, *268*, 5504–5511.
86. Vazquez-Flota, F.; Carolis, E. D.; Alarco, A.-M.; Luca, V. D. *Plant Mol. Biol.* **1997**, *34*, 935–948.
87. De Luca, V.; Balsevich, J.; Kurz, W. G. W. *J. Plant Physiol.* **1985**, *121*, 417–428.
88. Fahn, W.; Gundlach, H.; Deus-Neumann, B.; Stöckigt, J. *Plant Cell Rep.* **1985**, *4*, 333–336.
89. Daddona, P. E.; Hutchinson, C. R. *J. Am. Chem. Soc.* **1974**, *96*, 6806–6807.
90. Scott, A. I. *Bioorg. Chem.* **1974**, *3*, 398–429.
91. Hassam, S. B.; Hutchinson, C. R. *Tetrahedron Lett.* **1978**, *19*, 1681–1684.
92. Daddona, P. E.; Wright, J. L.; Hutchinson, C. R. *Phytochemistry* **1976**, *15*, 941–945.
93. Neuss, N.; Gorman, M.; Cone, N. J.; Huckstep, L. L. *Tetrahedron Lett.* **1968**, *9*, 783–787.
94. Potier, P.; Langlois, N.; Langlois, Y.; Guéritte, F. *J. Chem. Soc., Chem. Commun.* **1975**, 670–671.
95. Scott, A. I.; Gueritte, F.; Lee, S. L. *J. Am. Chem. Soc.* **1978**, *100*, 6253–6255.
96. Baxter, R. L.; Dorschel, C. A.; Lee, S.-L.; Scott, A. I. *J. Chem. Soc., Chem. Commun.* **1979**, 257–259.
97. Kutney, J. P.; Choi, L. S. L.; Honda, T.; Lewis, N. G.; Sato, T.; Stuart, K. L.; Worth, B. R. *Helv. Chim. Acta* **1982**, *65*, 2088–2101.
98. Endo, T.; Goodbody, A.; Vukovic, J.; Misawa, M. *Phytochemistry* **1987**, *26*, 3233–3234.
99. McLauchlan, W. R.; Hasan, M.; Baxter, R. L.; Ian Scott, A. *Tetrahedron* **1983**, *39*, 3777–3780.
100. Misawa, M.; Endo, T.; Goodbody, A.; Vukovic, J.; Chapplet, C.; Choi, L.; Kutney, J. P. *Phytochemistry* **1988**, *27*, 1355–1359.
101. Goodbody, A. E.; Endo, T.; Vukovic, J.; Kutney, J. P.; Choi, L. S. L.; Misawa, M. *Planta Med.* **1988**, *54*, 136–140.
102. Endo, T.; Goodbody, A.; Vukovic, J.; Misawa, M. *Phytochemistry* **1988**, *27*, 2147–2149.
103. Sottomayor, M.; de Pinto, M. C.; Salema, R.; Dicosmo, F.; Pedreõo, M. A.; Barcelo, A. R. *Plant, Cell Environ.* **2006**, *19*, 761–767.
104. Sottomayor, M.; López-Serrano, M.; DiCosmo, F.; Barceló, A. R. *FEBS Lett.* **1998**, *428*, 299–303.
105. Sottomayor, M.; Barceló, A. R. *Protoplasma* **2003**, *222*, 97–105.

106. Costa, M. M. R.; Hilliou, F.; Duarte, P.; Pereira, L. G.; Almeida, I.; Leech, M.; Memelink, J.; Barceló, A. R.; Sottomayor, M. *Plant Physiol.* **2008**, *146*, 403–417.
107. Tognolli, M.; Penel, C.; Greppin, H.; Simon, P. *Gene* **2002**, *288*, 129–138.
108. Welinder, K. G.; Justesen, A. F.; Kjærsgård, I. V. H.; Jensen, R. B.; Rasmussen, S. K.; Jespersen, H. M.; Duroux, L. *Eur. J. Biochem.* **2002**, *269*, 6063–6081.
109. Passardi, F.; Longet, D.; Penel, C.; Dunand, C. *Phytochemistry* **2004**, *65*, 1879–1893.
110. Duroux, L.; Welinder, K. G. *J. Mol. Evol.* **2003**, *57*, 397–407.
111. Sottomayor, M.; DiCosmo, F.; Ros Barceló, A. *Enzyme Microb. Technol.* **1997**, *21*, 543–549.
112. Sariaslani, F. S.; Duffel, M. W.; Rosazza, J. P. *J. Med. Chem.* **1985**, *28*, 629–633.
113. Goodbody, A.; Endo, T.; Vukovic, J.; Misawa, M. *Planta Med.* **1988**, *54*, 210–214.
114. Peter Kutney, J.; Stuart, K. L.; Worth, B. R. *Heterocycles* **1978**, *9*, 1015.
115. Peter Kutney, J.; Aweryn, B.; Choi, L. S. L.; Kolodziejczyk, P.; Kurz, W. G. W.; Chatson, K. B.; Constabel, F. *Heterocycles* **1981**, *16*, 1169.
116. Elaev, N. R.; Ryzhakov, A. V. *Bull. Exp. Biol. Med.* **1986**, *102*, 928–930.
117. Sagui, F.; Chirivì, C.; Fontana, G.; Nicotra, S.; Passarella, D.; Riva, S.; Danieli, B. *Tetrahedron* **2009**, *65*, 312–317.
118. Shao, Y.; Ding, H.; Tang, W.; Lou, L.; Hu, L. *Bioorg. Med. Chem.* **2007**, *15*, 5061–5075.
119. Kutney, J. P.; Hibino, T.; Jahngen, E.; Okutani, T.; Ratcliffe, A. H.; Treasurywala, A. M.; Wunderly, S. *Helv. Chim. Acta* **1976**, *59*, 2858–2882.
120. Langlois, N.; Gueritte, F.; Langlois, Y.; Potier, P. *J. Am. Chem. Soc.* **1976**, *98*, 7017–7024.
121. Potier, P. *J. Nat. Prod.* **1980**, *43*, 72–86.
122. Sundberg, R. J.; Gadamasetti, K. G.; Hunt, P. J. *Tetrahedron* **1992**, *48*, 277–296.
123. Peter Kutney, J.; Ratcliffe, A. H.; Treasurywala, A. M.; Wunderly, S. *Heterocycles* **1975**, *3*, 639.
124. Sundberg, R. J.; Hong, J.; Smith, S. Q.; Sabat, M.; Tabakovic, I. *Tetrahedron* **1998**, *54*, 6259–6292.
125. Mangeney, P.; Zo Andriamialisoa, R.; Langlois, N.; Langlois, Y.; Potier, P. *J. Am. Chem. Soc.* **1979**, *101*, 2243–2245.
126. Peter Kutney, J.; Siu Leung Choi, L.; Nakano, J.; Tsukamoto, H.; McHugh, M.; Andre Boulet, C. *Heterocycles* **1988**, *27*, 1845.
127. Vukovic, J.; Goodbody, A. E.; Kutney, J. P.; Misawa, M. *Tetrahedron* **1988**, *44*, 325–331.
128. Ishikawa, H.; Colby, D. A.; Boger, D. L. *J. Am. Chem. Soc.* **2008**, *130*, 420–421.
129. Ishikawa, H.; Colby, D. A.; Seto, S.; Va, P.; Tam, A.; Kakei, H.; Rayl, T. J.; Hwang, I.; Boger, D. L. *J. Am. Chem. Soc.* **2009**, *131*, 4904–4916.
130. Alehashem, M. S.; Lim, C.-G.; Thomas, N. F. *RSC Adv.* **2016**, *6*, 18002–18025.
131. Sears, J. E.; Boger, D. L. *Acc. Chem. Res.* **2015**, *48*, 653–662.
132. Gotoh, H.; Sears, J. E.; Eschenmoser, A.; Boger, D. L. *J. Am. Chem. Soc.* **2012**, *134*, 13240–13243.
133. Tam, A.; Gotoh, H.; Robertson, W. M.; Boger, D. L. *Bioorg. Med. Chem. Lett.* **2010**, *20*, 6408–6410.
134. Gotoh, H.; Duncan, K. K.; Robertson, W. M.; Boger, D. L. *ACS Med. Chem. Lett.* **2011**, *2*, 948–952.
135. Roepke, J.; Salim, V.; Wu, M.; Thamm, A. M. K.; Murata, J.; Ploss, K.; Boland, W.; Luca, V. D. *Proc. Natl. Acad. Sci.* **2010**, *107*, 15287–15292.
136. Hirsch, C. N.; Robin Buell, C. *Annu. Rev. Plant Biol.* **2013**, *64*, 89–110.